

Dissertation

zur Erlangung des Doktorgrades der Fakultät für Chemie und
Pharmazie der Ludwig-Maximilians-Universität München



Role of Bid and AIF in Glutamate-induced Neuronal Cell Death

vorgelegt von

Stefan Landshamer

aus München

2007

Erklärung:

Diese Dissertation wurde im Sinne von § 13 Abs. 3 bzw. 4 der Promotionsordnung vom 29. Januar 1998 von Privat-Dozent Dr. Carsten Culmsee und Professor Dr. Ernst Wagner betreut.

Ehrenwörtliche Versicherung:

Diese Dissertation wurde selbständig, ohne unerlaubte Hilfe erarbeitet.

München, am 15.01.2007

Stefan Landshamer

Dissertation eingereicht am 15.01.2007.

1. Gutacher: Prof. Dr. Ernst Wagner

2. Gutacher: PD Dr. Carsten Culmsee

Mündliche Prüfung am 22.02.2007.

Meinen Eltern

Table of Contents

1	<u>INTRODUCTION</u>	1
1.1	APOPTOSIS IN NEURODEGENERATIVE DISEASES	1
1.2	CASPASES AND CASPASE-INDEPENDENT MECHANISMS IN APOPTOSIS	4
1.3	OXIDATIVE STRESS AND MITOCHONDRIA	7
1.4	BCL-2-FAMILY PROTEINS.....	9
1.5	ACTIVATION OF BID IN APOPTOSIS	10
1.6	AIMS OF THE THESIS.....	13
2	<u>MATERIALS AND METHODS</u>	15
2.1	CHEMICALS AND REAGENTS	15
2.1.1	RECOMBINANT PROTEINS.....	15
2.1.2	CASPASE SUBSTRATES	15
2.1.3	INDUCERS AND INHIBITORS OF APOPTOSIS	15
2.1.4	TRANSFECTION REAGENTS.....	17
2.1.4.1	Plasmid vectors	17
2.1.4.2	siRNA	18
2.1.5	PRIMARY ANTIBODIES.....	19
2.1.6	SECONDARY ANTIBODIES.....	19
2.2	CELL BIOLOGICAL METHODS	19
2.2.1	CELL CULTURE AND INDUCTION OF APOPTOSIS.....	19
2.2.1.1	HT-22 neurons	20
2.2.1.2	Primary rat neurons.....	21
2.2.2	CELL VIABILITY ASSAYS AND MITOCHONDRIAL STAINING.....	21
2.2.2.1	MTT-assay	22
2.2.2.2	DAPI /Hoechst 33342 staining	22
2.2.2.3	Annexin-V-FITC staining	23
2.2.2.4	JC-1-assay (Mitochondrial function)	23
2.2.2.5	MitoTracker Green staining (Mitochondrial visualization)	24
2.2.3	TRANSMISSION LIGHT AND EPIFLUORESCENCE MICROSCOPY	24

2.2.4	TRANSFECTION PROTOCOLS.....	25
2.2.4.1	DNA-transfections.....	25
2.2.4.2	Flow cytometric analysis of DNA transfection efficiency in HT-22 neurons.....	26
2.2.4.3	siRNA-transfections.....	26
2.2.5	IMMUNOCYTOCHEMISTRY AND CONFOCAL LASER SCANNING MICROSCOPY (CLSM).....	26
2.2.6	CONFOCAL LASER SCANNING MICROSCOPY OF HT-22 NEURONS.....	27
2.3	PROTEIN ANALYSIS.....	28
2.3.1	PROTEIN SAMPLE PREPARATION FROM HT-22 NEURONS AND FROM PRIMARY RAT NEURONS.....	28
2.3.2	DETERMINATION OF PROTEIN AMOUNT.....	29
2.3.3	POLYACRYLAMID GEL ELECTROPHORESIS AND WESTERN BLOT.....	30
2.3.4	CASPASE-ACTIVITY ASSAY.....	31
2.4	RNA ANALYSIS.....	32
2.4.1	RNA SAMPLE PREPARATION.....	32
2.4.2	DETERMINATION OF RNA AMOUNT.....	33
2.4.3	REVERSE TRANSCRIPTASE POLYMERASE CHAIN REACTION (RT-PCR).....	33
2.4.3.1	Reverse transcription.....	33
2.4.3.2	Polymerase chain reaction (PCR).....	34
2.4.4	AGAROSE GEL ELECTROPHORESIS.....	34
2.4.5	STATISTICAL ANALYSIS.....	35
3	RESULTS.....	36
3.1	GLUTAMATE-SENSITIVITY OF HT-22 NEURONS.....	36
3.1.1	BID TRANSLOCATES TO MITOCHONDRIA EARLY DURING APOPTOSIS.....	37
3.1.2	BID KNOCKDOWN ATTENUATES OXIDATIVE STRESS AND PREVENTS CELL DEATH.....	38
3.1.3	SMALL MOLECULE BID INHIBITOR PREVENTS GLUTAMATE-INDUCED CELL DEATH.....	39
3.1.4	PREVENTION OF GLUTAMATE-INDUCED APOPTOSIS BY BID INHIBITOR.....	40
3.1.5	SPECIFICITY OF THE BID INHIBITOR.....	41
3.1.6	THERAPEUTIC TIME WINDOW OF BI-6C9.....	42
3.1.7	BAX INHIBITION DOES NOT PROTECT AGAINST GLUTAMATE.....	43
3.1.8	MECHANISMS DOWNSTREAM OF BID.....	43
3.1.8.1	Effect of BI-6C9 on mitochondrial translocation of Bid.....	44
3.1.8.2	Mitochondrial membrane potential.....	45
3.1.8.3	Bid inhibition reduces effector caspase-3 activity.....	46

3.1.9	INVOLVEMENT OF EFFECTOR CASPASES IN GLUTAMATE-INDUCED APOPTOSIS	46
3.1.9.1	Inhibition of caspase-3 does not attenuate glutamate toxicity	47
3.1.9.2	Lamin cleavage in glutamate-induced neurotoxicity	48
3.1.10	INVOLVEMENT OF AIF IN APOPTOSIS OF HT-22 NEURONS	48
3.1.10.1	AIF-siRNA prevents glutamate-induced cell death	50
3.1.10.2	Bid inhibition prevents translocation of apoptosis inducing factor (AIF).	53
3.1.10.3	AIF-knockdown prevents tBid-induced cell death	54
3.1.11	MECHANISMS UPSTREAM OF BID-ACTIVATION IN GLUTAMATE NEUROTOXICITY	54
3.1.11.1	Calpains	55
3.1.11.2	Cathepsins	56
3.1.11.3	P38 MAP kinase	56
3.1.11.4	PARP1/PARG	57
3.1.11.5	Caspase-8	59
3.1.11.6	Caspase-2	60
3.1.11.7	Caspase-1	61
3.1.11.8	Omi/HtrA2	62
3.2	BID AND AIF ARE NOT REQUIRED IN STAUROSPORINE-INDUCED APOPTOSIS	68
3.2.1	NO PROTECTION FROM STS-INDUCED CELL DEATH BY BID-INHIBITION	69
3.2.2	STS-INDUCED CELL DEATH DOES NOT INVOLVE AIF TRANSLOCATION	70
3.2.3	AIF-KNOCKDOWN DOES NOT RESCUE HT-22 NEURONS FROM APOPTOSIS BY STS-TREATMENT.	71
3.3	ROLE OF BID AND AIF IN GLUTAMATE-INDUCED APOPTOSIS OF PRIMARY RAT NEURONS...	71
3.3.1	AIF-KNOCKDOWN RESCUES PRIMARY NEURONS FROM APOPTOSIS.....	72
3.3.2	BID INHIBITOR PREVENTS TRANSLOCATION OF AIF	74
3.3.3	BID-INHIBITION PREVENTS APOPTOSIS OF PRIMARY RAT NEURONS	74
4	<u>DISCUSSION</u>.....	76
4.1	GLUTAMATE DAMAGE IN HT-22 NEURONS: A MODEL FOR OXIDATIVE STRESS INDUCED APOPTOSIS.....	76
4.2	BID-DEPENDENT AIF-RELEASE IN GLUTAMATE-INDUCED APOPTOSIS OF HT-22 NEURONS .	77
4.2.1	CASPASE-DEPENDENT VERSUS CASPASE-INDEPENDENT APOPTOSIS	79
4.2.2	STAUROSPORINE-INDUCED APOPTOSIS IS INDEPENDENT OF BID	81
4.3	ACTIVATION OF BID	83

4.4	GLUTAMATE TOXICITY IN HT-22 NEURONS IS A RELEVANT MODEL FOR NEURODEGENERATIVE DISEASES:	85
5	SUMMARY	88
6	APPENDIX	89
6.1	ABBREVIATIONS	89
6.2	PUBLICATIONS	93
6.2.1	ORIGINAL PAPERS	93
6.2.2	REVIEWS	94
6.2.3	ORAL PRESENTATIONS AND POSTERS	94
7	REFERENCES	96
8	ACKNOWLEDGEMENTS	107
9	CURRICULUM VITAE	109

1 Introduction

1.1 Apoptosis in neurodegenerative diseases

Apoptosis, first described by Kerr et al. in 1972 [1], is morphologically characterized by nuclear condensation (pyknosis) and fragmentation, membrane blebbing and subsequent formation of apoptotic bodies. The resulting cell fragments, which are surrounded by an intact plasma membrane, can be absorbed by other cells via phagozytosis. Altogether this provides a 'silent' degradation of cells without release of cell cytosol which would lead to inflammation and damage of adjacent tissue. In contrast, necrotic cell death is associated with rapid cell swelling and rupture of the plasma membrane followed by substantial cell damage in the surrounding tissue by inflammation [2]. In proliferative tissues, apoptosis is an important mechanism to replace old or excessive cells [3]; but also in non proliferating tissues as for example brain tissue, apoptotic mechanisms are needed during development of synapses and specialized nerve cells [4]. Since this so called programmed cell death occurs all the time and almost everywhere in an organism's life, the pathways involved in apoptosis must ensure that dying cells do not adversely affect adjacent cells. While apoptosis is a mechanism developed by nature to assure the survival and the function of tissues, its dysregulation in neurodegenerative diseases is a major reason for pathological neural cell demise, subsequent loss of brain function, and many clinical symptoms in patients suffering from acute and chronic neurodegenerative diseases.

In the last years evidence increased that neurodegeneration associated with Alzheimer's disease, Parkinson's disease, stroke and even brain trauma, but also with many other neurodegenerative diseases, is commonly featured by apoptotic mechanisms [5]. There are many triggers described for neuronal apoptosis: Neurotrophic factor withdrawal [6], activation of glutamate receptors (excitotoxicity) [7], oxidative stress (formation of reactive oxygen species 'ROS') [8], metabolic stress (loss of ATP) [9] and environmental toxins [10]. For example, in acute neurological

disorders such as brain trauma and stroke, cell death is caused by glutamate-mediated excitotoxicity. Ionotropic glutamate receptors such as N-methyl-D-aspartate- (NMDA) receptors, 2-amino-3-(3-hydroxy-5-methylisoxazol-4-yl) proprionate (AMPA) receptors or kainate receptors are activated by excessive and prolonged extracellular glutamate levels after ischemia or mechanical stimulation of these receptors after trauma [11, 12]. This leads to elevated calcium levels in the neurons followed by increased ROS production due to mitochondrial dysfunction and stimulation of enzymes such as nitric oxide synthase, activation of proteases such as calpains and last but not least activation of caspases, the biochemical executors of apoptosis. However, it has been shown that both necrosis and apoptosis can occur in glutamate-induced excitotoxic cell death in neurons [13].

Alzheimer's disease is a chronic neurodegenerative disease, where accumulation of amyloid plaques formed by aggregates of amyloid- β -peptide is associated with the death of neurons. Debris of β -amyloid induces apoptosis in a direct way [14] or by sensitizing the neurons to oxidative stress and reduced energy availability [7], both occurring in brains during ageing. The molecular mechanisms of β -amyloid toxicity involves membrane lipid peroxidation, resulting in membrane depolarization through impairment of ion transporting ATPases and other membrane transporter proteins. Membrane depolarization is followed by calcium influx, ROS production and mitochondrial dysfunction and subsequent execution of apoptotic mechanisms [15]. The involvement of apoptotic mechanisms has been also demonstrated in neuronal cell death that occurs in Parkinson's disease: Expression and activation of caspases seems to be involved in cell death of dopaminergic neurons in the substantia nigra and the striatum [16, 17]; furthermore, formation of ROS and mitochondrial dysfunction are described as mechanisms involved in neuronal death associated with Parkinson's disease [18].

All the different acute and chronic neurodegenerative disorders as exemplified above exhibit different reasons for cell death of neurons. The resulting apoptotic mechanisms that play a major role in these disorders follow highly conserved

mechanisms although they are induced by many different triggers [19]. Acute brain insults such as brain trauma and ischemic stroke are leading causes of death and disability in our population and, most notably, chronic neurodegenerative diseases are of increasing relevance due to the rising lifespan in our societies. Until now, still very few is known about the underlying pathology and efficient treatments for these neurodegenerative diseases are not available. Therefore, it is of utmost interest to understand mechanisms which are involved in neuronal apoptosis. This is an important first step for the development of efficient therapeutic strategies. Therefore, a major aim of this thesis was to further elucidate mechanisms of glutamate-induced neuronal cell death, a major feature that apparently triggers apoptosis in many different neurodegenerative diseases. Immortalized HT-22 neurons were used as a glutamate sensitive neuronal cell line. They are derived from mouse hippocampus and feature sensitivity to glutamate. From their origin and their glutamate-sensitivity, HT-22 neurons act as a representative for neuronal cells. In this model system glutamate mediates cell death by glutathione depletion. Glutamate blocks the glutamate-cysteine antiporter system X_c^- which is important for the cysteine-uptake of the cells and therefore limiting for the cells' glutathione synthesis [20]. Consequently, levels of ROS increase within a few hours after glutamate treatment of HT-22 neurons due to the breakdown of the glutathione pools in the cells. Later, the ROS levels further increase in an explosive burst because of the damage of mitochondria and the subsequent breakdown of the cellular redox homeostasis. Furthermore an elevation of cytosolic calcium levels has been observed following the ROS formation in glutamate-exposed HT-22 neurons [21]. Thus, ROS formation, increased calcium levels and mitochondrial dysfunction are pre-requisites for the induction of apoptosis in this model system similar to the pathological mechanisms that occur in neurodegenerative diseases.

1.2 Caspases and caspase-independent mechanisms in apoptosis

Activation of caspases is a well established biochemical hallmark of apoptosis [22]. Caspases are cysteine proteases with an aspartyl-specificity [23]. Under physiologic conditions, they reside in the cytosol as inactive pre-cursors that are activated during apoptosis by autoproteolysis, other caspases or other proteases. For example, activation of caspases is triggered through death receptor signaling in the so-called extrinsic pathway of apoptosis. Complexes of ligand (TNF, Fas-ligand) and respective death receptor (p55 or p75, Fas) rapidly activate pro-caspase-1 or pro-caspase-8, the so-called initiator caspases.

Pro-caspase-1 or -8 have long pro-domains, such as the death effector domain (DED) or the caspase recruitment domain (CARD) which can interact with activating proteins containing death domains (DD) or other binding domains. In contrast to the initiator caspases, the so-called executing caspases (-3, -6, -7) have shorter pro-domains with up to now unknown functions [24]. Upon death receptor activation, initiator caspases-1, -2, -8 or -10 are cleaved to their active forms. The functional initiator caspases then activate the executing caspases-3, -6 and -7 which cleave downstream substrates such as, for example, inhibitor of caspase-activated deoxyribonuclease (ICAD) [25], inhibitors of apoptosis (IAPs) [26], Rho-associated kinase (ROCK) [27], Lamin A [28], or poly(ADP-ribose) polymerase (PARP) [29], among others. This caspase-dependent cascade ends up in typical DNA laddering, membrane blebbing and forming of apoptotic bodies. For example, the typical DNA laddering in apoptotic cells is caused by the activation of caspase-activated deoxyribonuclease (CAD) and subsequent DNA fragmentation into 180 bp internucleosomal DNA fragments or multiples thereof [30, 31].

However the extrinsic pathway of the caspase activation cascade can also be amplified in an indirect way, involving mitochondrial damage via the so called intrinsic pathway [32]. Mitochondrial damage alone is able to initiate the apoptotic pathway without death receptor signaling by the release of cytochrome c and subsequent activation of caspase-9 [33]. A well known link between the extrinsic and the intrinsic

apoptotic pathway is the activation of caspase-8. Besides caspase-3, BH3-interacting domain death agonist (Bid), a pro-apoptotic member of the B-cell lymphoma-2 (Bcl-2) family, can be cleaved and activated by caspase-8 which results in damage of mitochondria, therefore activation of the intrinsic pathway featuring the release of cytochrome c from the mitochondrial intermembrane space. Cytochrome c forms the apoptosome complex together with apoptosis protease-activating factor-1 (Apaf-1) and pro-caspase-9 leading to activation of the initiator caspase-9 [34], which then cleaves and activates caspase-3 [35]. Further proteins released from mitochondria have been identified to promote caspase-dependent apoptosis: For example, second mitochondrial derived activator of caspase (Smac/Diablo) and high temperature requirement protein A2 (Omi/HtrA2). Both are able to inhibit IAPs thereby supporting caspase-dependent apoptosis, either by binding to IAPs (Smac) or by cleaving these through serine protease activity (Omi) [36, 37]. Omi/HtrA2 is a 36-kDa serine protease residing in the mitochondria intermembrane space which can be released by different pro-apoptotic stimuli [38] exhibiting its pro-apoptotic function by caspase-dependent and even caspase-independent mechanisms [39].

Another protein that can execute apoptosis independent of caspases is the apoptosis inducing factor (AIF), a 63-kDa flavoprotein, localized to the mitochondria intermembrane space [40]. Once released from mitochondria, AIF translocates to the nucleus, binds DNA with its pro-apoptotic binding domain [41] and produces large scale DNA strand breaks, different from CAD-induced DNA laddering [42]. In addition, under physiologic conditions, AIF binds to flavin adenine dinucleotide (FAD) and acts as an oxidoreductase [43]. The need of its physiologic expression is demonstrated in Harlequin (Hq) mice, in which expression of AIF is reduced to 10-20%. Hq mice develop ataxia and blindness due to progressive neurodegenerative processes in the cerebellum and the retina, respectively. This neurodegeneration is linked to higher susceptibility of the neurons to oxidative stress resulting in abnormal apoptosis, suggesting that AIF with its oxidoreductase function is an endogenous cytoprotector [44]. The name 'Harlequin mice' has been imposed due the patchy hair loss, which they also develop and which let the mice look like Harlequins.

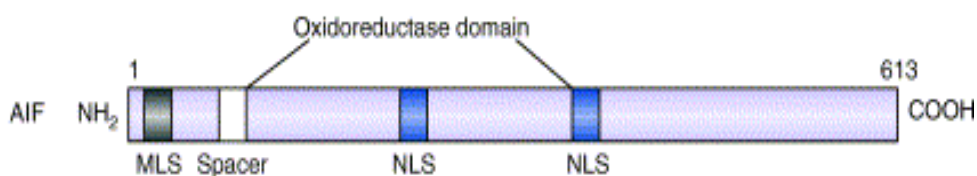


Figure 1: Schematic illustration of human AIF.

MLS: Mitochondrial localization sequence, NLS Nuclear localization sequence. The DNA binding domains reside in the oxidoreductase domain and at the C-terminus

In this thesis, it was a major aim to examine the involvement of caspase-dependent factors, such as caspase-8 and caspase-3, and caspase-independent, pro-apoptotic proteins such as AIF in glutamate-induced apoptosis of neuronal cells. For example, AIF has been shown in 2003 to be a main mediator of neuronal apoptosis after hypoxia-ischemia in neonatal rats [45]. In addition, proteins which induce the execution of apoptosis upstream of caspase-3 or AIF were of particular interest.

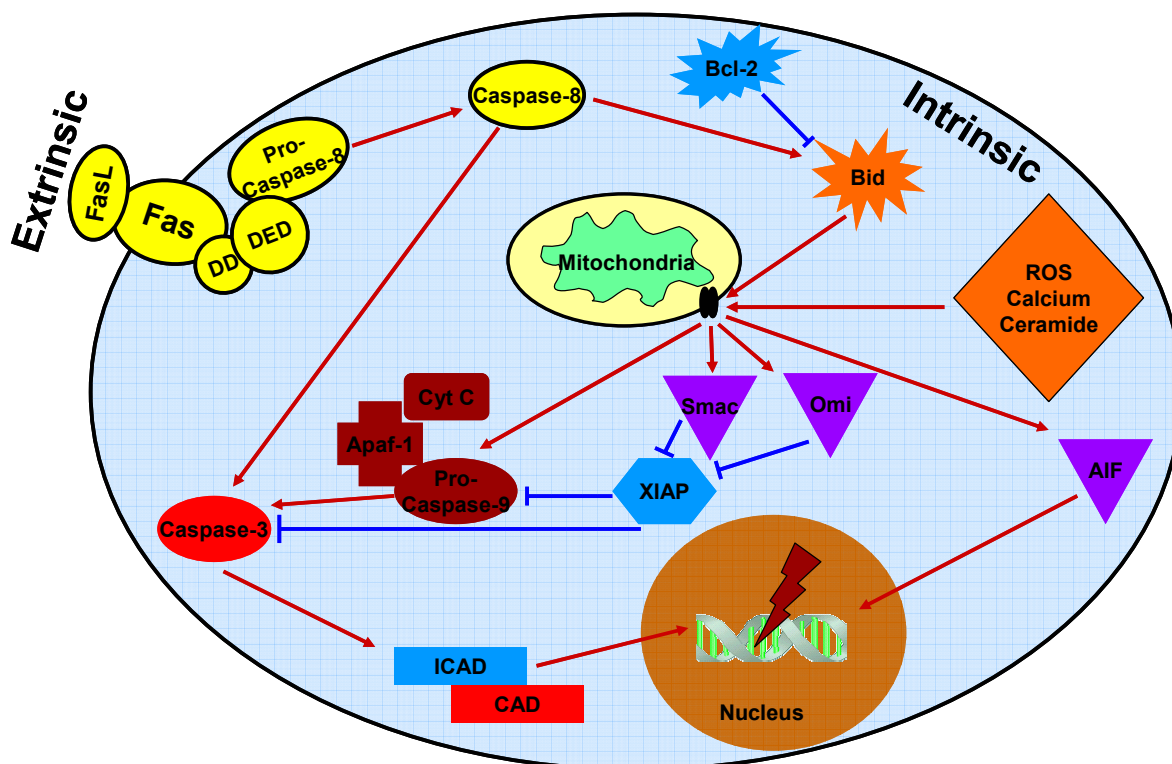


Figure 2: Regulation of apoptotic pathways.

Extrinsic pathway: Death receptors, such as Fas are activated by ligand (FasL) binding, resulting in the sequential binding of a Fas associated death domain (DD). Pro-caspase-8, containing the death effector domain (DED) in its pro-domain can bind to this complex and becomes activated. Caspase-8

*either directly activates caspase-3, which leads to the release of CAD (caspase-activated deoxyribonuclease) from its inhibitory ligand ICAD and subsequent DNA laddering, or caspase-8 cleaves the pro-apoptotic protein Bid which activates the **intrinsic pathway**. Bid cleavage, increased ROS- or calcium-levels are capable to induce mitochondrial membrane permeabilization, which leads to the release of cytochrome c, Omi/HtrA2, Smac or AIF. Cytochrome c builds a complex with Apaf-1 and pro-caspase-9 (Apoptosome) which amplifies caspase-3-activation. Omi/HtrA2 and Smac block the x-chromosomal linked inhibitor of apoptosis (XIAP), which leads to an indirect activation of caspase-3 and 9. AIF is able to execute apoptosis by a caspase-independent way: It translocates to the nucleus where it induces large scale (50 kb) DNA fragmentation. Pro-apoptotic Bcl-2-family members, such as Bid are inhibited by their anti-apoptotic family members, such as Bcl-2.*

1.3 Oxidative stress and Mitochondria

Mitochondria exhibit a crucial role in apoptotic mechanisms. On the one hand they are the well known 'power plants' of a cell which are responsible for ATP synthesis and therefore energy supply. On the other hand, they are a compartment that can generate large amounts of reactive oxygen species [46] and the mitochondrial intermembrane space harbors different proteins such as cytochrome c, Smac/Diablo, Omi/HtrA2, Endonuclease G and AIF, which are capable to mediate programmed cell death upon their release into the cytosol [47]. The mitochondrial pathway (intrinsic pathway) of apoptosis can amplify cascades of the extrinsic pathway as described above. In addition, the intrinsic mitochondrial pathway may be activated by different death receptor-independent stimuli as for example ROS, increased calcium levels, pro-apoptotic Bcl-2-family members or lipid mediators, such as ceramide [48].

For ATP synthesis, electrons are transferred inside the mitochondria from one complex of respiratory enzymes to the next and finally to molecular oxygen. Protons are translocated across the mitochondrial inner membrane. Thereby the ATP synthase gets powered and, as a side effect of the proton gradient, the mitochondrial transmembrane potential arises [49]. Since there is a continuous turnover of molecular oxygen and electrons, mitochondria are a potential source of huge amounts of reactive oxygen species, including superoxide anion radicals, hydroxyl radicals, singlet oxygen, hydrogen peroxides and peroxidized nitrogen derivatives. Formation and release of ROS are increased after mitochondrial damage and, therefore, dysfunctional mitochondria are not only susceptible to oxidative damage, but also a source of oxidative stress [46]. Mitochondrial dysfunction by oxidative

stress can originate from a disturbance of detoxifying mechanisms as superoxide dismutase (SOD), glutathione peroxidase or catalase and results in mitochondrial membrane permeabilization and the subsequent breakdown of the mitochondrial outer membrane potential. In addition high calcium levels (10-100 μM) can induce mitochondrial membrane permeabilization [50]. In neurons, high calcium levels result from excitotoxic activation of glutamate receptors. Upon its release from stores in the endoplasmic reticulum (ER), calcium can also link endoplasmic reticulum stress (ER stress) and mitochondrial dysfunction. ER stress results, for example, after accumulation of unfolded proteins in the ER, as a consequence of various stimuli, including ischemia, lack of trophic support and other neurodegenerative triggers [51]. One feature of ER stress is the crosstalk with mitochondria via calcium and cytochrome c. Small amounts of cytochrome c from mitochondria can bind to and stimulate endoplasmic reticular IP_3 -receptors. The subsequent release of calcium can trigger the mitochondrial membrane permeabilization, further release of cytochrome c from mitochondria and therefore execution of apoptosis [52]. Another feature of ER stress is the direct activation of executioner caspases independent of mitochondrial involvement: Accumulation of unfolded proteins in the ER leads to the activation of chaperones to facilitate protein folding or to suppress mRNA translation to block further protein accumulation [53]. In murine cells, ER stress induces the activation of caspase-12 which can subsequently activate executioner caspases like caspase-3 [54]. Caspase-4 is considered as the human homologue of mouse caspase-12 [53, 55].

Another regulation pathway of mitochondrial membrane permeabilization is represented by the members of the Bcl-2 family [56]. The correlation between mitochondrial membrane permeabilization and the breakdown of the mitochondrial membrane potential as well as the proteins which are involved in the formation of pores for the release of high molecular proteins from mitochondria are controversially discussed in the literature. However, there are common features of mitochondrial demise during apoptosis of a single cell: Upon induction of apoptosis involving the intrinsic pathway, mitochondrial membrane permeabilization occurs with subsequent increasing ROS levels, leading to a vicious circle of ROS production and the release

of cytochrome c and pro-apoptotic factors, which may activate caspase-dependent or caspase-independent pathways and ER stress. In particular, Smac/Diablo or Omi/HtrA2 can be released from mitochondria, thereby amplifying the activation of caspases. Also caspase-independent proteins, as for example AIF, can be released from mitochondria, executing apoptosis by nuclear translocation and DNA cleavage, independent from CAD [57]. In this thesis, the pathways of neuronal apoptosis downstream of mitochondrial dysfunction were identified. In addition, key players upstream of mitochondrial damage and caspase-dependent and caspase-independent mechanisms were identified in the context of glutamate toxicity in neuronal cells.

1.4 Bcl-2-family proteins

Multiple evidence demonstrates that the balance of pro- and anti-apoptotic B-cell lymphoma-2 (Bcl-2) protein family members is crucial for the regulation of mitochondrial integrity and function, thereby sealing a cell's fate after severe stress [58]. The Bcl-2 family consists of two large groups of proteins that either prevent (e.g. Bcl-2, Bcl-xl, Bcl-w) or promote apoptosis (e.g. Bax, Bad, Bak, Bid, Bim). These proteins can form either homo- or heterodimers and thus either function independently or in concert to regulate apoptosis. Bcl-2 and Bcl-xl can form heterodimer complexes with Bax to prevent its apoptogenic activity [59]. Upon activation, Bad- or Bak-mediated release of Bax from the Bax/Bcl-xl heterodimers or by conformational changes after interaction with truncated pro-apoptotic Bid, Bax forms a pore in the mitochondrial membrane which allows the release of cytochrome c and other pro-apoptotic factors from mitochondria. Bax has been identified as a key factor for mitochondrial damage in various models of neuronal apoptosis [58, 60]. In contrast to other cells where Bax or Bak can equally mediate mitochondrial damage, the prerequisite role of Bax in neuronal apoptosis may be explained by the absence of full-length Bak in neurons [61].

The translocation of truncated Bid (tBid) to the mitochondria where it interacts with Bax [62, 63] has been identified as a major pathway in neuronal cell death triggered by death receptor signaling and after cerebral ischemia [64, 65]. The subsequent

release of mitochondrial proteins such as cytochrome c or AIF amplifies pathways of apoptosis execution downstream of mitochondria. In this thesis, the involvement and importance of Bid, as a pro-apoptotic protein upstream of mitochondrial damage, in glutamate-induced apoptosis in neuronal cells had to be established. In addition, the executors of apoptosis downstream of Bid-mediated apoptosis had to be identified.

1.5 Activation of Bid in apoptosis

Bid is the only Bcl-2 family member that can act as a direct agonist of Bax or Bak after its activation. It has been shown that cleavage of Bid to tBid is essential for the activation of the intrinsic pathway and the subsequent amplification of pro-apoptotic mechanisms [60, 62]. For example, Bid-deficient neurons are highly resistant to cell death stimuli including oxygen glucose deprivation (OGD) in vitro or cerebral ischemia in vivo [65, 66]. Furthermore, Bid knockout mice were protected from secondary brain damage after trauma [67]. In sum, various models of neurodegeneration with relevance to different neurological diseases, revealed a key role for Bid. Usually, inactive full-length Bid resides in the cytosol of healthy cells and removing the N-terminal repressor of the C-terminal membrane-anchoring segment by proteolytic cleavage is necessary to activate the pro-apoptotic function of Bid [68]. The most prominent activator which cleaves Bid to tBid is caspase-8, which itself gets activated downstream of stimulated Fas or TNF death receptors. Activation of caspase-8 has been shown in primary cultured neurons, after OGD and also in rodent brains after an ischemic insult [69, 70] (Figure 3A). Inhibition of both, Fas ligand or TNF α protected neurons from apoptosis after OGD. Furthermore, Bid has been demonstrated as an ataxia telangiectasia mutated (ATM) effector after DNA damage in non-neuronal cells [71, 72].

In addition to caspases, other proteases, for example calpains, granzyme B or lysosomal hydrolases, can cleave Bid. Activation of calpains depends on elevated calcium levels, a common feature of neuronal apoptosis. Calpains cleave different substrates, including cytoskeletal proteins, protein kinases and phosphatases, membrane receptors and transporter proteins that play important roles in the

regulation of cell survival [73, 74]. In addition, calpains can cleave Bid. Calpains could therefore amplify pro-apoptotic signaling through mitochondrial damage and the subsequent release of pro-apoptotic factors like AIF, cytochrome c or Smac/Diablo [58, 75] (Figure 3B). Calpain inhibitors prevented neuronal cell death in many different models including, for example, transient forebrain ischemia in rats [76] or traumatic brain injury [77], suggesting that calpains play a key role in neuronal cell death after acute brain injury [78]. In addition caspase-2 may act as a linker between oxidative DNA damage and Bid cleavage [79] (Figure 3D); further, in vitro models of hypoxia as well as ischemia models in vivo demonstrated that caspase-1 is capable to cleave Bid. Therefore, caspase-1 may mediate mitochondrial damage and subsequent execution of cell death after cerebral ischemia [80] (Figure 3C).

The necessity of Bid cleavage to tBid to activate its pro-apoptotic function is recently challenged by the finding that translocation of full-length Bid to mitochondria resulted in a breakdown of the mitochondrial membrane potential and subsequent nuclear condensation in models of glutamate-induced neurotoxicity [81]. In an epithelial cell line full-length Bid also mediated apoptosis without previous cleavage by caspase-8 or interaction with other Bcl-2 family members; in this study, cell death was induced by removing the epithelial cells from extracellular matrix and plating them onto polyhydroxyethylmethacrylate-coated dishes, which resulted in Bid-dependent anoikis [82].

Altogether, Bid and its truncated form tBid seem to be central players in the mechanisms of apoptotic cell death, in particular in neurons. Therefore, it needs further studies to elucidate the exact mechanisms of Bid activation the particular role of Bid or tBid in mediating caspase-dependent or caspase-independent apoptosis. In this thesis, the involvement of Bid in glutamate-induced apoptosis of neuronal cells was addressed, including the mechanisms of Bid activation and downstream mechanisms such as mitochondrial damage.

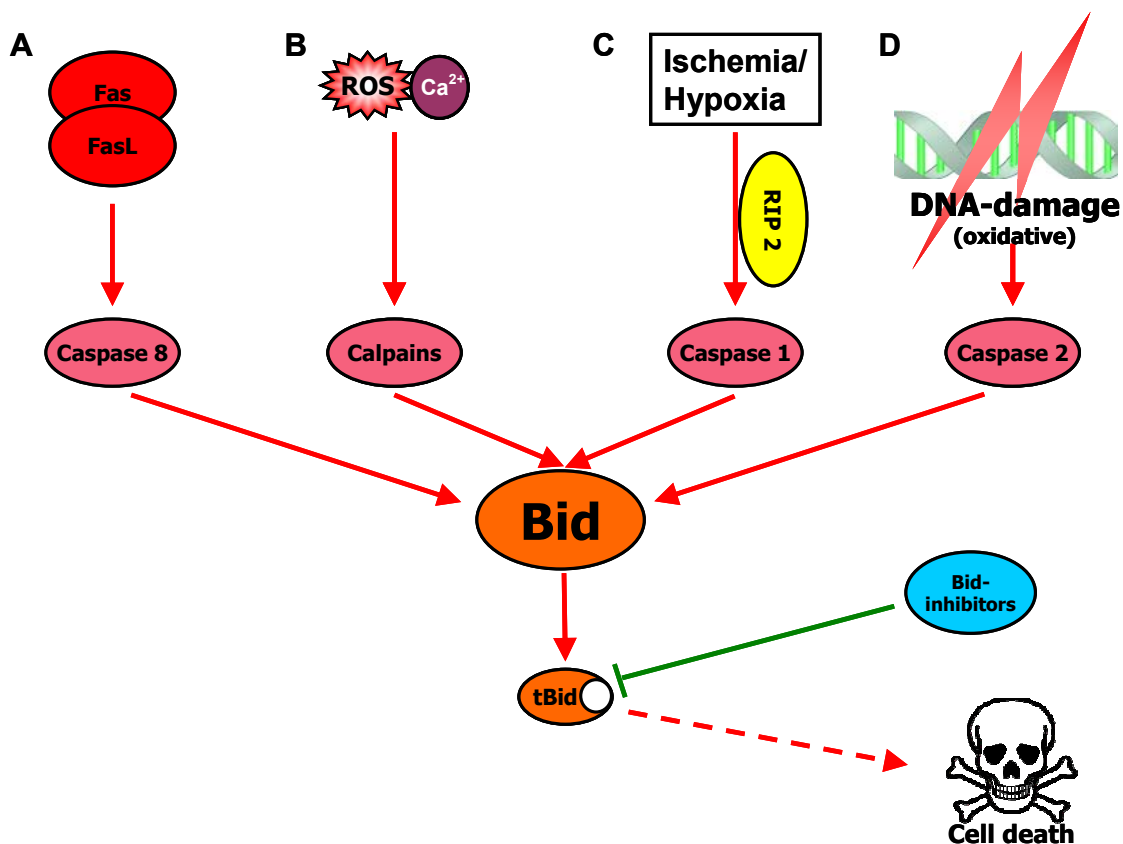


Figure 3: Activators of Bcl-2 family member Bid in different models of cell death.

A. Stimulation of death receptors results in activation of caspase-8, which cleaves Bid and leads to the mitochondrial release of cytochrome *c*. **B.** Bid cleavage is mediated by calpains after increases in intracellular calcium levels. **C.** After cerebral ischemia, activation of caspase-1 via RIP 2 modulator and subsequent Bid cleavage occur. This is followed by mitochondrial release of cytochrome *c* and AIF. **D.** Caspase-2 is activated in response to oxidative DNA damage and activates Bid which leads to mitochondrial demise and subsequent processing of caspase-9.

To elucidate the particular role of the different factors in apoptotic processes during glutamate-induced neuronal cell death in HT-22 neurons or primary neurons, established inhibitors of pro-apoptotic proteins, such as caspase- or calpain-inhibitors were applied in the present study as well as novel small molecular Bid inhibitors. These Bid inhibitors were developed in the laboratory of Maurizio Pellecchia, The Burnham Institute, La Jolla, USA by NMR-based molecular modeling [83]. These 4-phenyl-sulfanyl-phenylamine-derivatives, as for example BI-6C9 (Figure 4), are the first small molecule compounds which exhibited high affinity to pro-apoptotic Bid and were able to prevent tBid-induced mitochondrial damage and the subsequent release

of pro-apoptotic proteins such as cytochrome c and Smac/Diablo from mitochondria, by inhibition of tBid-translocation to mitochondria in non-neuronal cells [83]. These inhibitors have not been applied in neurons previously. In addition, small interfering RNA (siRNA) applications were established in the neuronal cell model systems to allow specific gene silencing of pro-apoptotic factors, in particular when small molecule inhibitors were not available. RNA interference was used as a powerful tool in neuronal cells to downregulate genes encoding pro-apoptotic proteins, such as Bid and AIF, and therefore to examine involvement of these factors in glutamate-induced neuronal apoptosis.

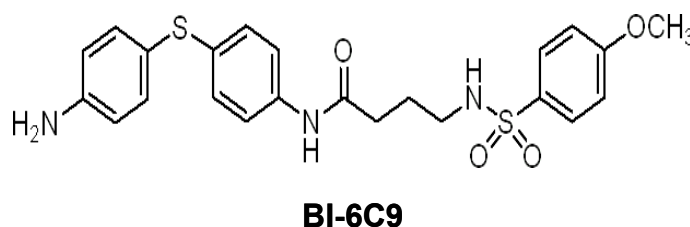


Figure 4: Bid inhibitor BI-6C9.

1.6 Aims of the thesis

A major aim of this work was to describe the involvement of AIF and thus caspase-independent mechanisms in glutamate-induced neuronal cell death. In addition, it was of interest which proteins and events were involved upstream the release of AIF from mitochondria. An understanding of the exact mechanisms, which execute apoptosis in neurons after glutamate treatment, may provide important information for the development of efficient therapeutic strategies against neurodegenerative diseases.

1. It was an aim to describe the role of Bid in glutamate-induced apoptosis of neuronal cells. Mechanisms which are involved in the activation of Bid were investigated as well as downstream pathways that mediate the execution of Bid-dependent apoptosis after glutamate damage in neurons.

2. In order to differentiate between caspase-dependent and caspase-independent mechanisms downstream of mitochondrial damage during glutamate toxicity the particular roles of AIF and caspases were addressed.

3. The findings obtained in the model of glutamate-induced apoptosis in HT-22 neurons were verified in model systems of primary neurons with relevance to stroke, brain trauma and Alzheimer's disease.

2 Materials and methods

2.1 Chemicals and reagents

All standard chemicals were obtained from Sigma-Aldrich (Taufkirchen, Germany) and Merck (Darmstadt, Germany), if not described otherwise.

2.1.1 Recombinant proteins

Human recombinant caspase-8, caspase-1 (ICE) and Omi/HtrA2 (each Merck, Darmstadt, Germany) were incubated separately or together for 5-20 minutes at 37°C with 50 µg protein of HT-22 neuron cell lysate at a final concentration of 100 U / 40 µl or 1-10 µg / 40 µl, respectively. Volumes were adjusted with 50 mM HEPES buffer (Biomol, Hamburg, Germany).

2.1.2 Caspase substrates

Fluorogenic substrates of caspase-1 (Z-YVAD-AFC, Merck, Darmstadt, Germany), caspase-3 (Ac-DEVD-AMC, Sigma-Aldrich, Taufkirchen, Germany) and caspase-8 (Ac-IETD-AMC, Sigma-Aldrich, Taufkirchen, Germany) were used for caspase activity measurements at final concentrations of 50 µM in 20 µl of HT-22 neuron cell lysate.

2.1.3 Inducers and inhibitors of apoptosis

Bid inhibitor BI-6C9 (kindly provided by Maurizio Pellecchia, The Burnham Institute, La Jolla, California, USA, and from Sigma-Aldrich, Taufkirchen, Germany) was dissolved in dimethyl sulfoxide (DMSO) to a stock concentration of 20 mM. It was used at a final concentration of 10 µM in Dulbecco's modified eagle medium (DMEM; Biochrom, Berlin, Germany) for HT-22 neurons. Bid inhibitor BI-11A7 (kindly provided by Maurizio Pellecchia) was dissolved in DMSO to a stock concentration of 20 mM. It was used at a final concentration of 2 µM in Earle's balanced salt solution (EBSS, Biochrom, Berlin, Germany) for primary rat neurons. Bax channel blocker (Tocris, Ellisville, Missouri, USA) was dissolved in DMSO to a stock concentration of 20 mM

and used at final concentration of 0.1-10 μM . Omi/HtrA2 inhibitor UCF-101 (Merck, Darmstadt, Germany) was dissolved in DMSO to a stock concentration of 20 mM. It was used at final concentrations of 10 μM and 20 μM in DMEM for HT-22 neurons. Glutamate (Sigma-Aldrich, Taufkirchen, Germany) was dissolved to a stock concentration of 200 mM in EBSS. The pH was adjusted to 7.2 with concentrated sodium hydroxide solution (NaOH). It was used at final concentrations from 1 mM to 5 mM in DMEM for HT-22 neurons and at a final concentration of 20 μM in EBSS for primary rat neurons. Staurosporine (STS, Sigma-Aldrich, Taufkirchen, Germany) was dissolved in DMSO to a stock concentration of 100 μM . It was used at a final concentration of 100-300 nM in DMEM for HT-22 neurons and EBSS for primary rat neurons. Caspase-1 inhibitor II (ICE inhibitor, Merck, Darmstadt, Germany) was dissolved in DMSO to a stock concentration of 9.24 mM. It was used at final concentrations of 1-50 μM in DMEM for HT-22 neurons. Caspase-2 inhibitor I (Z-VAD-FMK, Merck, Darmstadt, Germany) was dissolved in DMSO to a stock concentration of 10 mM. It was used at final concentrations of 5-50 μM in DMEM for HT-22 neurons. General caspase inhibitor (Z-VAD-FMK, R&D Systems, Wiesbaden, Germany) was dissolved in DMSO to a stock concentration of 2 mM. It was used at final concentrations of 10-100 μM in DMEM for HT-22 neurons. P38 MAPK inhibitor SB 203580 (Tocris, Ellisville, Missouri, USA) was dissolved in DMSO to a stock concentration of 20 mM. It was used at final concentrations of 5-20 μM . poly(ADP-ribose) polymerase (PARP) inhibitor (PJ34, Merck, Darmstadt, Germany) was dissolved in aqua dest. to a stock concentration of 20 mM and was used at final concentrations of 10 μM . Calpastatin Exon 1B-Derived Peptide was synthesized by Genzentrum (München, Germany) and the activated penetratin 1 was purchased from Qbiogene (Morgan Irvine, California, USA). The activated penetratin (100 μM in H_2O) was coupled onto the calpastatin exon 1B-derived peptide (100 μM in H_2O) by adding an equimolar amount of calpastatin and activated penetratin, and incubated for 2 hours at room temperature (RT). The conjugated peptide (50 μM) functioned as calpain inhibitor [84] and was used at final concentrations of 0.5 μM to 2 μM . Cathepsin inhibitor (E-64-d, Biomol, Hamburg, Germany) was dissolved in DMSO to

a stock concentration of 20 mM and was used at final concentrations of 1-50 μ M in DMEM for HT-22 neurons.

2.1.4 Transfection reagents

Opti-MEM I (Invitrogen, Karlsruhe, Germany) was used to form DNA- or siRNA transfection complexes. Lipofectamine 2000 (Invitrogen, Karlsruhe, Germany) was used at a final concentration of 1.5 μ l/ml in antibiotic free DMEM or in antibiotic and B27-free Neurobasal medium (NB) to complex DNA plasmids or siRNA.

2.1.4.1 Plasmid vectors

The mouse AIF-GFP vector (mAIF_pd2EGFP-N1) was derived from a pd2pEGFP-N1 vector (Clontech, Palo Alto, California, USA) and an AIF expressing vector (pcDNA3.1_mAIF, kind gift of S. Susin, CNRS, Paris, France). The mAIF insert was cut out from the pcDNA3.1_mAIF with *EcoRI*, the stop codon was removed by mutagenesis from tga to tCga and then fused to the d2EGFP construct. The resulting vector expresses EGFP fused to the C-terminus of mouse AIF that is located in mitochondria and allows analysis of AIF-GFP translocation to the nucleus in apoptotic cells. The construct was provided by Gerlinde Schwake. ptBid-plasmid was generated as described [85]. Plasmids pEGFP-N1 and pEGFP-Luc were purchased from Clontech Laboratories (Palo Alto, California, USA). Plasmid pgWIZ-GFP was derived from Gene Therapy Systems (San Diego, California, USA) and plasmid pCDNA 3.1+ used as a control vector was obtained from Invitrogen (Karlsruhe, Germany). The ApoAlert[®] pDsRed2-Bid Vector which encodes a biologically active fluorescent fusion protein of Bid and DsRed monomer was derived from Clontech (Palo Alto, California, USA). All the plasmids were amplified using a Quiafilter Giga Kit (Qiagen, Hilden, Germany) according to the manufacturer's protocol. Prior to use, their DNA concentrations were determined in a Biophotometer (Eppendorf, Hamburg, Germany) and digestion by restriction enzymes with subsequent gel electrophoresis analysis was performed. These steps were performed by Melinda Kiss.

2.1.4.2 *siRNA*

AIF-siRNA (5'-AAG AGA AAC AGA GAA GAG CCA-3'), non functional control siRNA (mut-siRNA. 5'-AAG AGA AAA AGC GAA GAG CCA-3') and Parg-siRNA (5'- AAA TGG GAC TTT ACA GCT TTG -3', [86]) were purchased at MWG Biotech (Ebersberg, Germany) or AIF and Bid siRNA mixtures were generated using recombinant dicer enzyme kit following the instructions of the manufacturer (Gene Therapy Systems, San Diego, California, USA). The following steps were performed by Miriam Hoehn. An AIF (750bp) or Bid copy DNA (cDNA; 521bp) template for T7-RNA polymerase in vitro transcription was generated from mouse (for Bid) or rat (for AIF) mRNA by reverse transcription polymerase chain reaction [RT-PCR; initial denaturation at 95°C for 2 min; 28-30 cycles of 30 s 95°C, 1 min 57°C (AIF) or 60°C (Bid), and 2 min 72°C; final extension at 70°C for 10 min] using the following AIF primers: forward, 5'-GCG TAA TAC GAC TCA CTA TAG GGA GAT CCA GGC AAC TTG TTC CAGC-3', and reverse, 5'-GCG TAA TACGAC TCA CTA TAG GGA GAC CTC TGC TCC AGC CCT ATC G-3'. Following Bid primers were used: forward, 5'-GCG TAA TAC GAC TCA CTA TAG GGA GAT GGG CTT CTG TCT AAG GAGA-3', and reverse, 5'-GCG TAA TAC GAC TCA CTA TAG GGA GAA GTG AGG CCT TGT CTC TGAA-3'. In vitro transcription was performed with the cDNA template by using the TurboScript-T7-Transcription kit (Gene Therapy Systems, San Diego, California, USA). The resulting double-stranded RNA (dsRNA) template was purified by lithium chloride (LiCl) precipitation. Briefly, 30 µl of LiCl solution and 30 µl Nuclease-free water were added to the dsRNA template. Mixture was chilled for at least 30 minutes at -20°C. Afterwards, it was centrifuged for 15 minutes at maximum speed and unincorporated nucleotides were removed by adding 1 ml 70% ethanol. After removing the ethanol, the mixture was exposed to the recombinant Dicer enzyme at 37°C for 16 h overnight, and the siRNA fragments were again purified on the RNA Purification Columns 1 (removing salts and unincorporated nucleotides) and 2 (removing undigested dsRNA) (Gene Therapy Systems, San Diego, California, USA). The amount of the purified siRNA was determined in a Biophotometer (Eppendorf, Hamburg, Germany) and siRNA was used in concentrations of 10-20 nM.

2.1.5 Primary antibodies

All primary antibodies were diluted in Tris-buffered saline with Tween 20 (TBST). The dilution of the Bid-antibody (Cell signaling, Danvers, Massachusetts, USA) was 1:1,000, of AIF-Antibody (Santa Cruz, Santa Cruz, California, USA) 1:500. α -Tubulin-antibody (Sigma-Aldrich, Taufkirchen, Germany) was diluted 1:20,000, p38-MAP-kinase-Antibody (Cellsignaling, Danvers, Massachusetts, USA) was diluted 1:2,000. Cleaved-Lamin-A-antibody (Cell signaling, Danvers, Massachusetts, USA) was used in a dilution of 1:1,000 and Lamin-A/C-antibody (Cell signaling, Danvers, Massachusetts, USA) was used 1:1,000 diluted.

2.1.6 Secondary antibodies

All secondary antibodies were purchased from Vector Labs (Burlingame, California, USA). Horse reddish peroxidase (HRP) labeled Anti-mouse IgG (H+L), Anti-goat IgG (H+L) and Anti-rabbit IgG (H+L) for western blot were used in 1:2,000 - 1:5,000 dilutions in TBST. The biotinylated Anti-goat IgG (H+L) for immunocytochemistry was used in a 1:200 dilution in phosphate-buffered saline (PBS) containing 3% horse-serum (Invitrogen, Karlsruhe, Germany).

2.2 Cell biological methods

Sterile plastic materials for the cell culture were purchased from TPP (T75 flasks, 96-well plates; Trasadingen, Switzerland), from Nunc (24- and 6-well plates; Wiesbaden, Germany) and Becton-Dickinson (35-mm, 60-mm Falcon culture dishes; BD, Wiesbaden, Germany).

2.2.1 Cell culture and induction of apoptosis

Cell culture media Dulbecco's modified eagle medium 4.5 g/l glucose (DMEM) and Earle's balanced salt solution (EBSS) were obtained from Biochrom (Berlin, Germany). DMEM was supplemented with 10% heat-inactivated fetal calf serum (FCS, Invitrogen, Karlsruhe, Germany), 8 ml/l L-alanyl-L-glutamine 200 mM stock solution (Biochrom, Berlin, Germany), 5 ml sodium pyruvate 100 mM stock solution (Biochrom, Berlin, Germany) and 5 ml Penicillin/Streptomycin 1000 U/ml (Biochrom,

Berlin, Germany) for culturing HT-22 neurons. Neurobasal Plus (NB+) contained 500 ml Neurobasal (Invitrogen, Karlsruhe, Germany) supplemented with 10 ml B27 supplement (Invitrogen, Karlsruhe, Germany), 1.145 g 4-(2-Hydroxyethyl)piperazine-1-ethanesulfonic acid (HEPES, Biomol, Hamburg, Germany), 0.176 g L-glutamine (Sigma-Aldrich, Taufkirchen, Germany) and 25 mg gentamicin sulfate (Sigma-Aldrich, Taufkirchen, Germany) for primary rat neurons. MEM+ was obtained from Eagle's minimum essential medium (Invitrogen, Karlsruhe, Germany) by addition of 1 mM HEPES (Biomol, Hamburg, Germany), 26 mM NaHCO₃, 40 mM glucose, 20 mM KCl, 1.2 mM L-glutamine (each Sigma-Aldrich, Taufkirchen, Germany), 1 mM sodium pyruvate (Biochrom, Berlin, Germany), 10% (v/v) FCS (Invitrogen, Karlsruhe, Germany) and 10 mg/l gentamicin sulfate (Sigma-Aldrich, Taufkirchen, Germany) for seeding primary rat hippocampal neurons. Hank's balanced salt solution (HBSS) was made from 100ml 10x HBSS (Invitrogen, Karlsruhe, Germany), aqua dest. (Millipore) 800 ml, 2.4g HEPES (Biomol, Hamburg, Germany) and 10 mg gentamicin sulfate (Sigma-Aldrich, Taufkirchen, Germany). All cells were grown at 37°C in 5% CO₂ humidified atmosphere, provided by a Hera Cell incubator (Kendro Laboratory Products GmbH, Hanau, Germany).

2.2.1.1 HT-22 neurons

HT-22 neurons were obtained from Gerald Thiel with kind permission by David Schubert (Salk Institute, San Diego, California, USA). The HT-22 line was originally selected from HT-4 cells based on glutamate sensitivity. HT-4 cells were immortalized from primary hippocampal neurons using a temperature-sensitive SV-40 T antigen [87]. They were cultured in T75 flasks and splitted 1:10 - 1:20 every 3-4 days. This was performed as follows: Growth medium was replaced by 2 ml PBS containing 0.05% trypsin and 0.02% ethylenediaminetetraacetic acid disodium salt (EDTA) (1x TE, Invitrogen, Karlsruhe, Germany). Afterwards, cells were incubated 2-5 min at 37°C. After detaching of the cells, trypsin was inhibited by addition of serum containing growth medium. The cells were centrifuged at 179 x g; the cell pellet was resuspended in fresh growth medium. Then cells were seeded in 6-well plates with a density of 4×10^5 cells / well, in 24-well plates with a density of 8×10^4 / well or in 96-

well plates with a density of 8×10^3 / well for further treatment. Induction of apoptosis was performed 24 h after seeding the cells. Growth medium was removed and replaced by medium containing inhibitors of apoptosis. After 1 h preincubation, glutamate or STS were added to final concentrations of 1-5 mM or 100-300 nM, respectively. Between 0.5 h and 18 h later, cells were analyzed following standard procedures for flow cytometry, epifluorescence microscopy, protein or RNA analysis. To harvest cells for flow cytometry, epifluorescence microscopy or protein analysis, 200 μ l of 1x TE was used per well for a 24 well plate.

2.2.1.2 Primary rat neurons

Embryonic hippocampal cultures: Hippocampi were removed from embryonic day 18 Sprague-Dawley rats (Charles River Laboratories, Sulzfeld, Germany) and dissociated by mild trypsinization and trituration as followed: Isolated hippocampi were incubated for 10 min in a solution of 1 mg/ml trypsin (Sigma, Taufkirchen, Germany) on Ca^{2+} -and Mg^{2+} -free HBSS. The hippocampi were then rinsed with fresh HBSS, exposed for 2 min 1 mg/ml trypsin inhibitor (Sigma, Taufkirchen, Germany), and then washed with HBSS. Cells were mechanically dissociated by trituration and were then seeded onto 35-mm polyethylenimine-coated culture dishes (for survival analysis), 35-mm culture dishes containing glass coverslips (for immunocytochemistry), or 60-mm culture dishes (for immunoblot analysis) containing 1 ml or 2 ml MEM+, respectively. After 4 h incubation, the medium was replaced with NB+. Medium was exchanged after 5 days in culture. Since cultures of primary neurons develop functional glutamate receptors after 8 days in culture, experimental treatments were performed with 9- to 10-day old cultures in EBSS. Apoptosis was induced by glutamate (20 μ M) in EBSS and quantified 6 - 24 h later.

2.2.2 Cell viability assays and mitochondrial staining

For cell viability assays HT-22 neurons were grown in 96-well plates. Primary rat hippocampal neurons were grown in 35 mm dishes. For Annexin-V and JC-1 assay, HT-22 neurons were cultured in 24-well plates. MitoTracker Green staining was

performed in cells cultured on Collagen A-coated Ibitreat μ -slide 8-well plates (Ibidi, München, Germany) immediately before confocal microscopic analysis.

2.2.2.1 *MTT-assay*

Metabolic activity of HT-22 neurons was determined by using a 3-(4,5-Dimethylthiazol-2-yl)-2,5-diphenyltetrazolium bromide (MTT) reduction assay in 96-well plates: To each well 10 μ l of a 5 mg/ml MTT solution (Sigma-Aldrich, Taufkirchen, Germany) in sterile PBS buffer were added. Cells were incubated at 37°C for 1.5 h, medium was removed and the samples were frozen at -80°C for at least 1 h. Afterwards 100 μ l of DMSO were added and samples were incubated at 37°C for 30 min under constant shaking. Absorbance was measured at 590 nm (reference wavelength 630 nm) using a microplate reader (Spectrafluor Plus, Tecan Austria GmbH, Grödig, Austria), and cell viability levels were expressed as percentage of absorption levels in untreated control cells (100% viability).

2.2.2.2 *DAPI/Hoechst 33342 staining*

Cultured primary neurons were stained in 35 mm-dishes with the fluorescent DNA-binding dye 4', 6-diamidino-2-phenylindole dihydrochloride (DAPI) or Hoechst 33342, respectively. After removing the medium, cells were fixed in 1 ml of a PBS solution containing 4% paraformaldehyde (PFA). Cells were then exposed to 1 μ g/ml of the respective staining dye in PBS. Cells were washed twice with PBS and kept in 1 ml PBS. Stained nuclei were visualized under epifluorescence illumination at an excitation wavelength of 365 nm and an emission detected through a 420 nm longpass filter (Filter set 02, Carl Zeiss, Jena, Germany) using an Axiovert 200 microscope (Carl Zeiss, Jena, Germany) with a 20x 0.40 NA objective (Carl Zeiss, Jena, Germany). Neurons with condensed and fragmented nuclei were considered apoptotic, whereas healthy neurons exhibited low staining intensity and the staining was evenly distributed over the nuclei.

2.2.2.3 *Annexin-V-FITC staining*

Apoptotic cells were detected after labeling with annexin-V and subsequent flow cytometry. Annexin-V binds in the presence of calcium to phosphatidylserine, which appears on the cell surface in early phases of apoptosis [88]. HT-22 neurons were harvested 17-20 h after glutamate- or STS-treatment by using trypsin/EDTA, washed once in PBS and resuspended in 1x annexin-V binding buffer (Sigma-Aldrich, Taufkirchen, Germany) at a concentration of approximately 1.6×10^5 cells / 500 μ l. The DNA stain propidium iodide (PI, Sigma-Aldrich, Taufkirchen, Germany) and annexin V-FITC (Sigma-Aldrich, Taufkirchen, Germany) were added at 1 μ g/ml each and incubated for 10 min at RT. Apoptotic and necrotic cells were determined using a Cyan™ MLE flow cytometer (DakoCytomation, Copenhagen, Denmark). Annexin V-FITC fluorescence was excited at a wavelength of 488 nm and emission was detected using a 530 \pm 40 nm bandpass filter. Propidium iodide fluorescence was excited at a wavelength of 488 nm and emission was detected using a 680 \pm 30 nm bandpass filter. To exclude cell debris and doublets, cells were appropriately gated by forward versus side scatter and pulse width, and 1×10^4 gated events per sample were collected. Cells which are at an early stage of apoptosis were stained with annexin-V alone. Living cells did not show any staining. Necrotic cells were stained by both, annexin-V and propidium iodide.

2.2.2.4 *JC-1-assay (Mitochondrial function)*

Mitochondrial membrane potential of HT-22 neurons was determined by 5, 5', 6, 6'-tetrachloro-1, 1', 3, 3'-tetraethylbenzimidazolylcarbocyanine iodide (JC-1) reduction. HT-22 neurons were stained with JC-1 (Mitoprobe, Invitrogen, Karlsruhe, Germany) according to the manufacturer's protocol and analyzed by subsequent flow cytometry or epifluorescence microscopy. After glutamate treatment (6-12 hours), JC-1 was added to each well of each condition at a final concentration of 2 μ M. Living-control cells were left untreated and damage-control cells were treated with carbonyl cyanide m-chlorophenylhydrazone (CCCP) 5 minutes before staining to induce mitochondrial membrane depolarization. Supernatants of each condition were collected (to avoid the loss of detached cells) and cells harvested using 1x TE. After detaching of the

HT-22 neurons TE reaction was stopped by adding 800 μ l serum-containing medium to each well. Cells were resuspended and transferred to their respective supernatant. Cells were centrifuged at 179 x g, supernatants were removed, pellet washed once in PBS, resuspended in 700 μ l PBS and kept on ice. Mitochondrial membrane potential was determined using a Cyan™ MLE flow cytometer (DakoCytomation, Copenhagen, Denmark). JC-1 green fluorescence was excited at 488 nm and emission was detected using a 530 \pm 40 nm bandpass filter. JC-1 red fluorescence was excited at 488 nm and emission was detected using a 613 \pm 20 nm bandpass filter. To exclude cell debris and doublets, cells were appropriately gated by forward versus side scatter and pulse width, and 1 x 10⁴ gated events per sample were collected. All mitochondria get loaded by JC-1 dye which leads to a green fluorescence. Living cells with intact mitochondria are able to reduce JC-1 and produce an additional red fluorescence.

2.2.2.5 *MitoTracker Green staining (Mitochondrial visualization)*

To 50 μ g MitoTracker Green (Invitrogen, Karlsruhe, Germany) 74.4 μ l DMSO were added. The resulting 1 mM solution was diluted 1:10,000 in DMEM and 300 μ l were added to HT-22 neurons after their respective treatment in Collagen A-coated Ibitreat μ -slide 8 well plates. Cells were incubated for 15 minutes at 37°C with the staining medium. Afterwards, the staining medium was replaced with DMEM and mitochondria were visualized using a confocal laser scanning microscope at an excitation wavelength of 488 nm (Carl Zeiss, Jena, Germany). Light was collected through a 100 x 1.3 NA oil immersion objective. MitoTracker Green fluorescence was excited at a wavelength of 488 nm and emission was detected using a 560 nm longpass filter.

2.2.3 **Transmission light and epifluorescence microscopy**

Transmission light microscopy of living HT-22 neurons was performed using an Axiovert 200 microscope (Carl Zeiss, Jena, Germany) equipped with a Sony DSC-S75 digital camera (Sony Corporation, Tokyo, Japan). Light was collected through 5 x 0.12 NA, 10 x 0.25 NA or 32 x 0.40 NA objectives (Carl Zeiss, Jena, Germany), and

images were captured using phase contrast. Imaging of JC-1-stained HT-22 neurons or DAPI-stained primary rat hippocampal neurons was performed using an Axiovert 200 fluorescence microscope, equipped with a Zeiss Axiocam camera (Carl Zeiss, Jena, Germany). JC-1 green fluorescence was excited using a 470 ± 20 nm bandpass filter, and emission was collected using a 540 ± 25 nm bandpass filter (Filter set 10, Carl Zeiss, Jena, Germany). JC-1 red fluorescence was excited using a 557.5 ± 27.5 nm bandpass filter, and fluorescence emission was collected using a 615 nm longpass filter (Filter set 00, Carl Zeiss, Jena, Germany). DAPI fluorescence was excited using a G 365 nm bandpass filter, and emission was collected using a 420 nm longpass filter (Filter set 02, Carl Zeiss, Jena, Germany). For digital imaging the software LSM 510 3.20 SP2 (Carl Zeiss, Jena, Germany) was used.

2.2.4 Transfection protocols

HT-22 neurons were transfected in 24 well plates, 24 hours after seeding at a density of 8×10^4 cells per well. Antibiotic containing growth medium was replaced by 900 μ l antibiotic free DMEM per well. Six days old primary rat hippocampal neurons were transfected in 35 mm culture dishes at a density of 3.5×10^5 cells per dish. NB+ was replaced by 900 μ l NB without B27 supplement and antibiotics.

2.2.4.1 DNA-transfections

Lipofectamine 2000 (Invitrogen, Karlsruhe, Germany) and the respective DNA plasmids were dissolved separately in Opti-MEM I (Invitrogen, Karlsruhe, Germany). After 10 min of equilibration at room temperature each DNA solution was combined with the respective volume of the Lipofectamine solution, mixed gently, and allowed to form plasmid liposomes for further 20 min at room temperature. The transfection mixture was added to the antibiotic-free cell culture medium to a final concentration of 1 μ g DNA and 1.5 μ l/ml Lipofectamine 2000 in HT-22 neurons. Controls were treated with 100 μ l/ml Opti-MEM I only, and vehicle controls with 1.5 μ l/ml Lipofectamine 2000. Cells were transfected for at least 24 h, before further treatment.

2.2.4.2 *Flow cytometric analysis of DNA transfection efficiency in HT-22 neurons*

To determine transfection efficiency, HT-22 were transfected with different EGFP-encoding plasmids, i.e. pEGFP-N1, pEGFP-Luc and pgWIZ-GFP, followed by analysis of the relative percent of transfected to non-transfected cells. Twenty-four hours after transfection with the plasmids, cells were harvested after 1x TE-exposure and kept on ice. The number of EGFP-positive cells was quantified using a Cyan MLE flow cytometer (DakoCytomation, Copenhagen, Denmark). Fluorescence of EGFP was excited at a wavelength of 488 nm and emission was detected using a 530±40 nm bandpass filter. To exclude cell debris and doublets, cells were appropriately gated by forward versus side scatter and pulse width, and 1 x 10⁴ gated events per sample were collected.

2.2.4.3 *siRNA-transfections*

For siRNA transfections, Lipofectamine 2000 (Invitrogen, Karlsruhe, Germany) and AIF-siRNA, Bid-siRNA, Parg-siRNA, or non-functional mut-siRNA were dissolved separately in Opti-MEM I (Invitrogen, Karlsruhe, Germany). After 10 min of equilibration at RT, each siRNA solution was combined with the respective volume of the Lipofectamine 2000 solution, mixed gently, and allowed to form siRNA liposome complexes for further 20 min at room temperature. The transfection mixture was added to the antibiotic-free cell culture medium to a final concentration of 10-20 nM (dicer products) and up to 80 nM siRNA (single siRNA sequences), and 1.5 µl/ml or 2µl/mL Lipofectamine in HT-22 neurons. Controls were treated with 100 µl/ml Opti-MEM I only, and vehicle controls with 1.5-2 µl/ml Lipofectamine 2000.

2.2.5 Immunocytochemistry and confocal laser scanning microscopy (CLSM)

For immunocytochemistry primary rat hippocampal neurons cultured on PEI-coated 35 mm culture dishes containing glasscoverslips were fixed with 4% PFA after their respective treatment. Culture medium was removed and cells were washed once with PBS. Afterwards, cells were fixed in 1 ml 4% paraformaldehyde for 20 minutes, washed 1x in PBS and then membranes were permeabilized by exposure for 5 min to 0.4% Triton X-100 (Sigma-Aldrich, Taufkirchen, Germany) in PBS, and cells were

placed in blocking solution [3% horse serum (Invitrogen, Karlsruhe, Germany) in PBS] for 30 min. Cells were then exposed to a polyclonal anti-AIF antibody (1:100 in block solution, Santa Cruz Biotechnology, Santa Cruz, California, USA), overnight at 4°C and subsequent 2.5 h at room temperature, followed by an incubation for 1 h with biotinylated anti-goat IgG antibody (1:200, Vector Labs, Burlingame, CA, USA) and 30 minutes in the presence of streptavidin oregon green 514 conjugate (Invitrogen, Karlsruhe, Germany) according to the manufacturers protocol. The specificity of AIF immunoreactivity was controlled by omission of the primary antibody. Nuclei were counterstained with DAPI as described above. Images were acquired using a confocal laser scanning microscope (LSM 510, Carl Zeiss, Jena, Germany) equipped with an UV and an argon laser delivering light at 364 nm and 488 nm, respectively. Light was collected through a 63 x 1.4 NA oil immersion objective. DAPI fluorescence was excited at 364 nm and emission was achieved by using the 385 nm longpass filter. Fluorescence of oregon green was excited at a wavelength of 488 nm and emission was detected using a 505 nm longpass filter. For digital imaging, the software LSM 510 3.20 SP2 (Carl Zeiss, Jena, Germany) was used.

2.2.6 Confocal laser scanning microscopy of HT-22 neurons

For detection of AIF or Bid localization during apoptosis, HT-22 neurons were transfected with the mAIF_pd2EGFP-N1 or the pDsRed2-Bid plasmid, respectively. Twenty four hours after transfection HT-22 neurons were seeded in collagen A-coated Ibitreat μ -slide 8-well plates (Ibidi, München, Germany) at a density of 1×10^4 / well for endpoint analysis or, for time lapse pictures in a microscope-attached CO₂-chamber at the LSM 510, Zeiss, Germany) onto a round glasscoverslip (H. Saur, Reutlingen, Germany) with a diameter of 42 mm and a thickness of 0.17 mm. Mitochondria were stained with MitoTracker Green (Invitrogen, Karlsruhe, Germany) as described above. Endpoint pictures were taken after fixation with 4% PFA and DAPI counterstaining of the nuclei between 5 h to 17 h after onset of treatment. Images were acquired using a confocal laser scanning microscope (LSM 510, Carl Zeiss, Jena, Germany) equipped with an UV, an argon and a Helium/Neon laser,

delivering light at 364 nm, 488 nm and 543 nm respectively. Light was collected through a 40 x 1.3 NA, 63 x 1.4 NA or 100 x 1.3 NA oil immersion objectives. DAPI fluorescence was excited at 364 nm and emission was achieved by using the 385 nm longpass filter. Fluorescences of MitoTracker Green or AIF-GFP and DsRed were excited at 488 nm and 543 nm and emissions were observed using 505-530 nm bandpass (green) and 560 nm longpass filters (red), respectively. For real time confocal microscopy the CO₂-chamber was adjusted to 37°C, 5% CO₂ and a humidified atmosphere. Images were acquired every five minutes up to 17 hours after onset of treatments with the same laser settings as for 'endpoint pictures'. They were exported to a movie file, using the software LSM 510 3.20 SP2 (Carl Zeiss, Jena, Germany).

2.3 Protein analysis

For protein extraction and subsequent analysis, HT-22 neurons were grown at a density of 8×10^4 cells per well in 24-well plates (western blot) or 4×10^5 cells per well in 6-well plates (caspase activity assays). Primary rat neurons were cultured in PEI-coated 60 mm culture dishes at 1 density of 1.5×10^6 cells per dish.

2.3.1 Protein sample preparation from HT-22 neurons and from primary rat neurons

For western blot analysis, HT-22 neurons were harvested as described using 1x TE solution to detach cells. At least 4 wells per condition were pooled. Cells were washed in PBS and lysed with 50-150 μ l 1:5 diluted cell lysis reagent 5x (Promega, Mannheim, Germany), supplemented with 1 tablet /10 ml Complete Mini protease inhibitor cocktail (Roche, Mannheim, Germany), containing a cocktail of several reversible and irreversible protease inhibitors. Protein extracts were kept on ice for 15 minutes and then extracts were centrifuged at 15,000 x g for 15 minutes at 4°C to remove insoluble membrane fragments. The supernatants were stored at -80°C until further use. For nuclear and cytosolic protein extracts, HT-22 neurons were harvested using 1x TE solution. The resulting cell pellets were fractionated using the Nuclear Extract Kit (Active Motif, Rixensart, Belgium) according to the manufacturer's

instructions. Briefly, the pellet was dissolved in hypotonic buffer and incubated for 15 minutes on ice. The suspension was centrifuged at 15,000 x g at 4°C. Supernatant (cytosolic extract) was stored at -80°C. The pellet containing the nuclei was incubated in lysis buffer (Active Motif, Rixensart, Belgium) and stored at -80°C. For caspase activity assays, 6-well plates were put on ice and incubated for 15 min. Medium was removed and cells were washed once with 3 ml ice cold PBS. 150 µl lysis buffer (5 mM MgCl₂, 1 mM EGTA, 0.1% Triton X-100, 25 mM HEPES in 50 ml aqua dest.) were added to the first well. Cells were harvested using a cell scraper (Sarstedt, Newton, North Carolina, USA). The lysate was then transferred into the next well of the same condition and cells were scraped. At least 3 wells of each condition were pooled. Lysates were transferred to an Eppendorf tube and homogenated by 10 strokes through a 20-gauge needle. Insoluble membrane fragments were separated by centrifuging at 15,000 x g for 15 minutes at 4°C. Pellets were discarded, and supernatants were stored at -80°C.

To achieve full protein extract of primary rat neurons, cells were scraped as described above for HT-22 in PBS containing 1 tablet Complete Mini protease inhibitor cocktail (Roche, Mannheim, Germany) per 10 ml and centrifuged at 64 x g for 15 min at 4°C. The pellet was washed once in PBS and was resuspended in 50-150 µl cell lysis reagent (Promega, Mannheim, Germany), supplemented with Complete Mini protease inhibitor cocktail (Roche, Mannheim, Germany). Protein extracts were kept on ice for 15 minutes. To remove insoluble membrane fragments, extracts were centrifuged at 15,000 x g for 15 minutes at 4°C and supernatants were stored at -80°C.

2.3.2 Determination of protein amount

Protein amounts in extracts were determined with the Pierce BCA kit (Perbio Science, Bonn, Germany). To this end, 5 µl of each sample were diluted in 95 µl PBS. A standard curve containing 0-100 µg bovine serum albumin (Perbio science, Bonn, Germany) per 100 µl, 5 µl of the respective lysis buffer and PBS ad 100 µl was prepared. Then, 500 µl of a 1 : 50 mixture of reagent B : reagent A (Perbio Science, Bonn, Germany) was added to each sample. Samples were incubated for 30 minutes

at 60°C; 150 µl of each sample were pipetted into a 96-well plate (Nunc, Wiesbaden, Germany). Absorption at 590 nm was determined using a SpectrafluorPlus plate reader (Tecan, Grödig, Austria) and protein amounts of the test samples were calculated from the standard curve.

2.3.3 Polyacrylamid gel electrophoresis and western blot

For gel electrophoresis and western blot analysis, the following solutions were used: 0.5 M Tris [7.88 g Tris-HCl (Sigma-Aldrich, Taufkirchen, Germany) in 100 ml Millipore water, adjusted to pH 6.8 by concentrated HCl], 1.5 M Tris [23.6 g Tris-HCl (Sigma-Aldrich, Taufkirchen, Germany) in 100 ml Millipore water, adjusted to pH 8.8 by concentrated HCl], 10% APS [Ammoniumpersulfat (Sigma-Aldrich, Taufkirchen, Germany) 1 g in 10 ml Millipore water], N,N,N',N'-Tetramethylethylenediamine (TEMED, Promega, Mannheim, Germany), sodium dodecyl sulfate 10% (SDS, Roth, Karlsruhe, Germany) 10 g in 100 ml Millipore water], electrophoresis buffer [3.0 g trizma base (Sigma-Aldrich, Taufkirchen, Germany), 14.4 g glycine (Roth, Karlsruhe, Germany) and 1 g SDS (Roth, Karlsruhe, Germany) in 1000 ml Millipore water], transfer buffer [3.0 g trizma base (Sigma-Aldrich, Taufkirchen, Germany), 14.4 g glycine (Roth, Karlsruhe, Germany), 100 ml methanol p.a. ad 1000 ml Millipore water], TBST [2.42 g trizma base (Sigma-Aldrich, Taufkirchen, Germany), 29.2 g sodium chloride (Sigma-Aldrich, Taufkirchen, Germany), 0.5 ml Tween 20 (Roth, Karlsruhe, Germany) ad 1000 ml Millipore water], loading buffer [7 ml 1M Tris-HCl pH 6,8, 3 ml glycerol (Sigma-Aldrich, Taufkirchen, Germany), 1 g SDS (Roth, Karlsruhe, Germany), 0.93 g DTT (D,L-dithiotreitol, Sigma-Aldrich, Taufkirchen, Germany), 100 µl β-mercaptoethanol (Merck, Darmstadt, Germany), 1.2 mg bromophenol blue sodium salt (Sigma-Aldrich, Taufkirchen, Germany), 5 g blocking buffer [non-fatty milk powder (Töpfer, Dietmannsried, Germany) in 100 ml TBST] and strip buffer [3.84 g trizma base (Sigma-Aldrich, Taufkirchen, Germany), 10.0 g SDS (Roth, Karlsruhe, Germany) in 500 ml Millipore water, adjusted to pH 6.7 by concentrated HCl; β-mercaptoethanol (Merck, Darmstadt, Germany) was added immediately before use (78 µl in 10 ml strip buffer)]. Discontinuous polyacrylamid gels (resolving gel 10% or 15% polyacrylamid, stacking gel 3.5% polyacrylamid) were cast using the Mini-

Protean 3 cell with 1.5 mm spacer and 10-pocket combs (Bio-RAD, München, Germany). Resolving gels contained following components: 2.5 ml 1.5 M Tris, 0.1 ml SDS 10%, 3.34 ml (10%) or 5 ml (15%) 30% Acrylamid/Bis solution 29:1 (Bio-Rad, München, Germany), 0.05 ml 10% APS, 0.01 ml TEMED and Millipore water ad 10 ml. Stacking gels were prepared with 2.5 ml 0.5 M Tris, 0.1 ml SDS 10%, 1.2 ml (3.5%) 30% Acrylamid/Bis solution 29:1 (Bio-Rad, München, Germany), 0.05 ml 10% APS, 0.01 ml TEMED and Millipore water ad 10 ml. An amount of 50 µg protein of each sample was filled up to 40 µl with RNase-free water (Sigma-Aldrich, Taufkirchen, Germany). 8 µl loading buffer were added and boiled at 95°C for 5 minutes. Then samples were loaded onto the gel and 10 µl of Precision Plus Protein Dual Color Standard (Bio-Rad, München, Germany) were used on each gel as molecular weight marker. The electrophoresis was performed at 100 V for 20 minutes and subsequent 60 mA for 1 h per 2 gels in electrophoresis buffer. After electrophoresis, proteins were blotted onto a porablot polyvinylidenfluorid membrane (PVDF, Macherey und Nagel, Düren, Germany) according to the Bio-Rad protocol at 15-20 V for 45 minutes. Blotting was performed in a Trans-Blot SD semi-dry transfer cell (Bio-Rad, München, Germany) using extra thick filter paper (Bio-Rad, München, Germany) and transfer buffer. Membranes were dried at 37°C for 1 h, before incubating in 8 ml blocking buffer + 36 µl Tween 20 (Sigma-Aldrich, Taufkirchen, Germany). Then blots were probed with an appropriate primary antibody in block solution at 4°C overnight; afterwards, membranes were washed and then exposed to a HRP-conjugated secondary antibody. Binding was detected by chemiluminescence using ECL (Visualizer Spray & Glow, Chemicon & Upstate, Hampshire, United Kingdom) and CL-X Posure Films 8 x 10 inches (Perbio Sciences, Bonn, Germany). Equal protein loading was controlled by re-probing the membrane with the monoclonal anti- α -tubulin antibody (Sigma-Aldrich, Taufkirchen, Germany) and the respective secondary antibody.

2.3.4 Caspase-activity assay

Triplicates of each sample (20 µl) were added to a black 96-well plate with flat and transparent bottom (Nunc, Wiesbaden, Germany) and incubated with 90 µl freshly

prepared substrate solution [37.5 μ l DTT 16% solution and 16.9 μ l of 10 mM caspase-3-substrate-solution Ac-DEVD-AMC (Sigma-Aldrich, Taufkirchen, Germany), caspase-8-substrate solution Ac-IETD-AMC (Sigma-Aldrich, Taufkirchen, Germany) or caspase-1-substrate Z-YVAD-AFC (Merck, Darmstadt, Germany) added to 3 ml Buffer B (5.96 g HEPES, 5.0 g Sucrose, 0.5 g 3-[(3-Cholamidopropyl)dimethylammonio]-1-propanesulfonate (CHAPS), aqua dest. ad 500.0 ml, pH 7.5)]. After 5 min of incubation, fluorescence (excitation 360 nm, emission 465 nm) was measured with a SpectraFluor Plus (Tecan, Grödig, Austria) reader. Fluorescence of caspase-1-substrate (excitation 400 nm, emission 505 nm) was measured with a Varian Cary Eclipse fluorimeter (Varian, Darmstadt, Germany). Background was determined after incubating lysis buffer with substrate buffer and fluorescence of protein extracts was normalized to individual sample protein concentrations determined by BCA assay Kit (Perbio Science, Bonn, Germany). Caspase activity was inhibited by using the general caspase inhibitor Z-VAD-FMK (R&D Systems, Wiesbaden, Germany) or the caspase-1 inhibitor (Merck, Darmstadt, Germany). Z-VAD-FMK was applied 1 h or 6 h before glutamate damage at a final concentration of 50 μ M. Caspase-1 inhibitor was applied 1 h before glutamate damage at a final concentration of 50 μ M.

2.4 RNA analysis

For RNA extraction and subsequent analysis HT-22 neurons were grown at a density of 8×10^4 cells per well in 24-well plates. Primary rat neurons were cultured in PEI-coated 60 mm culture dishes at 1 density of 1.5×10^6 cells per dish.

2.4.1 RNA sample preparation

For RT-PCR analysis, HT-22 neurons were harvested and then centrifuged at $179 \times g$, 4°C for 10 minutes and washed once in PBS. At least 4 wells per condition were pooled. Primary rat neurons (at least five 60-mm dishes per condition) were scraped in PBS, and centrifuged at $64 \times g$ for 15 min at 4°C . The pellet was washed once in PBS. Then RNA-extraction was performed following the same procedure for HT-22 and primary rat neurons. NucleoSpin RNA II Kit was used according to the

manufacturer's protocol (Macherey und Nagel, Düren, Germany). Briefly, samples were dissolved in SDS-containing cell lysis buffer RA1 (Macherey und Nagel, Düren, Germany) and β -mercaptoethanol (Merck, Darmstadt, Germany). To separate insoluble cell fragments, samples were filtered through Nucleospin Filter units. Ethanol was added to the filtrate and the sample was loaded onto a Nucleospin RNA II column. Salt and DNA were removed by Membrane Desalting Buffer and a subsequent DNase reaction. Membrane was washed with Nucleospin buffer RA2 and RA3. Finally purified RNA was eluted from the column with RNase-free water. The RNA samples were stored at -80°C until further use.

2.4.2 Determination of RNA amount

To determine the RNA amount in the samples, 4 μl were diluted in 156 μl RNase-free water (Sigma-Aldrich, Taufkirchen, Germany). RNA amount was determined by UV, using micro cuvettes (Brand, Wertheim, Germany) in a Biophotometer (Eppendorf, Hamburg, Germany) at a wavelength of 260 nm. Reference wavelength was 280 nm. OD of 1 at 260 nm represents a concentration of 40 $\mu\text{g}/\text{ml}$ RNA.

2.4.3 Reverse transcriptase polymerase chain reaction (RT-PCR)

2.4.3.1 Reverse transcription

CDNA was derived from RNA samples by reverse transcription using a M-MLV-reverse transcriptase and oligo-dT-primers; 5 μg total RNA were added to the following reaction components: 5 μl 10x PCR buffer (Abgene, Hamburg, Germany), 2.5 μl dNTP mix [dATP, dCTP, dGTP, dTTP (Abgene, Hamburg, Germany) each 10 mM], 2.5 μl D,L-dithiothreitol 0.4 mM, 2.5 μl Oligo-dT15-Primer (MWG-Biotech, Ebersberg, Germany) 100 μM , ad aqua dest. 45 μl . Sample was heated to 65°C for 5 minutes in a PX2 Thermal Cycler (Thermo electron corporation, Karlsruhe, Germany). Then 1 μl RNase inhibitor RNasin (40 U/ μl , Promega, Mannheim, Germany) and 5 μl M-MLV reverse transcriptase (50 U/ μl , Promega, Mannheim, Germany) were added and total sample was incubated for 1 h at 37°C . Finally, samples were heated at 95°C for 5 minutes. Derived cDNA was stored at -20°C until further use.

2.4.3.2 Polymerase chain reaction (PCR)

The PCR was used to amplify the cDNA of AIF, Bid or glyceraldehyde-3-phosphatedehydrogenase (GAPDH) to detectable amounts in the samples. The following primers were used: AIF, forward, 5'-GCG TAA TAC GAC TCA CTA TAG GGA GAT CCA GGC AAC TTG TTC CAGC-3', and reverse, 5'-GCG TAA TACGAC TCA CTA TAG GGA GAC CTC TGC TCC AGC CCT ATC G-3'. Bid, forward, 5'-GCG TAA TAC GAC TCA CTA TAG GGA GAT GGG CTT CTG TCT AAG GAGA-3', and reverse, 5'-GCG TAA TAC GAC TCA CTA TAG GGA GAA GTG AGG CCT TGT CTC TGAA-3'. For loading control, cDNA of housekeeping gene GAPDH was amplified, using the following primers: forward, 5'-CGT CTT CACCAC CAT GGA GAA GGC-3' and reverse, 5'-AAG GCC ATG CCA GTG AGC TTC CC-3'. The resulting cDNA fragments had a length of 750 (AIF), 521 (Bid) and 400 (GAPDH) base pairs, respectively. The cDNA sample (10 µl) was added to the following reaction components: 4 µl 10x PCR reaction buffer IV (Abgene, Hamburg, Germany), 1 µl dNTP mix [dATP, dCTP, dGTP, dTTP (Abgene, Hamburg, Germany) each 10 mM], 3 µl MgCl₂ 25 mM (Abgene, Hamburg, Germany), 1 µl of forward and reverse primers (MWG-Biotech, Ebersberg, Germany) 10 µM, 5µl Thermoprime Plus polymerase 0.2 U/µl (Abgene, Hamburg, Germany), 25 µl aqua dest. PCR was performed in a PX2 Thermal Cycler (Thermo electron corporation, Karlsruhe, Germany) with an initial denaturation at 95°C for 2 min followed by 26-30 cycles of 30 s 95°C, 1 min 57°C (AIF, GAPDH) or 60°C (Bid), and 2 min 72°C, and final extension at 70°C for 10 min. PCR products obtained for AIF, Bid or GAPDH gene were detected relative to control samples by ethidium bromide staining.

2.4.4 Agarose gel electrophoresis

Analysis of PCR amplification products was performed by fluorescence detection after agarose gel electrophoresis. To this end, 10 µl of each sample were mixed with bromophenol blue containing loading buffer 6x (2.4 ml EDTA solution 0.5 M, 12 ml glycerin, 5.6 ml aqua dest. and 0.04 g bromophenol blue) and were loaded onto a 1.5% agarose gel containing ethidiumbromide. The gel was prepared by dissolving 0.6 g agarose (Sigma-Aldrich, Taufkirchen, Germany) in 40 ml TBE buffer [10.8 g

trizma base, 5.5 g boric acid, 0.75 g disodium EDTA (all Sigma-Aldrich, Taufkirchen, Germany) ad 1000 m Millipore water], boiling everything up to 100°C and adding 40 µl of a 0.5 mg/ml ethidiumbromide (Sigma-Aldrich, Taufkirchen, Germany) solution after cooling down to about 70 °C. The electrophoresis was performed for 70 minutes at 80 V. 10 µl of 50 bp DNA-ladder (Peqlab, Erlangen, Germany) were used as a size marker. PCR amplification products were detected under UV light (excitation 260 nm) by photographing the emission light (560 nm) of ethidium bromide in a UV chamber (Raytest, Straubhardt, Germany), equipped with a CCD Camera (Raytest, Straubhardt, Germany) controlled by Diana/NT 1.6 software.

2.4.5 Statistical analysis

All data are given as means ± standard deviation (SD). For statistical comparisons between two groups student's t-test was used; multiple comparisons were performed by analysis of variance (ANOVA) followed by Scheffé's post hoc test. Calculations were performed with the Winstat standard statistical software package.

3 Results

3.1 Glutamate-sensitivity of HT-22 neurons

HT-22 neurons are immortalized hippocampal mouse neurons. They do not exhibit dendrites or axons and are an adhesive cell line with spindle shaped morphology. Glutamate (1-5 mM) induced cell death in HT-22 neurons (HT-22) in a concentration-dependent manner (Figure 5). After exposure to glutamate, HT-22 neurons round up and detach from the well bottom. It is important to note that sensitivity to glutamate toxicity varies in HT-22 neurons depending on density and passage number of cells. For example, when seeded at a density of 60,000 cells per well HT-22 neurons exhibited less sensitivity against glutamate than at seeding densities of 40,000 cells per well, as shown in Figure 5. Therefore, experiments were always performed at different glutamate concentrations between 1-5 mM, and representative results are always shown from individual experiments where the respective glutamate concentration induced at least 50% cell death as detected with the MTT assay. The protective effects observed after treatment with siRNA or pharmacological inhibition were always robust over the whole range of glutamate concentrations.

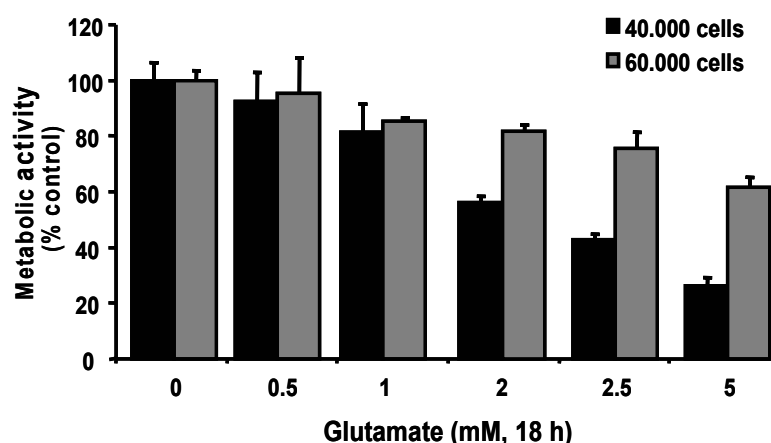


Figure 5: Glutamate toxicity

Glutamate reduces viability of HT-22 neurons in a concentration-dependent manner as evaluated by the MTT assay 17 h after onset of the treatment. When seeded at a density of 40,000 cells per well, HT-22 were more sensitive against glutamate than at densities of 60,000 cells per well.

3.1.1 Bid translocates to mitochondria early during apoptosis

Under physiological conditions, inactive Bid is distributed in the cytosol. The proapoptotic activation of Bid is best characterized by Bid truncation and translocation of Bid to the mitochondria. To detect Bid translocation to the mitochondria after a glutamate challenge, HT-22 neurons were transfected with the pDsRed2-Bid vector which results in the expression of a red fluorescing Bid residing in the cytosol (Figure 6). Mitochondria were stained with MitoTracker green immediately before treating the cells with glutamate. As shown in Figure 6 Bid translocated to mitochondria within 5 h after onset of the glutamate challenge, visualized by the co-localization of DsRed and MitoTracker Green fluorescence.

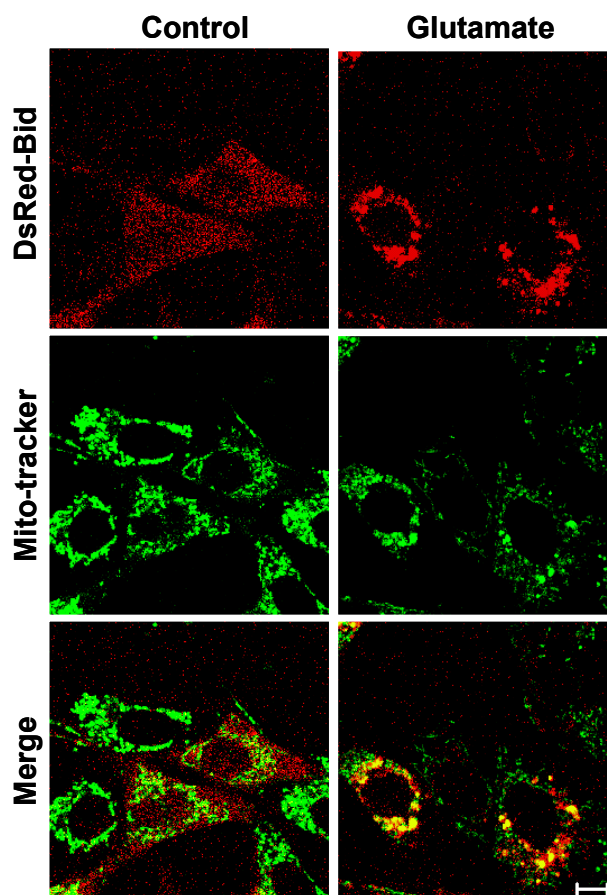


Figure 6: Translocation of Bid after glutamate damage of HT-22 neurons

Fluorescence photomicrographs of HT-22 neurons expressing a Bid-DsRed fusion protein show co-localization of MitoTracker Green- and DsRed-signal in glutamate-damaged (5 mM, 5 h) cells. Similar results were obtained in cells exposed to 3 mM glutamate. Note, that the homogenous distribution of Bid observed in control cells significantly changes in glutamate-damaged cells where Bid accumulates at mitochondria (yellow in merged panels).

3.1.2 Bid knockdown attenuates oxidative stress and prevents cell death

Bid-siRNA induced specific gene silencing of Bid as determined at mRNA and protein level. Messenger RNA and protein levels of housekeeping genes such as GAPDH and α -Tubulin were not affected by Bid-siRNA; the non-silencing mutant siRNA control sequence (mut-siRNA) did not alter Bid expression or any of the housekeeping genes (Figure 7A). Bid-siRNA significantly reduced glutamate-induced acceleration of reactive oxygen species (ROS) and attenuated glutamate-induced cell death as evaluated by DCF-fluorescence (Figure 7B) and MTT-assay (Figure 7C), respectively.

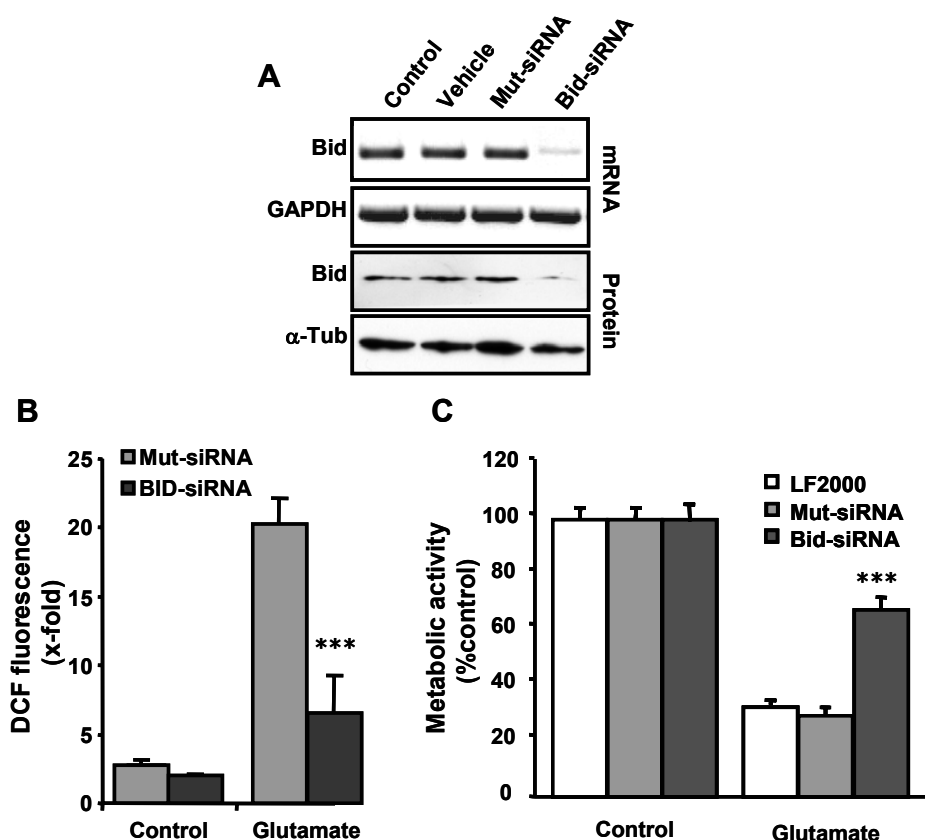


Figure 7: Bid-knockdown rescued HT-22 neurons from glutamate induced apoptosis.

A. RT-PCR analysis of Bid mRNA (upper panels) and Western blot analysis of Bid protein (lower panels) in HT-22 neurons pretreated with 20 nM Bid-siRNA for 48h. RT-PCR with primers specific for GAPDH and anti- β -actin antibodies served for respective control analyses. **B.** Bid siRNA (20 nM, 48 h pretreatment) significantly reduces oxidative stress as evaluated by the DCF assay after exposure of HT-22 neurons to glutamate (2 mM) for 6 hours. *** $p < 0.001$ compared to glutamate-exposed HT-22 neurons pretreated with nonfunctional Mut-siRNA (Student's *t*-test). **C.** Bid-siRNA significantly attenuated glutamate-induced cell death as determined by MTT assay. *** $p < 0.001$ compared to glutamate-exposed HT-22 neurons pretreated with nonfunctional Mut-siRNA or vehicle Lipofectamine 2000 (ANOVA, Scheffé's).

3.1.3 Small molecule Bid inhibitor prevents glutamate-induced cell death

In addition to the siRNA approach, the specific Bid inhibitor BI-6C9 was applied to confirm the essential role of Bid in glutamate-induced neuronal death. HT-22 neurons exposed to glutamate for 17 h show typical morphology of dying cells: the neuronal cells appear shrunken, rounded and detach from the culture dish (Figure 8A). HT-22 neurons pretreated with the Bid inhibitor BI-6C9 retained their normal spindle-shaped morphology and were completely rescued from glutamate-induced cell death as determined by the MTT assay in experiments with different concentrations of glutamate (Figure 8A/B/C). Cells treated with the Bid inhibitor alone, showed an enhanced metabolic activity.

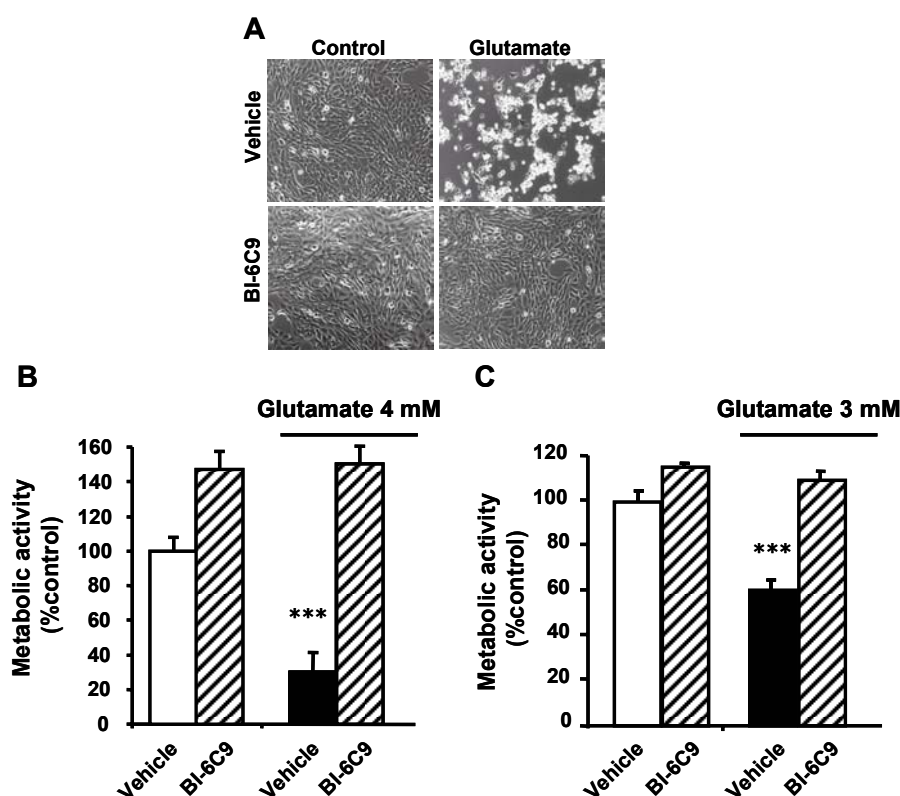


Figure 8: Bid inhibitor BI-6C9 protects HT-22 neurons against glutamate-induced cell death.

A. Photomicrographs (10x objective) show morphological evidence for severe damage of HT-22 neurons 17 h after glutamate (4 mM) exposure. Glutamate-treated cells lose their spindle-like morphology, shrink and detach from the culture well bottom; in contrast, cells pretreated with the Bid inhibitor BI-6C9 (10 μ M) are fully protected against glutamate-induced death and are not different from the controls. **B.** Quantification of glutamate-induced (4 mM, 17 h) severe cell damage and the protective effect of BI-6C9 (10 μ M) by the MTT assay. **C.** Quantification of glutamate-induced (4 mM, 17 h) weak cell damage and the protective effect of BI-6C9 (10 μ M) by the MTT assay. Note; the protective effect of BI-6C9 is independent from the severity of the cell damage. *** p <0.001 compared to vehicle controls and BI-6C9-treated cells (ANOVA, Scheffé's).

3.1.4 Prevention of glutamate-induced apoptosis by Bid inhibitor

FACS analysis of FITC-Annexin-V-stained HT-22 neurons confirmed the pronounced protective effect of the Bid inhibitor against glutamate-induced apoptotic cell death (Figure 9A). Concomitant detection of propidium iodide (PI) revealed that less than $9.4 \pm 1.6\%$ of the glutamate-treated cells were PI positive versus $5.4 \pm 0.6\%$ in the controls, suggesting that most HT-22 neurons exposed apoptotic features after glutamate exposure. Similar to the results obtained by Annexin binding analyses, the Bid inhibitor reduced the percentage of PI positive, i.e. necrotic cells to control levels ($4.7 \pm 0.3\%$) (Figure 9B).

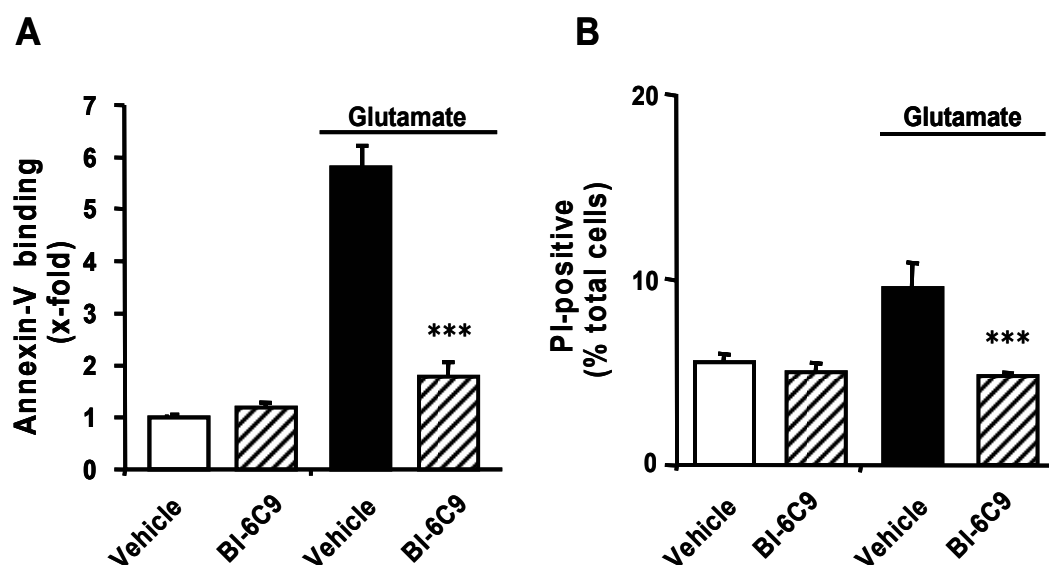


Figure 9: Bid inhibitor BI-6C9 protects HT-22 neurons against glutamate-induced apoptosis.

A. FACS analysis of HT-22 neurons after FITC- Annexin-V labeling to detect apoptotic cells. Exposure to glutamate (3 mM, 17 h) resulted in enhanced Annexin-V binding of apoptotic HT-22 neurons compared to controls. BI-6C9 (10 μ M, 1 h prior to damage) significantly reduced glutamate-induced apoptosis. *** $p < 0.001$ compared to glutamate-treated cells (Student's *t*-test). **B.** FACS analysis of necrotic HT-22 neurons after labeling with propidium iodide (PI). Note that the increase in PI positive cells (2-fold) after glutamate exposure is far less pronounced compared to the increase in Annexin-V-labeling (6-fold). BI-6C9 (10 μ M) treatment before glutamate-exposure significantly reduced the percentage of PI-positive cells to control levels. *** $p < 0.001$ compared to glutamate-treated cells (Student's *t*-test).

3.1.5 Specificity of the Bid inhibitor

The specificity of BI-6C9 in the presently used culture system was confirmed in HT-22 neurons transfected with a tBid expression vector. Overexpression of tBid reduced cell viability by approximately 40% (Figure 10) whereas cells pretreated with the Bid inhibitor were significantly protected from tBid-induced cell death (Figure 10).

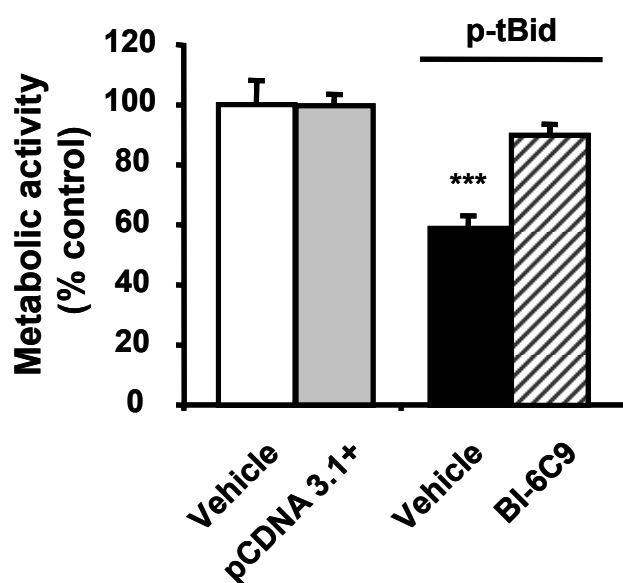


Figure 10: BI-6C9 prevents tBid-induced cell death.

HT-22 neurons were pretreated with BI-6C9 (10 μ M, 1 h) before transfection with a tBid expressing plasmid (p-tBid). Twenty four hours later cell viability was determined with the MTT assay. *** p <0.001 compared to controls and BI-6C9-treated cells (ANOVA, Scheffé's).

It is important to note that the percentage of cell death detected in tBid-transfected HT-22 neurons corresponds well to the transfection efficiency achieved with the current protocol for DNA vector transfection: Parallel transfection experiments in HT-22 neurons with gene vectors encoding green fluorescent protein (GFP) of a comparable vector size of 4.7 kbp to 5.8 kbp and subsequent FACS analysis revealed a transfection efficiency of $44.7 \pm 2.5\%$ to $51.2 \pm 1.2\%$, respectively (Figure 11).

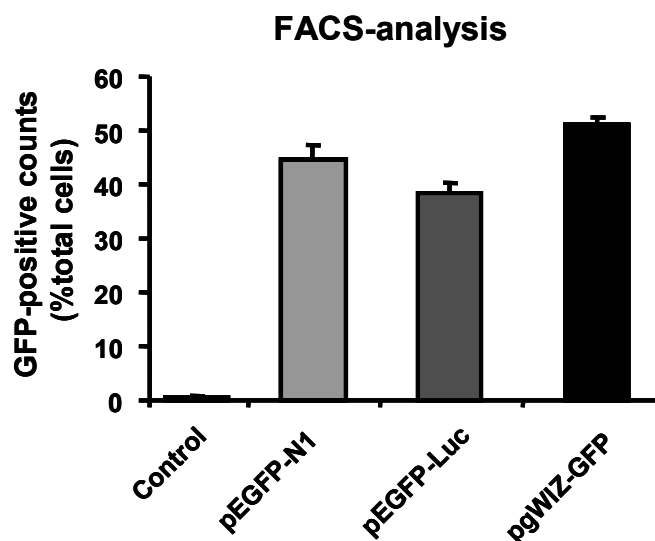


Figure 11: Efficiency of DNA vector transfections.

HT-22 neurons were transfected with different GFP encoding gene vectors. Twenty four hours later the number of green fluorescing cells was determined by FACS analysis.

3.1.6 Therapeutic time window of BI-6C9

Strikingly, morphological analysis and MTT assay revealed that the Bid inhibitor BI-6C9 rescued HT-22 neurons even when applied up to 6 h after glutamate-exposure, suggesting that Bid-mediated cell death depends on sustained Bid activation with a remarkable time window (Figure 12).

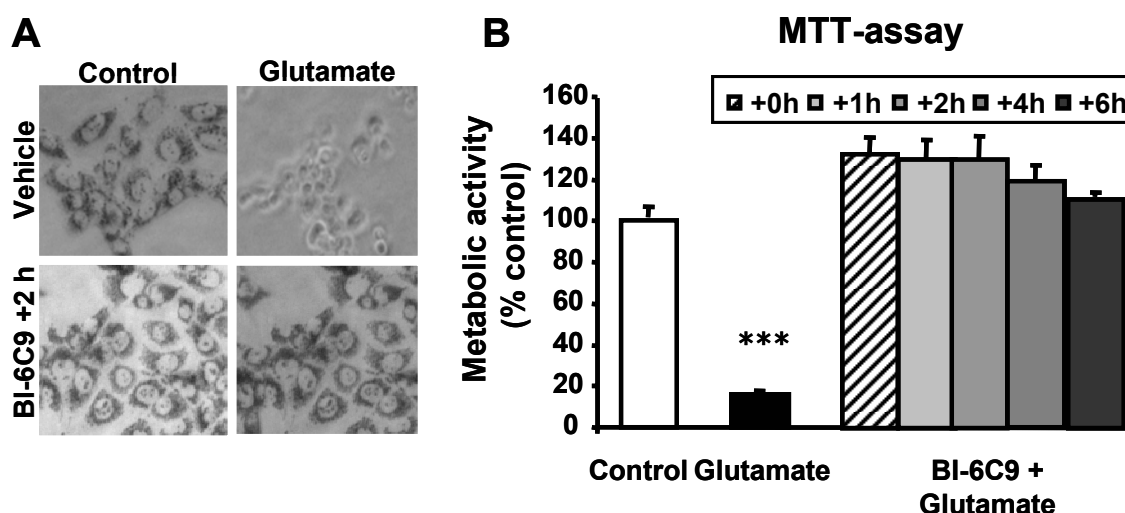


Figure 12: BI-6C9 blocks HT-22 neuronal cell death applied up to 6h hours after glutamate.

A. Photomicrographs of HT-22 MTT-incubated neurons after glutamate treatment (3 mM, 18 h) with or without BI-6C9 (10 μ M, applied 2 h after onset of glutamate damage) **B.** Quantification of the MTT assay performed 18 h after onset of glutamate-treatment (3 mM) of HT-22 neurons. BI-6C9 was applied together with glutamate (0 h) or up to 6 hours afterwards. The graph shows mean values and S.D. of $n=8$ independent experiments per group; *** $p<0.001$ compared to glutamate treatment alone.

3.1.7 Bax inhibition does not protect against glutamate

Bid and Bax are described as co-players in apoptotic processes of mitochondrial membrane permeabilization under various conditions [58, 60]. Therefore the effect of Bax inhibition in glutamate-induced apoptosis of HT-22 neurons was examined. In contrast to the findings with inhibition of Bid, blocking pro-apoptotic Bcl-2 family member Bax had no or only a very weak protective effect on HT-22 neurons as shown by MTT-assay, 18 hours after glutamate damage (Figure 13). Treatment of HT-22 neurons with Bax inhibitor alone increased the metabolic activity up to 140%. The protective effect of Bax inhibitor in glutamate-treated cells did not exceed the effect of the Bax inhibitor in control cells.

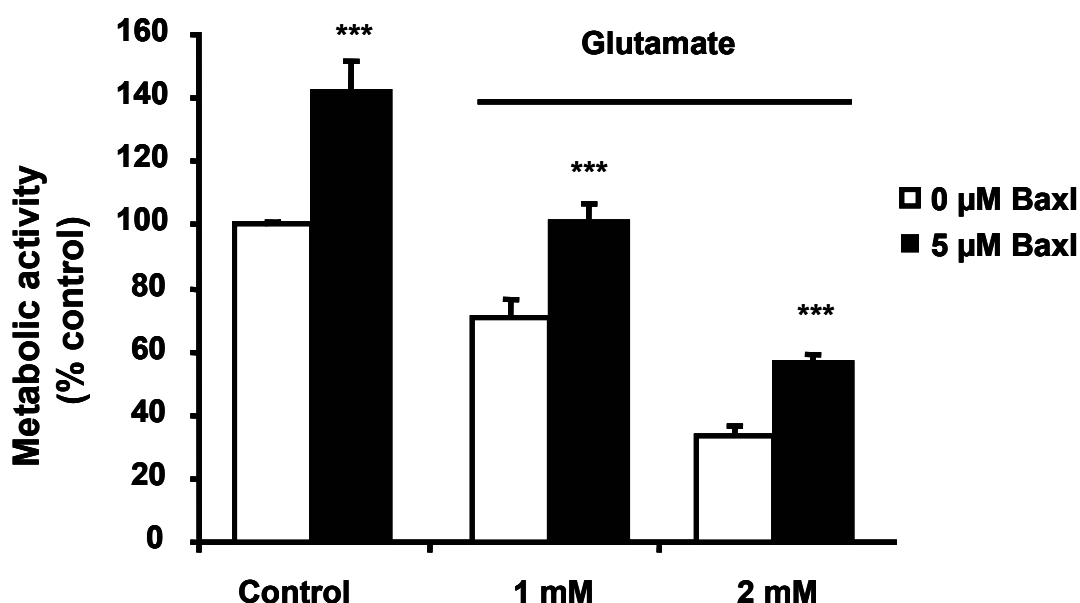


Figure 13: No protection of HT-22 neurons by Bax inhibition.

The Bax channel blocker (Baxl, 5 μ M) was applied 1 h prior to exposure of HT-22 neurons to glutamate (1-2 mM, 17 h). The MTT assay revealed an enhanced metabolic activity by the Baxl in control cells. The Baxl only moderately preserved the metabolic activity in glutamate-treated cells, and this moderate protective effect did not exceed the effect of Baxl on metabolic activity in control cells. *** $p < 0.001$ compared to respective glutamate-treated cells.

3.1.8 Mechanisms downstream of Bid

Since Bid is supposed to act upstream mitochondrial damage, the involvement of Bid in the breakdown of mitochondrial membrane potential and subsequent activation of caspase-dependent and caspase-independent mechanisms was examined.

3.1.8.1 Effect of BI-6C9 on mitochondrial translocation of Bid

To test the effect of BI-6C9 on the activation, i.e. the translocation of Bid to the mitochondria, confocal laser scanning microscopy of glutamate-treated HT-22 neurons expressing DsRed-Bid and mitochondrial co-staining with MitoTracker was used. An inhibition of aggregation and mitochondrial translocation of Bid could be demonstrated in glutamate-treated groups with simultaneous addition of Bid inhibitor BI-6C9 to the damage medium.

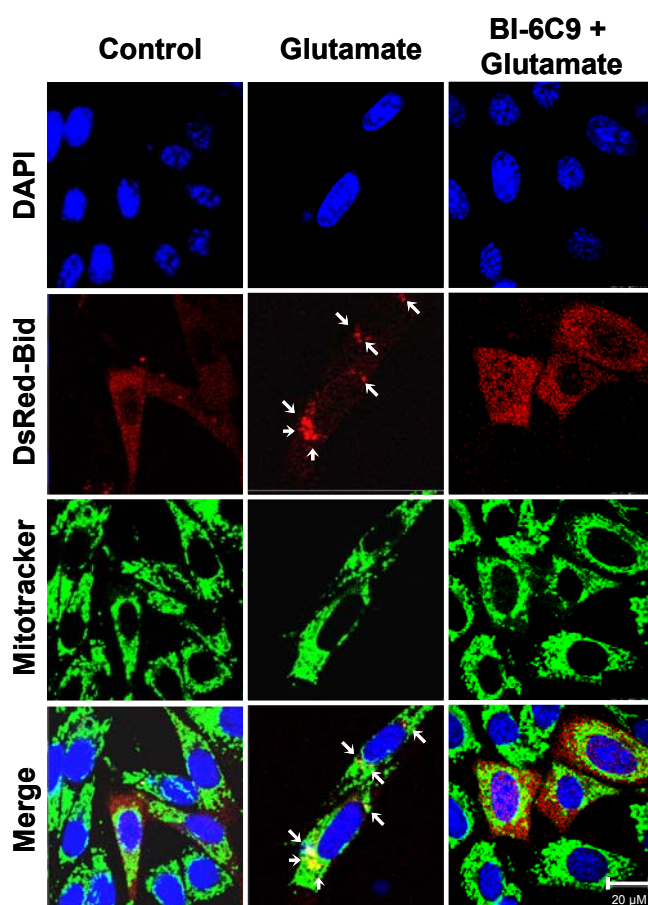


Figure 14: Bid inhibitor prevents translocation of Bid to the mitochondria.

Fluorescence photomicrographs of HT-22 neurons expressing a Bid-DsRed fusion protein show co-localization of MitoTracker Green- and DsRed-signal in glutamate-damaged (5 mM, 8 h) cells. Bid inhibitor BI-6C9 (10 μM) prevented the accumulation of Bid at the mitochondria and retained a homogenous distribution of Bid in the cytosol.

3.1.8.2 Mitochondrial membrane potential

Staining with JC-1 was used to evaluate the effect of Bid inhibition on glutamate-induced breakdown of the mitochondrial membrane potential. Glutamate treatment caused a significant loss of JC-1 red fluorescence, i.e. loss of mitochondrial membrane potential after glutamate treatment within 6-12 h (Figure 15A/B). In the HT-22 neurons, glutamate was as effective as carbonyl cyanide m-chlorophenylhydrazone (CCCP) to induce mitochondrial membrane depolarization (Figure 15C). Pre-treatment with the Bid inhibitor prevented glutamate-induced breakdown of the mitochondrial membrane potential.

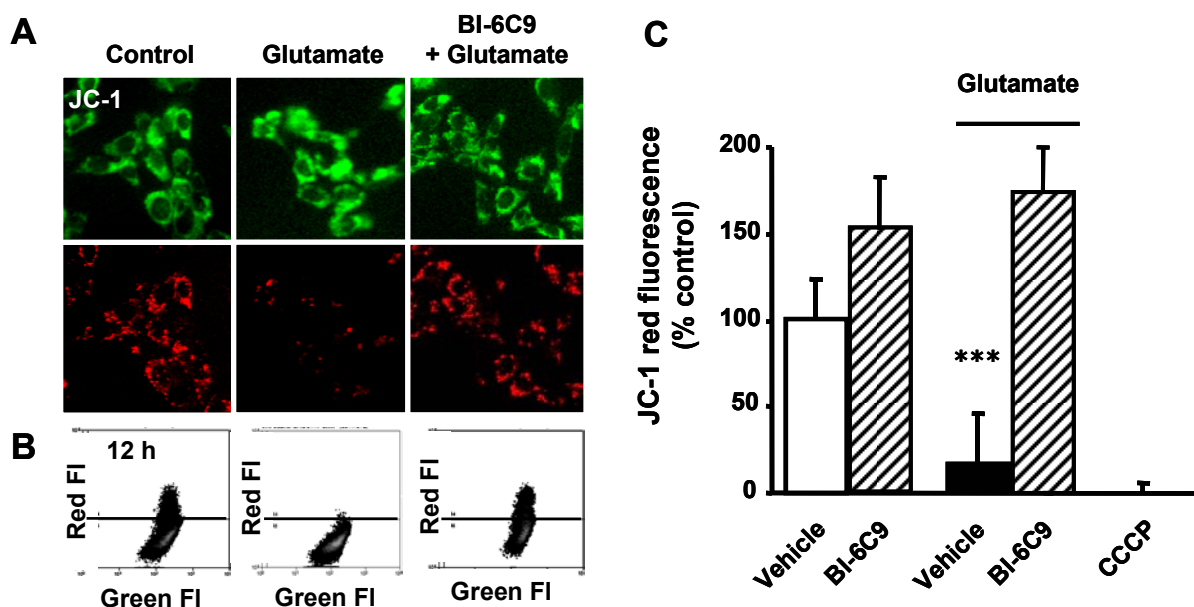


Figure 15: Bid-inhibitor BI-6C9 prevents glutamate-induced mitochondrial depolarization.

A. Mitochondrial membrane potential was analyzed by JC-1 fluorescence: upper panels show epifluorescence photomicrographs indicating equal cellular uptake of JC-1 by green fluorescence, lower panels depict intact mitochondria exposing red fluorescence. Glutamate-treated (3 mM, 12h) HT-22 neurons show significantly reduced red fluorescence compared to controls whereas BI-6C9 (10 μ M) prevents the breakdown of the mitochondrial membrane potential as indicated by preservation of the red JC-1 fluorescence. **B, C.** FACS analyses of $n=4$ independent experiments per group reveal a decrease of the red JC-1 fluorescence to 20% of control levels 12h after glutamate-treatment (3 mM) which is prevented by BI-6C9. Glutamate treatment was as effective as the positive damage-control CCCP which causes a fast breakdown of the mitochondrial membrane potential. *** $p < 0.001$ compared to controls and BI-6C9-treated cells (ANOVA, Scheffé's).

In sum these data reveal, that Bid is activated after glutamate treatment of HT-22 neurons, which leads to a breakdown of the mitochondrial membrane potential. Bid activation with subsequent mitochondrial membrane permeabilization may trigger both, caspase-dependent and caspase-independent execution of cell death through release of cytochrome c and AIF, respectively. Therefore, these caspase-dependent and caspase-independent mechanisms downstream mitochondrial damage were further examined.

3.1.8.3 Bid inhibition reduces effector caspase-3 activity

Measurements of caspase activity revealed a significant increase of caspase-3 activity in HT-22 neurons after exposure to glutamate and this caspase activation was fully blocked by the Bid inhibitor (Figure 16).

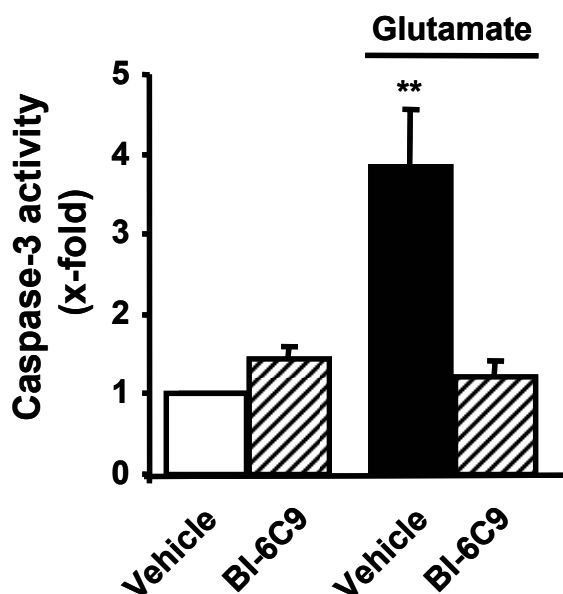


Figure 16: Bid inhibitor prevents glutamate induced activation of caspase-3.

Caspase-3-activity assay revealed an increased caspase-3 activity after glutamate-treatment (2 mM, 17h) that was prevented by BI-6C9 (10 μ M). ** $p < 0.01$ compared to controls and BI-6C9-treated cells (ANOVA, Scheffé's).

3.1.9 Involvement of effector caspases in glutamate-induced apoptosis

The data suggest activation of caspase-3 after glutamate-treatment of HT-22 neurons, which could be blocked by BI-6C9. Therefore analyses regarding the

involvement of effector caspases in glutamate neurotoxicity were performed by using caspase-inhibitors and examination of lamin cleavage as an indicator of caspase-6 activity.

3.1.9.1 Inhibition of caspase-3 does not attenuate glutamate toxicity

Significant inhibition of increased caspase-3 activity after the glutamate challenge was achieved with the membrane permeable general caspase inhibitor Z-VAD-FMK (Figure 17A). Although these and the data presented above implied an involvement of caspase-3 in the execution of glutamate-induced cell death in HT-22 neurons, the caspase inhibitor Z-VAD-FMK did not attenuate glutamate toxicity (Figure 17B). These data suggest that caspase-3 activation occurs after glutamate exposure in HT-22 neurons but is not required for execution of the cell death program.

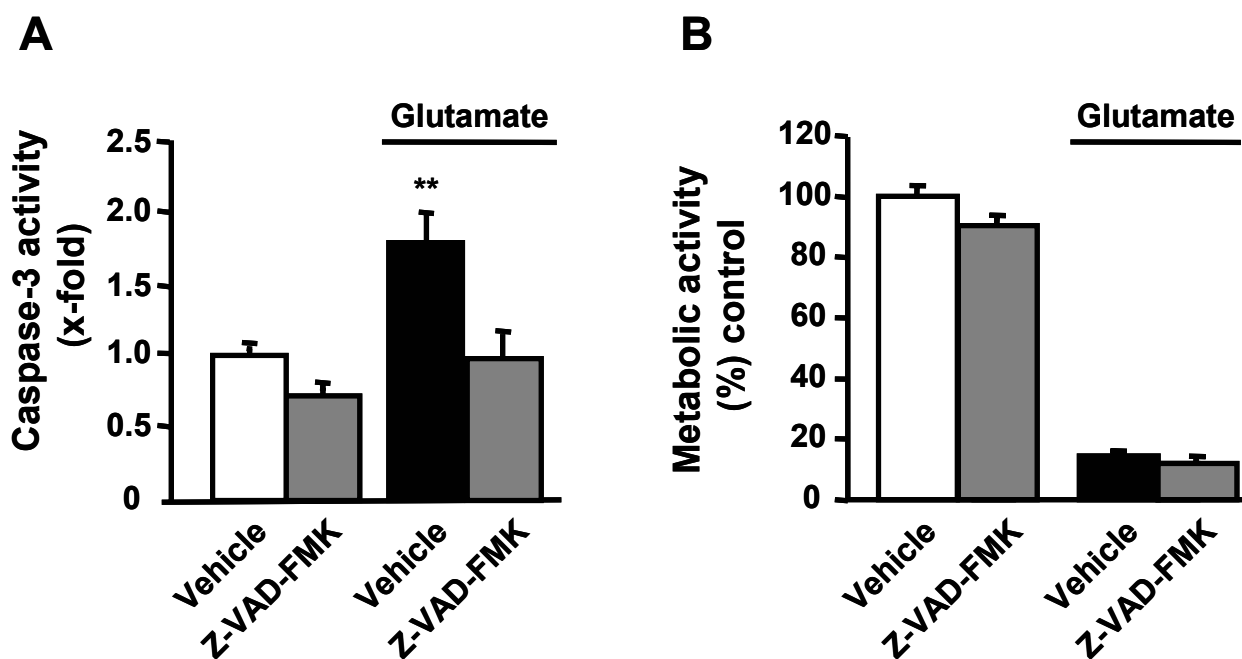


Figure 17: Pan-caspase inhibitor fails to prevent glutamate-induced cell death in HT-22 neurons.

A. Increased caspase-3 activity in glutamate-treated HT-22 neurons was prevented by the pan-caspase inhibitor Z-VAD-FMK (50 μ M) applied 1 h before glutamate exposure proving the efficiency of Z-VAD-FMK under these experimental conditions. ** $p < 0.01$ compared to controls and Z-VAD-FMK-treated cells, (ANOVA, Scheffé's). **B.** The MTT-assay revealed that Z-VAD-FMK (50 μ M) could not protect HT-22 neurons from glutamate-induced cell death.

3.1.9.2 Lamin cleavage in glutamate-induced neurotoxicity

Cleavage of Lamin, a structure protein within the nuclear lamina, was examined as an indicator for the involvement of effector caspase-6 in glutamate-induced neurotoxicity. However, proteolytic activity indicating caspase-6 activity was not detected. Western blot analysis of total protein cell extracts with an antibody detecting Lamin A/C and respective caspase-6 cleavage products revealed that no cleavage of Lamin A occurred during glutamate-induced apoptosis of HT-22 neurons (Figure 18).

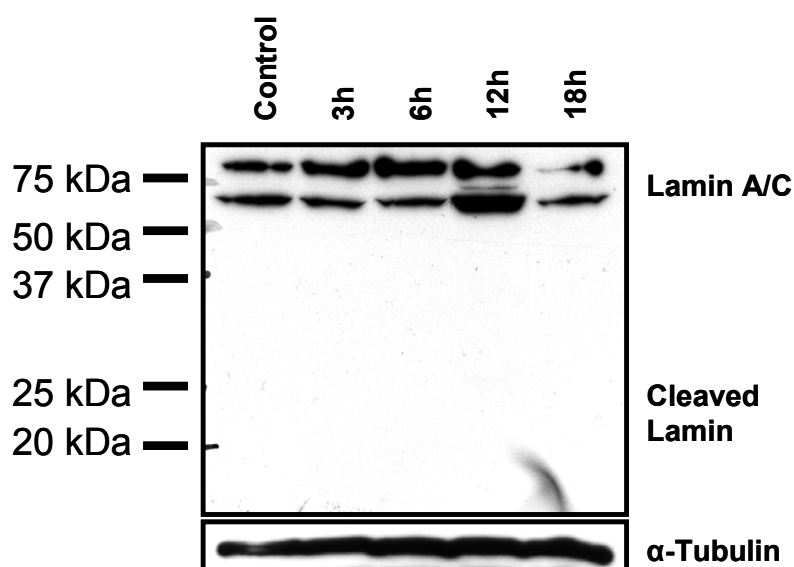


Figure 18: Lamin cleavage was not detected during glutamate-induced neurotoxicity. Western blot analysis of total protein extracts. No cleaved lamin (28kDa) could be detected during glutamate damage (2 mM, 0-18 h) of HT-22 neurons. α -Tubulin band shows loading control.

3.1.10 Involvement of AIF in apoptosis of HT-22 neurons

Having shown that apoptosis induced by glutamate in HT-22 neurons does not require the activity of effector caspases, the involvement of AIF as a representative of mitochondrial caspase-independent pro-apoptotic factors was determined. Addition of 2 mM glutamate to immortalized hippocampal neurons induced translocation of AIF to the nucleus, as demonstrated by Western blot analysis and immunocytochemistry (Figure 19A/B) in fixed HT-22 neurons.

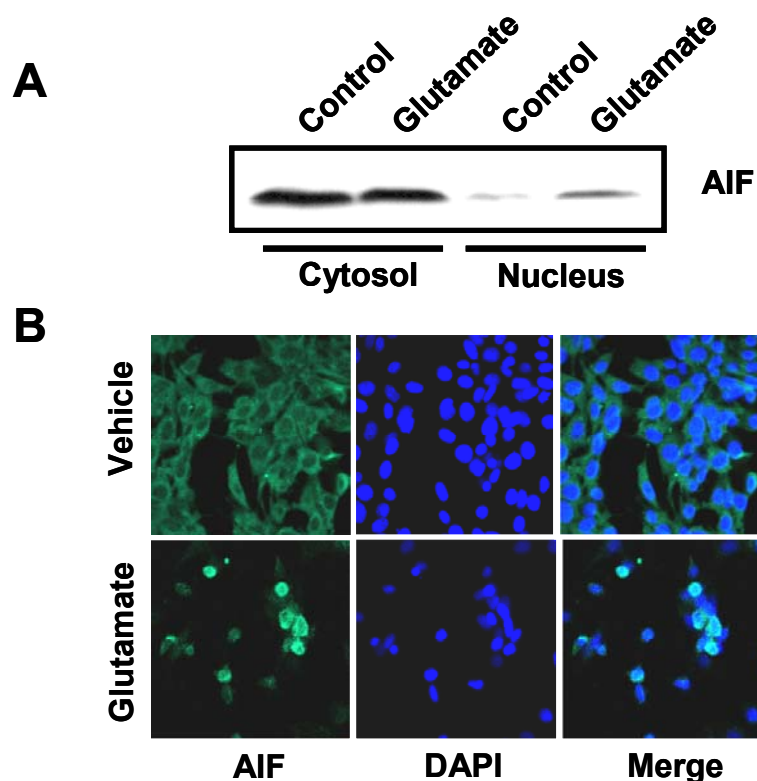


Figure 19: Nuclear translocation of AIF in glutamate-treated HT-22 neurons.

A. Western blot analysis of AIF protein in the crude cytosolic and in the nuclear fractions before and after exposure to 2 mM glutamate. **B.** Confocal laser scanning microscope images of AIF immunoreactivity (green) under control conditions and after 18 h exposure to glutamate (2 mM) in immortalized hippocampal neurons (HT22 neurons). Counter staining with DAPI (dark blue) allowed the identification of nuclear translocation of AIF (AIF/DAPI, light blue).

Confocal microscopy time laps recordings over a period of 18 h after glutamate exposure revealed that mitochondria containing AIF-GFP fusion protein translocated to the nucleus within 10 h after onset of the apoptotic challenge followed by a rapid release of AIF into the nucleus (see supplement movie). The movie was composed from fluorescence photomicrographs taken every 5 minutes from 7-14 h after onset of glutamate-treatment (3 mM) in HT-22 neurons expressing an AIF-GFP fusion protein. The movie shows accumulation of AIF around the nucleus in a damaged cell within 10 h after glutamate exposure. After accumulation around the nucleus AIF is released from mitochondria to the nucleus within 10-15 minutes followed by nuclear condensation and fragmentation of the cell. Co-localization of AIF-GFP- (green) and DAPI-signals (dark blue) reveal a nuclear localization of AIF (merged colour: light blue).

3.1.10.1 AIF-siRNA prevents glutamate-induced cell death

Since the translocation studies implied a major role for AIF in glutamate-induced neuronal cell death, AIF gene silencing by siRNA was applied to further address this issue. AIF gene silencing on mRNA and protein level using a dsRNA dicer product (Figure 20A) significantly enhanced survival of HT-22 neurons exposed to glutamate (Figure 20B).

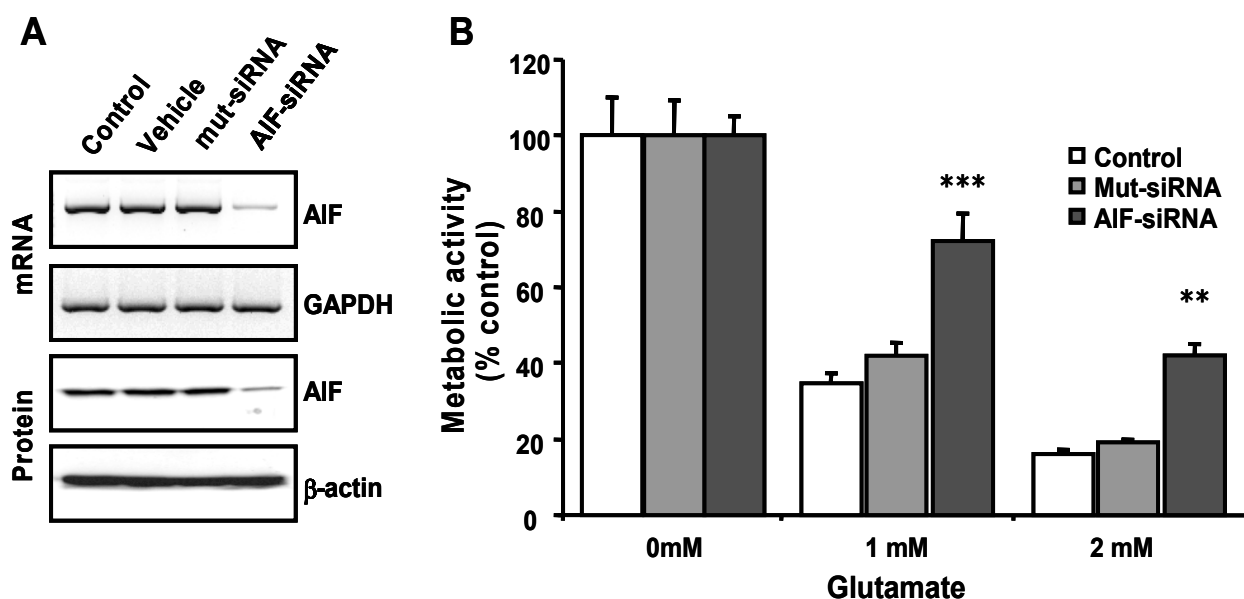


Figure 20: AIF-knockdown by dicer product attenuates glutamate-induced neuronal cell death in HT-22 neurons.

A. RT-PCR analysis of AIF mRNA (top rows) and Western blot analysis of AIF protein levels (bottom rows) in HT22 neurons pretreated with 20 nM AIF siRNA for 48 h. Controls were treated with mutant siRNA. RT-PCR with primers specific for GAPDH and anti- β -actin antibodies were used as controls for equal mRNA and protein amounts, respectively. HT22 neurons were pretreated with vehicle (Lipofectamine), nonfunctional mutant siRNA (mut-siRNA), or AIF-siRNA for 48 h. **B.** Cell viability was determined by the MTT assay, 20 nM mutant siRNA or AIF-siRNA for 48 h before 18 h 1-2 mM glutamate exposure. Cell viability in glutamate-exposed cultures pretreated with AIF-siRNA was significantly enhanced compared with controls ($n=8$; *** $p<0.001$; ** $p<0.01$).

Of note, AIF-siRNA-treated HT-22 neurons surviving glutamate toxicity did not show nuclear AIF translocation (Figure 21), thereby stressing the specific role for AIF during the cell death process.

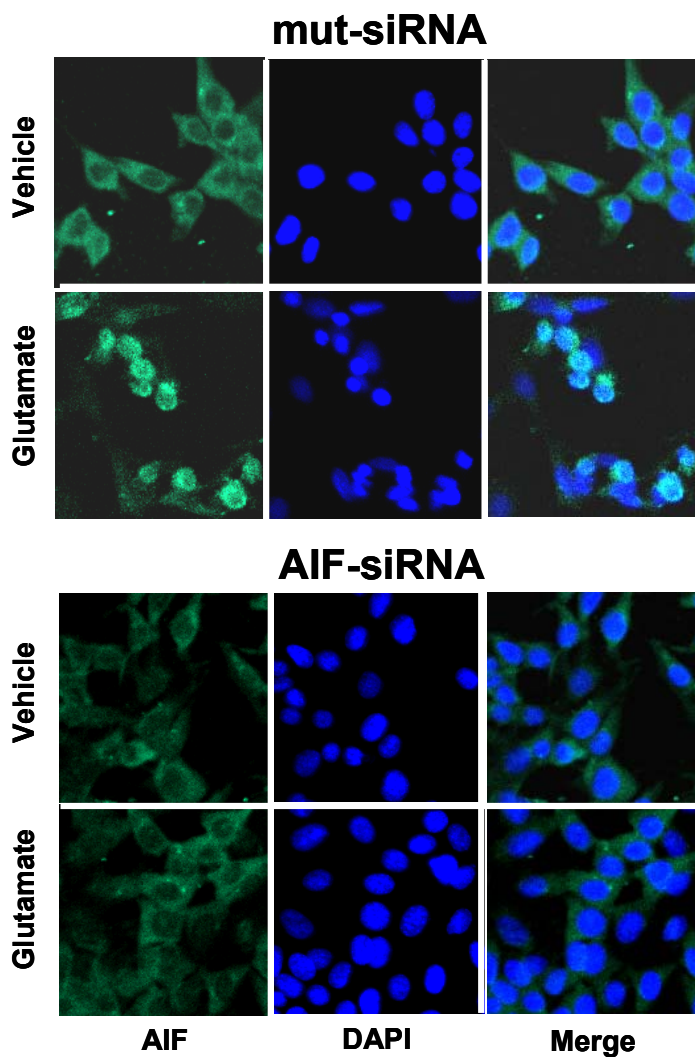


Figure 21: No AIF-translocation in HT-22 neurons surviving glutamate treatment by AIF-siRNA. Confocal laser scanning microscope images of AIF immunoreactivity (green) and nuclear DAPI staining (dark blue). Downregulation of AIF by siRNA (dicer product, see above) resulted in inhibition of nuclear AIF translocation after 18 h of exposure to glutamate (2mM).

Comparable results were also obtained with a single AIF-siRNA sequence (Figure 22B), which also specifically reduced AIF mRNA and protein levels (Figure 22A). This confirmation experiment was performed to exclude possible unspecific off-target effects of the siRNA cocktail, which was obtained by the dicer reaction. On the one

hand, the single sequence was not as effective as the dicer product, because of the higher variety of the siRNAs obtained by the dicer reaction; on the other hand, the significant protective effect of the single sequence confirmed the conclusion that AIF plays an important role during glutamate-induced apoptosis of HT-22 neurons.

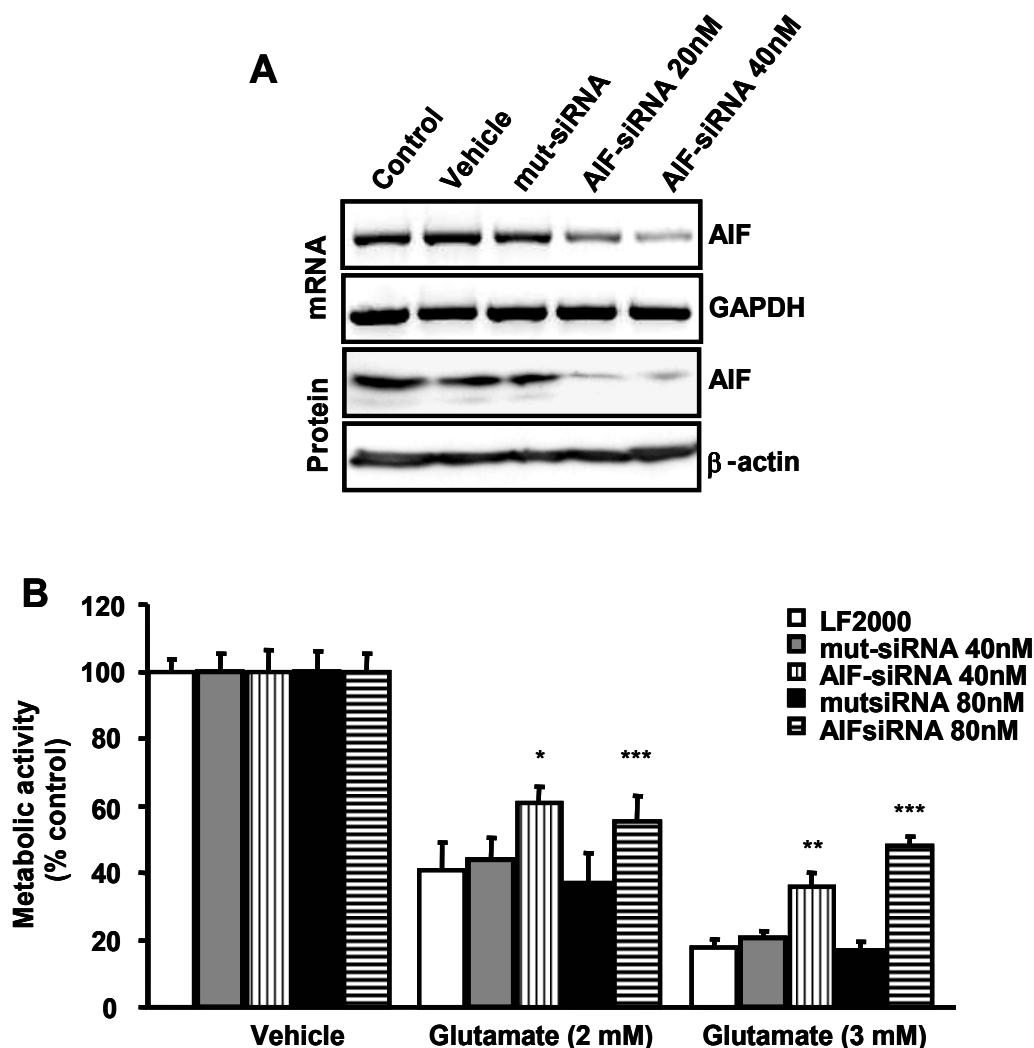


Figure 22: AIF-siRNA attenuates glutamate toxicity in HT-22 neurons.

A. AIF siRNA (20-40 nM) was applied to HT-22 neurons 48 h prior to analysis of mRNA levels by RT-PCR (upper panels) or protein analysis by Western blot (lower panels). Non-functional Mut-siRNA or Lipofectamine 2000 (vehicle) was applied in control experiments, GAPDH or β -actin was analyzed as respective controls for RT-PCR or Western blot, respectively. **B.** AIF-siRNA (40-80 nM) was applied to HT-22 neurons 48 h prior to glutamate (2-3 mM). Cell viability was assessed by the MTT assay 18 h later. Mean values and S.D. of $n=6$ experiments per group are shown; * $p<0.05$, ** $p<0.01$, and *** $p<0.001$ compared to respective mut-siRNA treatments (ANOVA, Scheffé's).

3.1.10.2 Bid inhibition prevents translocation of apoptosis inducing factor (AIF).

To evaluate the role of Bid in mitochondrial AIF release and subsequent nuclear translocation, HT-22 neurons expressing AIF-GFP fusion protein were exposed to glutamate and AIF translocation to the nucleus in the presence or absence of the Bid inhibitor was analyzed (Figure 23). The Bid inhibitor BI-6C9 blocked glutamate-induced AIF translocation as shown by confocal microscopy (Figure 23A) and Western blot analysis of cytosolic/mitochondrial and nuclear protein extracts (Figure 23B).

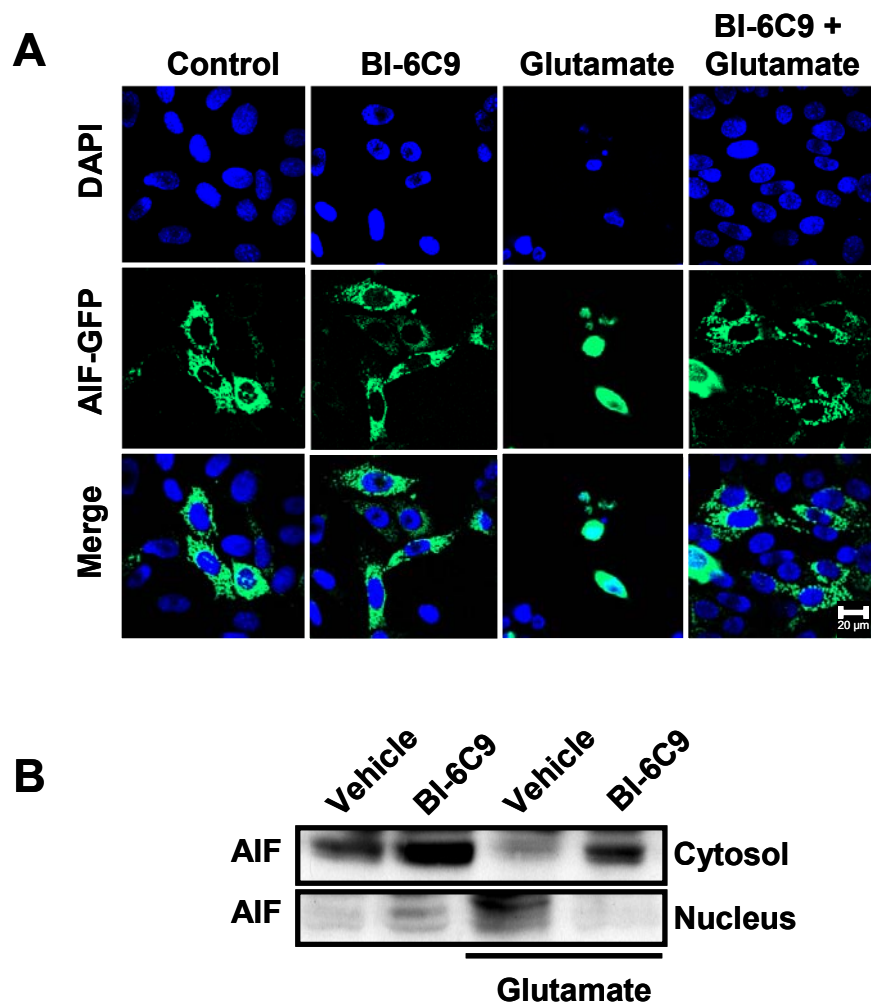


Figure 23: Bid-mediated glutamate toxicity requires AIF.

A. Fluorescence photomicrographs of HT-22 neurons expressing a AIF-GFP fusion protein show co-localization of GFP- and DAPI-signal in glutamate-damaged (2 mM, 17 h) cells. Bid inhibitor BI-6C9 (10 μ M) prevented the AIF translocation to the nucleus. **B.** Western blot analysis of cytosolic and nuclear protein extracts confirmed inhibition of glutamate-induced AIF translocation to the nucleus by the Bid inhibitor BI-6C9.

3.1.10.3 AIF-knockdown prevents tBid-induced cell death

In addition, experiments with AIF-silenced HT-22 neurons showed, that siRNA-mediated AIF knockdown prevented cell death induced by tBid-overexpression (Figure 24). This demonstrated that AIF mediates tBid-induced neurotoxicity.

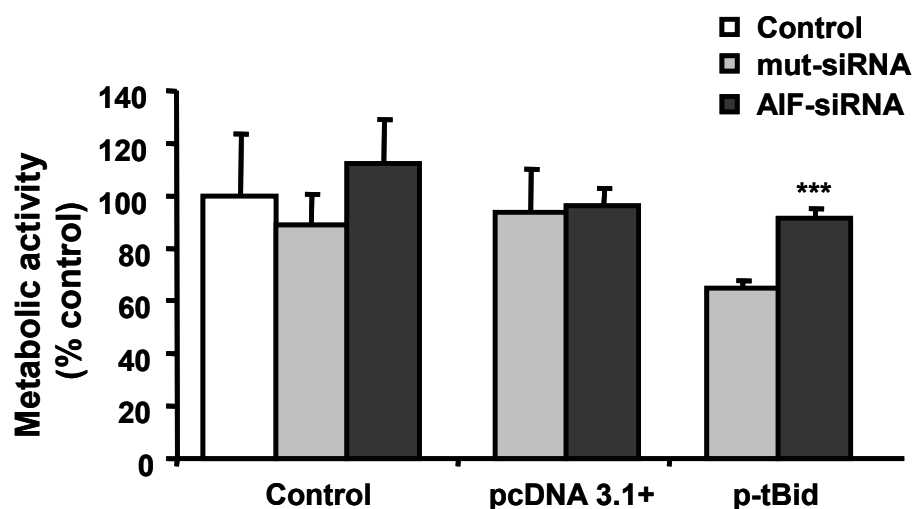


Figure 24: Bid-mediated cell death of HT-22 neurons requires AIF.

HT-22 neurons were transfected with AIF-siRNA (50 nM) 24 h prior to transfection with a tBid-expressing plasmid (1 μ g). Analysis of cell viability by the MTT assay 24 h later revealed protection of HT-22 neurons against tBid-induced cell death by AIF-siRNA. *** $p < 0.001$ compared to p-tBid transfected cells (Student's *t* test). Metabolic activity of HT-22 was neither affected by control plasmid 3.1+ or the nonfunctional mut-siRNA.

3.1.11 Mechanisms upstream of Bid-activation in glutamate neurotoxicity

Several proteases have been demonstrated to act upstream of Bid cleavage and mitochondrial transactivation, including, for example, caspases, calpains and cathepsins [89, 90]. In addition poly(ADP-ribose) polymerase (PARP1) and poly(ADP-ribose) glycohydrolase (PARG) have been described as major key mediators of apoptotic signaling [86], especially for the translocation of AIF from mitochondria [91]. Also, mitogen-activated protein kinases (Map kinases) are discussed in the literature to play a role in apoptosis and the release of pro-apoptotic factors from mitochondria. For example, inhibition of p38 Map kinase prevented the release of mitochondrial pro-apoptotic factors, such as AIF in ceramide-induced

neuronal apoptosis [92]. Thus, the influence of specific inhibitors of these potential pro-apoptotic factors was examined in glutamate-challenged HT-22 neurons.

3.1.11.1 Calpains

Calpains do not play a role in apoptosis of HT-22 neurons caused by glutamate. Pre-incubation of HT-22 neurons with the calpain inhibitor calpastatin in different concentrations, failed to prevent apoptosis induced by glutamate as determined by MTT-assay (Figure 25).

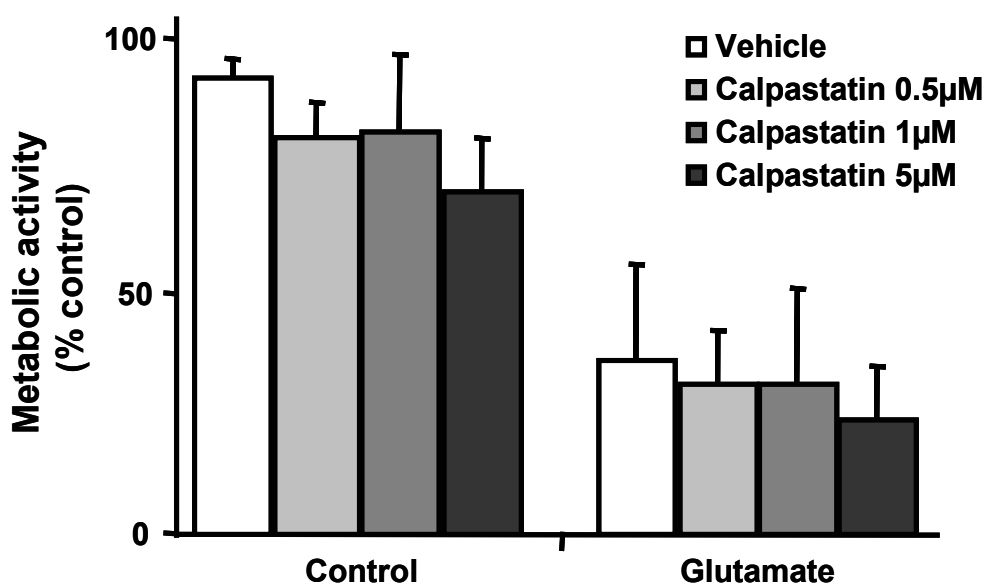


Figure 25: Calpastatin does not protect HT-22 neurons from glutamate-induced apoptosis. Inhibitor of calpain (calpastatin 0.5-5 µM) was applied 1 h prior to exposure of HT-22 neurons to glutamate (3 mM, 17 h). MTT assay showed no protective effect of calpastatin against glutamate toxicity.

3.1.11.2 Cathepsins

Cathepsins do not take part in mediation of apoptosis in HT-22 neurons after glutamate exposure. The Cathepsin inhibitor E-64-d showed no protective effect against glutamate toxicity in HT-22 neurons when applied one hour before glutamate-exposure. This was shown by the MTT-assay (Figure 26).

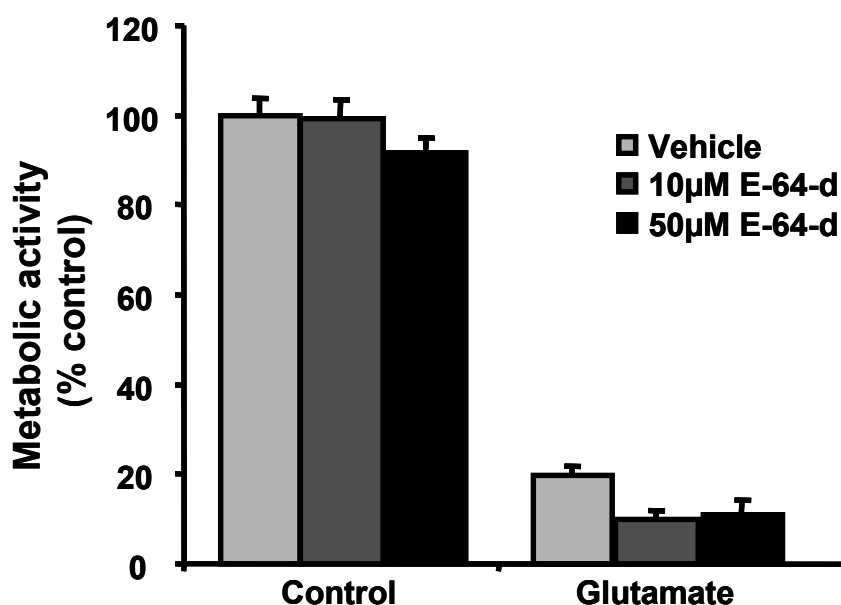


Figure 26: E-64-d showed no prevention of cell death in HT-22 neurons exposed to glutamate. Inhibitor of cathepsins (E-64-d 10-50 µM) was applied 1 h prior to exposure of HT-22 neurons to glutamate (3 mM, 17 h). MTT assay showed no protective effect of calpastatin against glutamate toxicity.

3.1.11.3 P38 MAP kinase

The p38 MAP kinase, a protein kinase involved in the cellular response to cytokines and stress does not participate in the mechanisms which are executed during glutamate treatment of HT-22 neurons. P38 MAP kinase phosphorylation was not altered during the cell death process (Figure 27A). Further, the involvement of p38 was investigated by applying the p38 inhibitor SB 203580, which did not prevent apoptosis at any concentration in glutamate-treated HT-22 neurons (Figure 27B).

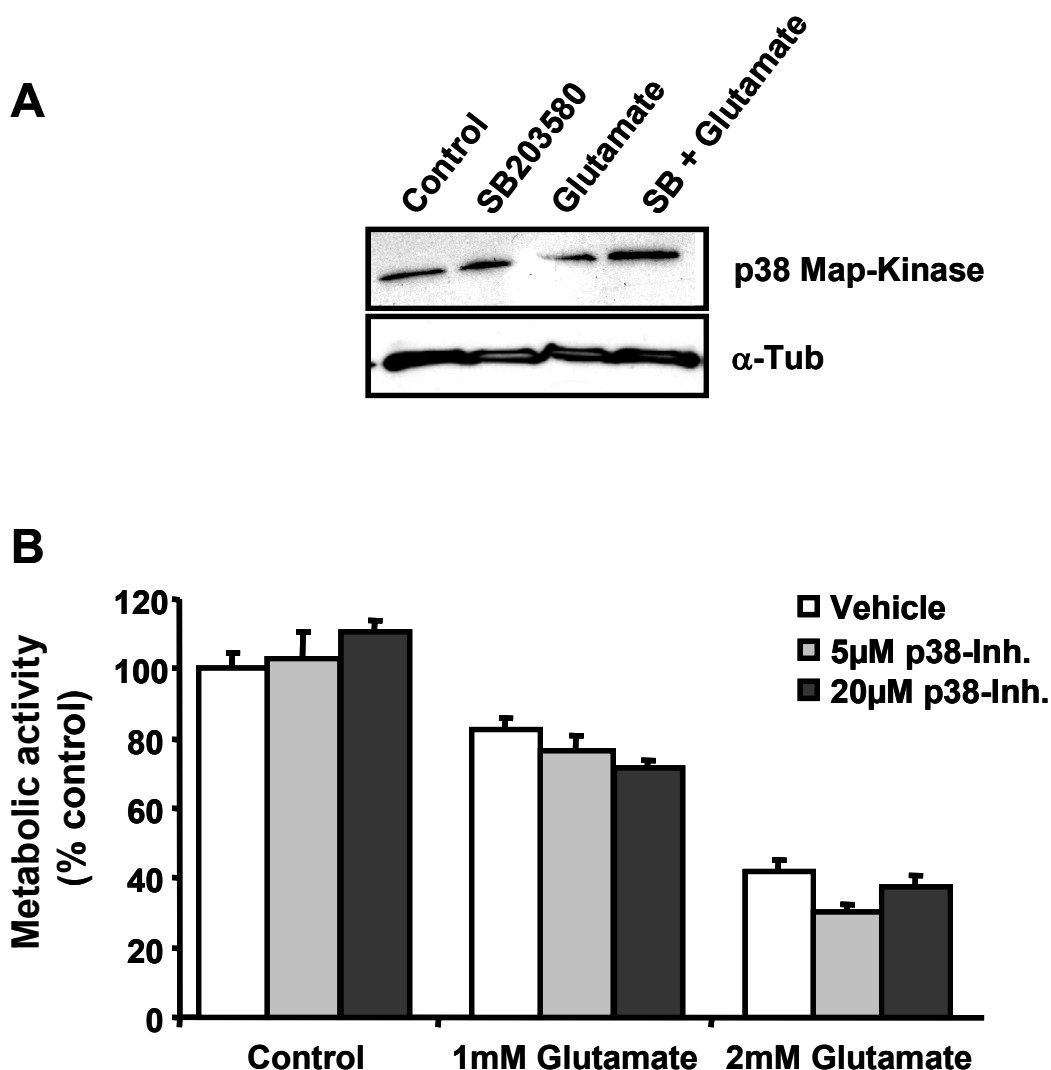


Figure 27: No enhanced phosphorylation of p38 MAPK after glutamate treatment and no prevention of cell death by inhibition of p38 MAPK in HT-22 neurons.

A. Western blot analysis of p38 MAP kinase phosphorylation in the total cell extract of HT-22 neurons before and after 6 hours of exposure to 3mM glutamate. Alteration of p38 phosphorylation was not detected. **B.** SB 203580 was applied 1h before glutamate-treatment of HT-22 neurons. Analysis of cell viability by the MTT assay 18 h later revealed no protection of HT-22 neurons against glutamate-induced cell death by SB 203580.

3.1.11.4 PARP1/PARG

It is interesting to note that inhibition of PARP1, which plays a role in the release of AIF, protects HT-22 neurons from glutamate toxicity (Figure 28A). In contrast, PJ34 did not protect HT-22 neurons against tBid-induced cell death. This result suggested

that PARP1 activation occurs upstream of Bid activation (Figure 28B). However, downregulation of PARG, which recently has been shown to be protective in cell death induced by oxidative stress, did not result in enhanced survival of HT-22 neurons challenged with glutamate (Figure 28C).

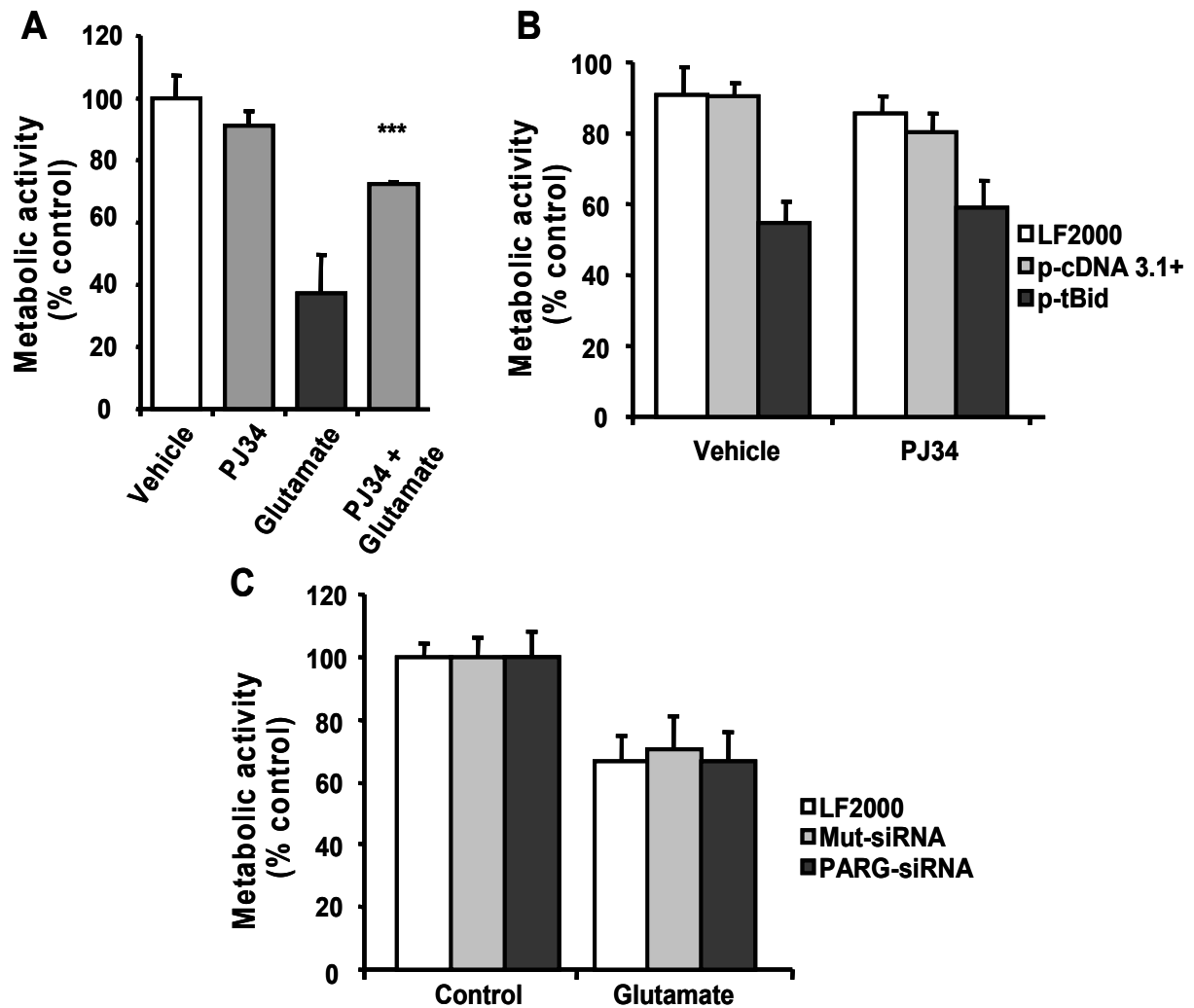


Figure 28: Inhibition of PARP1 but not PARG gene silencing reduces glutamate-induced cell death in HT-22 neurons.

A. The PARP inhibitor PJ34 (10 μ M) was applied 1 h before glutamate (2 mM) treatment. Cell viability, assessed by the MTT-assay 17 h later, showed attenuated decrease of metabolic activity in HT-22 neurons pretreated with PJ34. **B.** HT-22 neurons were pretreated with PJ34 (10 μ M, 1 h) before transfection with a tBid expressing plasmid (p-tBid). Twenty four hours later cell viability was determined with the MTT assay. **C.** Cells were transfected with mutant siRNA or PARG-siRNA (40 nM, 24 h) before glutamate exposure (3 mM, 18 h). Cell viability in glutamate-exposed cultures was significantly decreased by glutamate and was not influenced by PARG-siRNA.

3.1.11.5 Caspase-8

Since Bid is well known as a target of caspase-8 [25], the involvement of caspase-8 in glutamate-induced cell death was tested in HT-22 neurons. No activity of caspase-8 in HT-22 neurons exposed to glutamate could be detected in the activity assay (Figure 29A), suggesting that this pathway of Bid activation was not activated. This was confirmed by showing in the MTT-assay, that blocking caspase-8 activity by the specific inhibitor Z-IETD-FMK did not rescue HT-22 neurons from glutamate toxicity (Figure 29B).

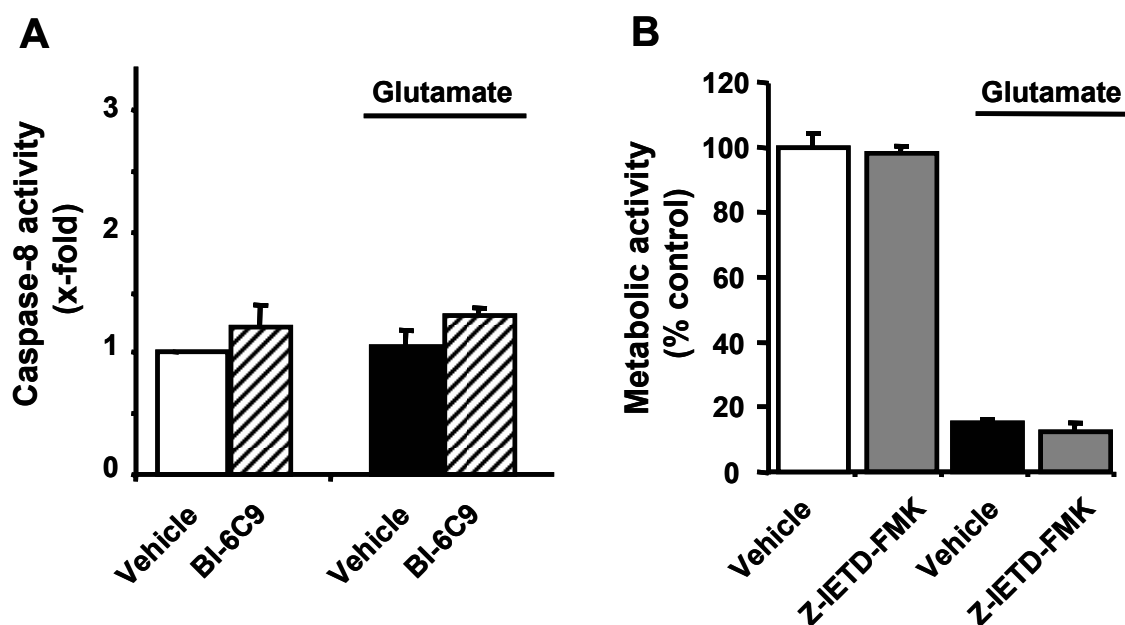


Figure 29: Caspase-8 is not activated during glutamate-induced cell death of HT-22 neurons.

A. Caspase-8 activity was analyzed in $n = 4$ independent experiments of the indicated treatment groups. Glutamate exposure (3 mM, 17 h) did not alter caspase-8 activity in HT-22 neurons. **B.** The specific caspase-8 inhibitor (Z-IETD-FMK, 50 μ M) was applied 1 h prior to exposure of HT-22 neurons to glutamate (3 mM, 17 h). Evaluation of cell viability by the MTT assay showed that Z-IETD-FMK failed to exert protection against glutamate-induced HT-22 cell death.

3.1.11.6 Caspase-2

DNA damage resulting from oxidative stress can lead to caspase-2 activation. Bid has been identified as a target of caspase-2 after cell death was induced by oxidative DNA damage. However, inhibition of caspase-2 by Z-VDVAD-FMK did not lead to an enhanced metabolic activity in glutamate-treated HT-22 neurons, as determined by the MTT-assay 17 hours after glutamate exposure (Figure 30).

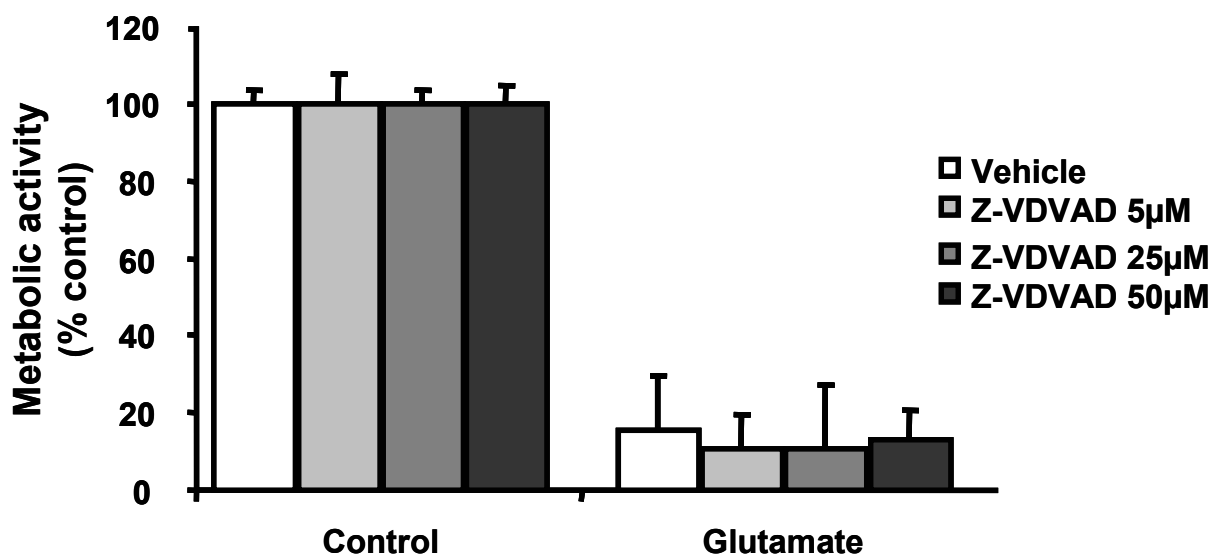


Figure 30: Inhibition of caspase-2 does not protect HT-22 neurons from glutamate. The specific caspase-2 inhibitor (Z-VDVAD-FMK, 5-50 µM) was applied 1 h prior to exposure of HT-22 neurons to glutamate (3 mM, 17 h). Evaluation of cell viability by the MTT assay showed that Z-VDVAD-FMK failed to protect against glutamate-induced HT-22 cell death.

3.1.11.7 Caspase-1

It has been reported, that caspase-1 is involved in hypoxia-induced Bid cleavage and in the burst of ROS levels after glutamate toxicity in neurons [21, 80]. In line with these previous findings, the caspase-1 inhibitor (ICE inhibitor II) attenuated glutamate toxicity in HT-22 neurons (Figure 31), but this protective effect was rather moderate compared to the pronounced protection achieved with the Bid inhibitor, in particular at high glutamate concentrations.

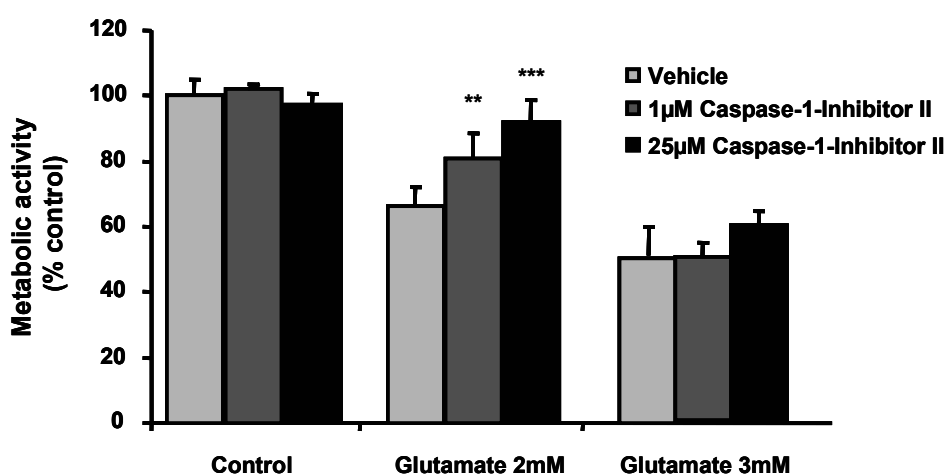


Figure 31: Moderate protection by caspase-1-inhibition.

Inhibitor for caspase-1 (ICE-inhibitor II, 1-25 µM was applied 1 h prior to exposure of HT-22 neurons to glutamate (2-3 mM, 17 h). Evaluation of cell viability by the MTT assay showed a moderate protective effect of the caspase-1 inhibitor. . ** $p < 0.01$ and *** $p < 0.001$ compared to glutamate-treated cells (ANOVA, Scheffé's).

3.1.11.8 Omi/HtrA2

In addition to the established potential proteases involved in Bid cleavage and AIF release, next the involvement of the serine protease Omi/HtrA2, which supports caspases by cleaving IAPs or caspase-independent pathways through its protease activity, was addressed [93, 94]. The MTT assay revealed a pronounced concentration-dependent protection by the Omi/HtrA2 inhibitor UCF-101 [38] (Figure 32A/B).

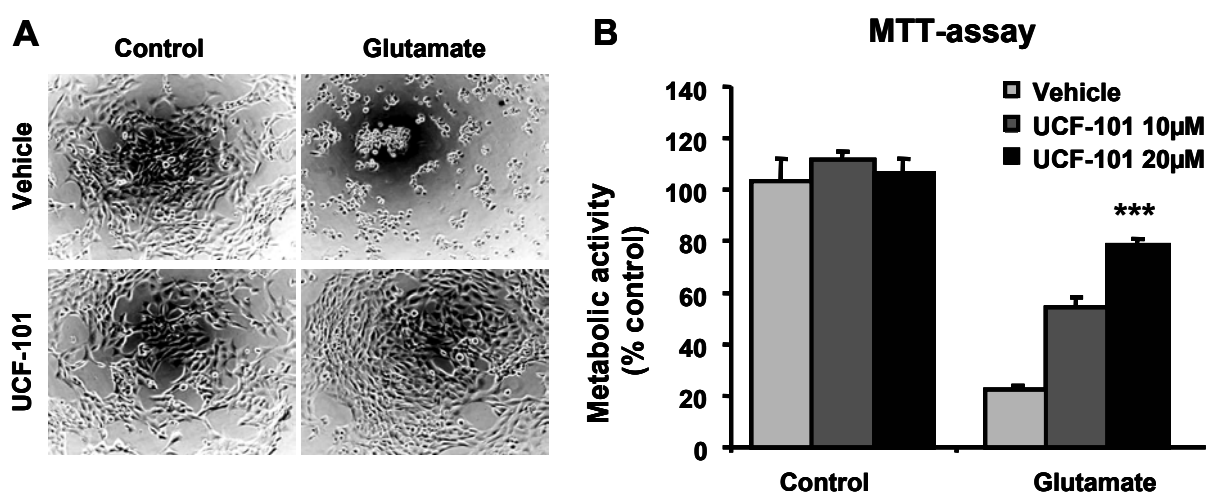


Figure 32: Involvement of Omi/HtrA2 activity in glutamate neurotoxicity.

A, B. The Omi/HtrA2 inhibitor UCF-101 (10-20 μ M) attenuates glutamate-induced cell death. UCF-101 was applied 1 h prior to glutamate exposure and cell viability was assessed by the MTT assay 18 h later. *** $p < 0.001$ compared to glutamate-treated cells (ANOVA, Scheffé's).

Moreover, the Omi/HtrA2 inhibitor prevented mitochondrial release and translocation of AIF to the nucleus of HT-22 neurons exposed to glutamate as shown in confocal microscopy pictures of HT-22, expressing the AIF-GFP fusion protein (Figure 32).

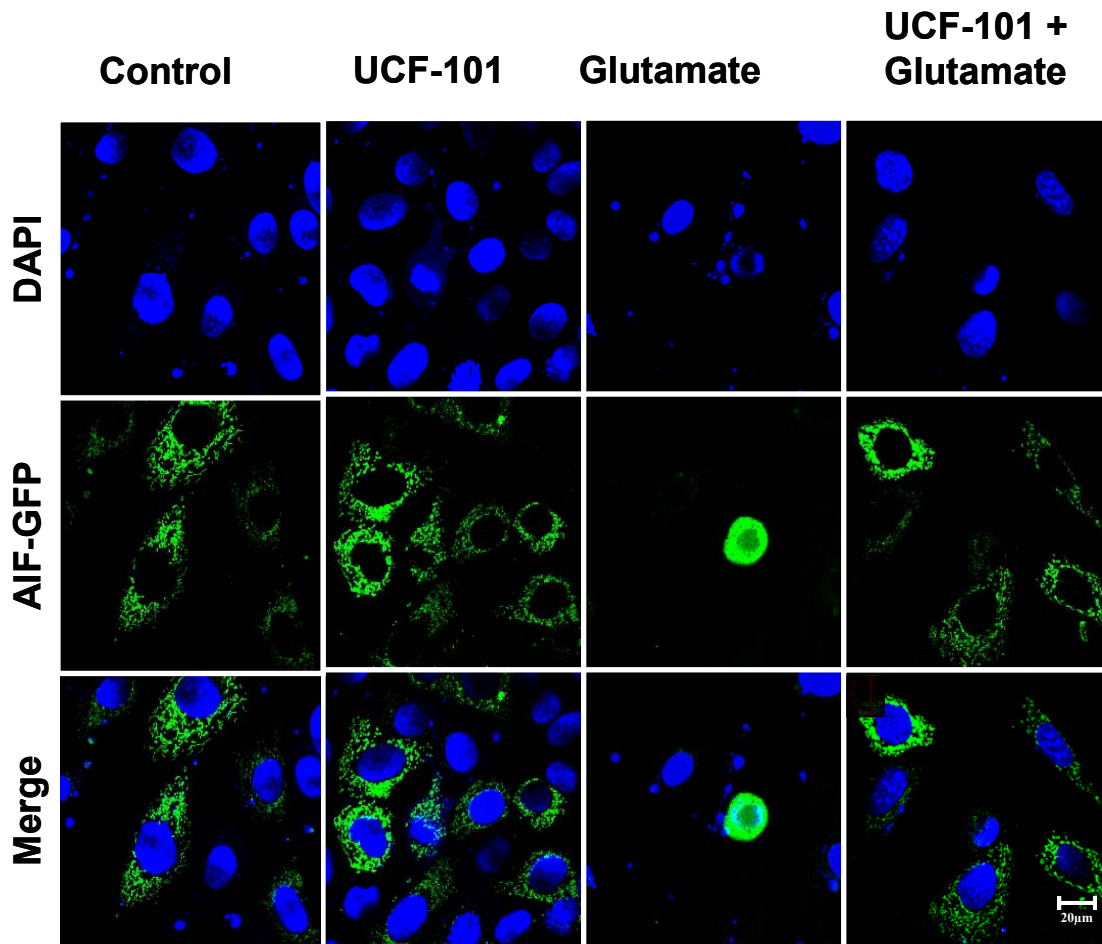


Figure 32: Inhibition of Omi/HtrA2 prevents AIF translocation in glutamate-treated HT-22 neurons.

Omi/HtrA2 inhibitor UCF-101 (10 μ M) prevents AIF translocation in AIF-GFP fusion protein-transfected HT-22 neurons exposed to glutamate. HT-22 neurons expressing AIF-GFP fusion protein (green) were treated with glutamate for 18 h, before staining with DAPI (blue) and analysis by confocal fluorescent microscopy. Glutamate-treated cells show translocation of AIF to the nucleus, whereas in controls and UCF-101-treated cells AIF remains located in the mitochondria.

However, UCF-101 did not prevent tBid neurotoxicity (Figure 33), suggesting that Omi/HtrA2 does rather act upstream than downstream of Bid-mediated mitochondrial demise.

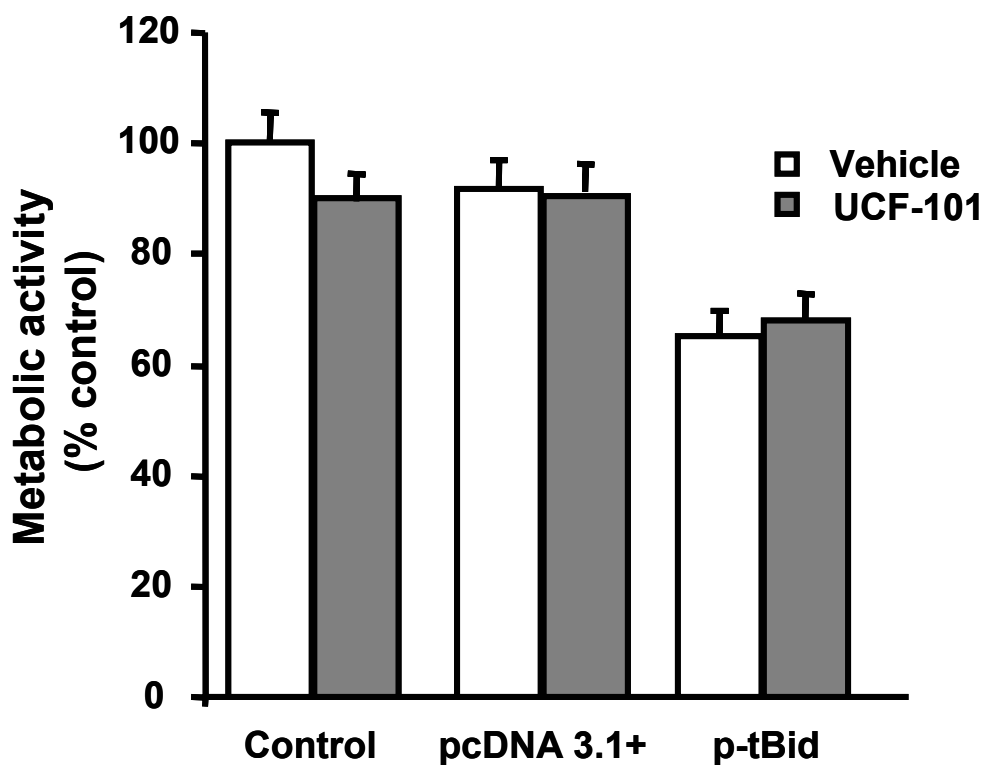


Figure 33: No protective effect of UCF-101 against tBid neurotoxicity. HT-22 neurons transfected with tBid expression vector showed reduced viability as assessed by MTT assay 24 h later. The Omi/HtrA2 inhibitor UCF-101 (10 μ M) failed to attenuate tBid-induced cell death in HT-22 neurons. Controls were transfected with an empty vector (pcDNA 3.1+).

This could be confirmed by the finding that HT-22 neurons pre-treated with AIF-siRNA, showed no enhanced protection against glutamate toxicity by additional application of the Omi/HtrA2 inhibitor UCF-101 (Figure 34). AIF-siRNA and UCF-101 alone exhibited similar significant protective effects in HT-22 neurons exposed to glutamate. When applied together, AIF-siRNA and UCF-101 showed no better protection of HT-22 neurons than AIF-siRNA in the UCF-101 lacking groups or UCF-101 in mut-siRNA- or un-transfected groups.

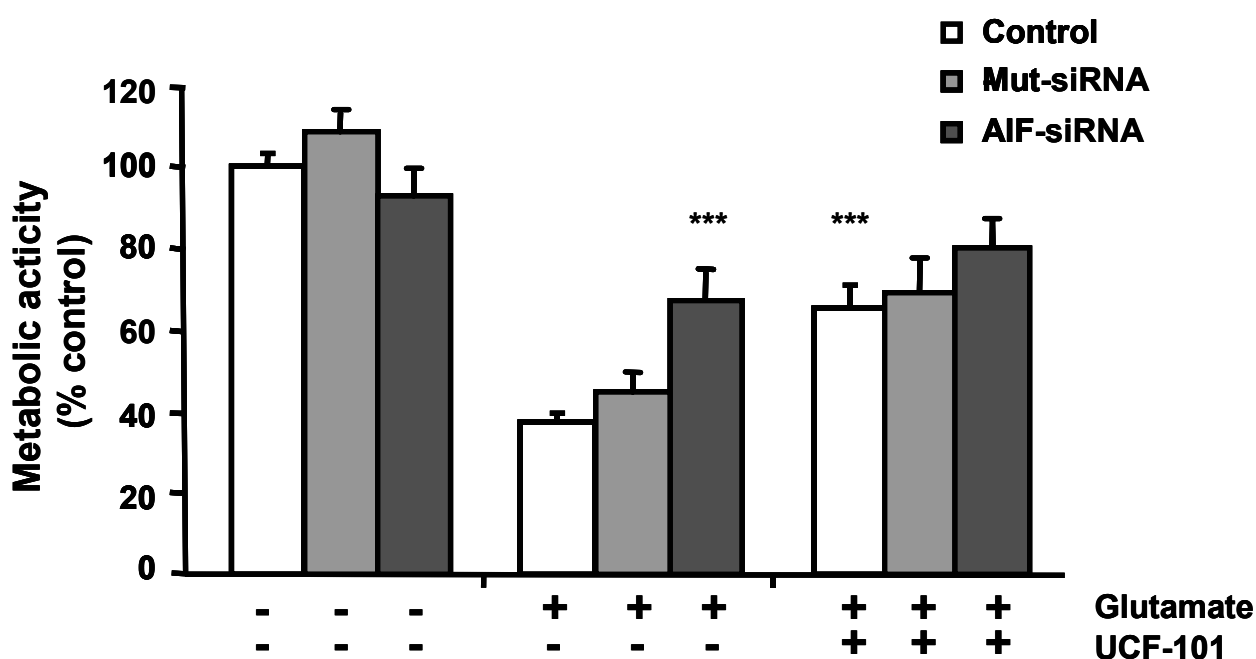


Figure 34: UCF-101 and AIF-siRNA protect HT-22 neurons against glutamate toxicity, but not in an additional manner.

AIF-siRNA (15 nM) was applied to HT-22 neurons 48 h prior to glutamate (1 mM) treatment which was performed on presence or absence of UCF-101 (10 μ M). Cell viability was assessed by the MTT assay 18 h later. *** $p < 0.001$ compared to glutamate-treated cells. Together, AIF-siRNA and UCF-101 showed no additional protective effect.

Similar to the caspase-1 inhibitor, the Omi/HtrA2-inhibitor provided only moderate protection when HT-22 neurons were exposed to high concentrations of glutamate (Figure 35). Compared with BI-6C9, UCF-101 never achieved protection efficiency as pronounced as the Bid inhibitor. A combination of caspase-1 inhibitor and UCF-101, however, provided an additive effect resulting in near complete protection against glutamate toxicity at moderate cell damage (60% with 3 mM glutamate) but not after severe cell damage (80% with 4 mM glutamate) (Figure 35).

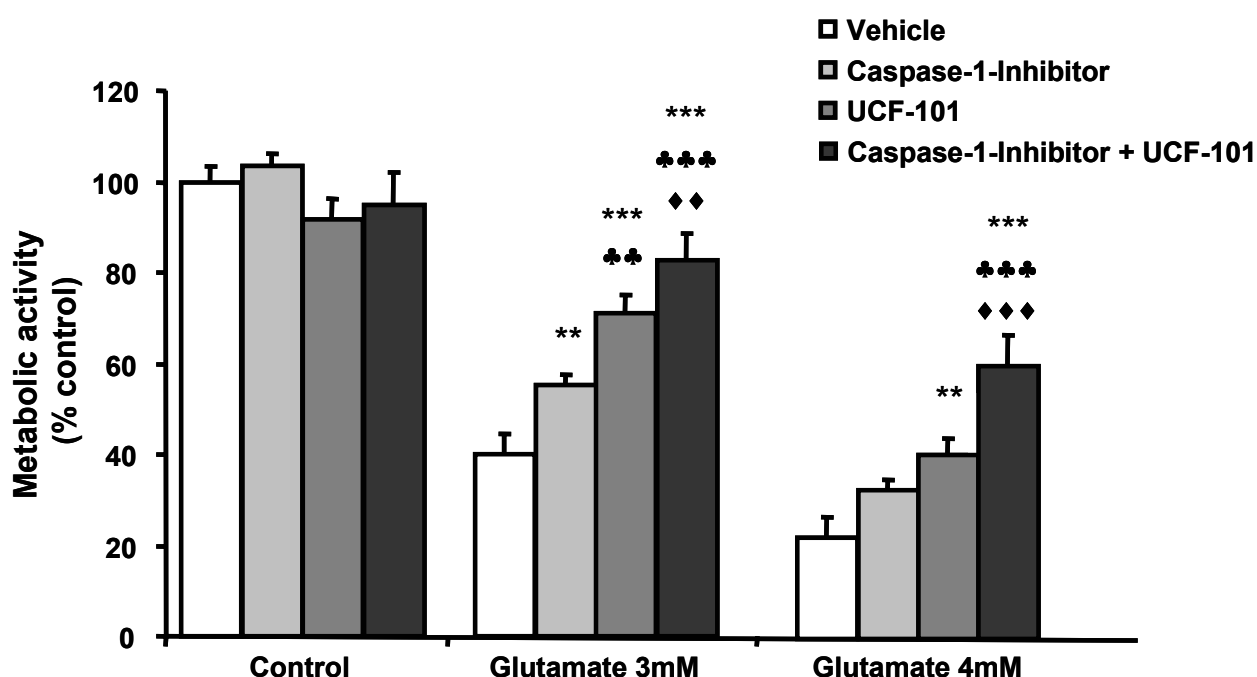


Figure 35: Inhibition of Omi/HtrA2 and caspase-1 exert additive protection against glutamate toxicity.

The caspase-1 inhibitor (ICE-Inhibitor, 25 μ M) and UCF-101 (10 μ M) were applied separately or in combination 1 h before exposure of HT-22 neurons to glutamate. Cell viability was determined 18 h later by the MTT assay. Note, that the caspase-1 Inhibitor and UCF-101 exert additive effects. The graph shows mean values and SD of 8 experiments per group. ** $p < 0.01$, *** $p < 0.001$ compared to the respective glutamate-treated cells. $\clubsuit\clubsuit\clubsuit p < 0.01$, $\clubsuit\clubsuit\clubsuit\clubsuit p < 0.001$ compared to caspase-1 inhibitor pretreated cells. $\blacklozenge\blacklozenge p < 0.01$, $\blacklozenge\blacklozenge\blacklozenge p < 0.001$ compared to the UCF-101 pretreated cells.

It is interesting to note that a combination of UCF-101 and the general caspase inhibitor (Z-VAD-FMK) exerted no additive protective effect against glutamate toxicity (Figure 36) as combinations of UCF-101 and the caspase-1 inhibitor (ICE inhibitor II) did. This suggests that the general caspase inhibitor did not efficiently block caspase-1, likely due to different IC₅₀ values of Z-VAD-FMK for the different caspases.

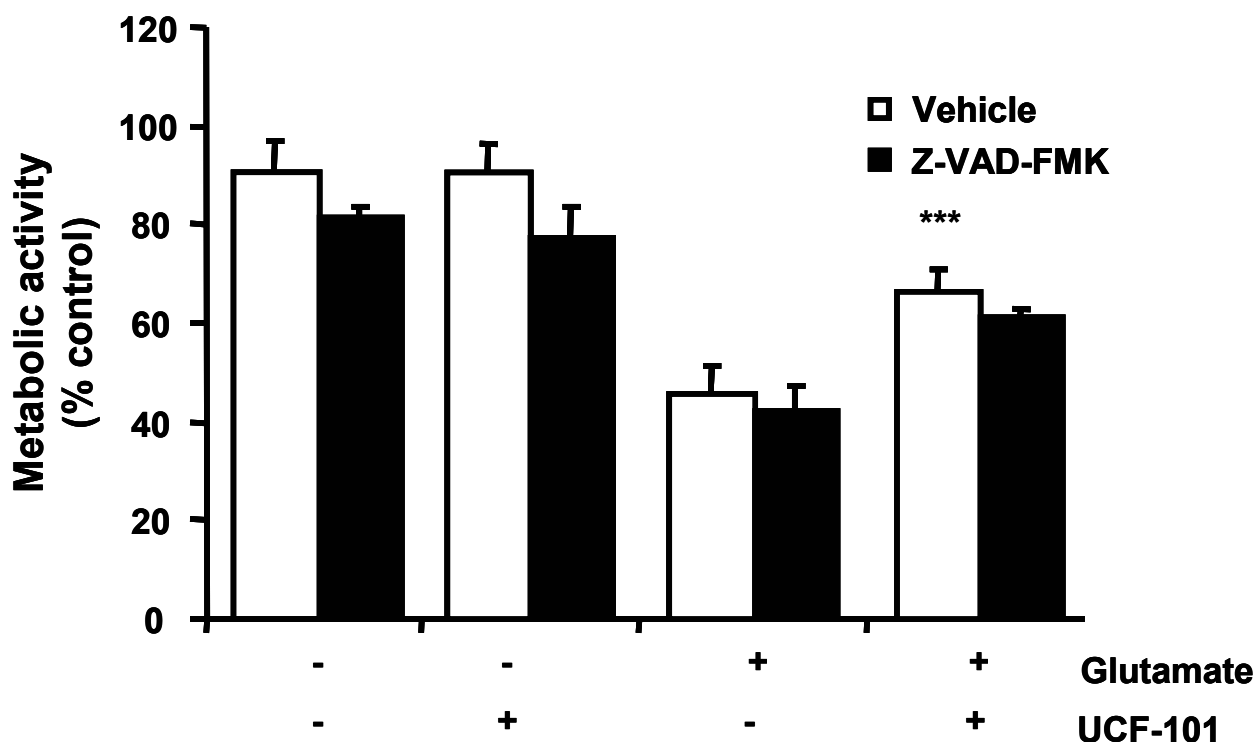


Figure 36: Combination of UCF-101 and Z-VAD-FMK did not exert additive protection against glutamate toxicity.

The general caspase inhibitor (Z-VAD-FMK, 50 μ M) and UCF-101 (10 μ M) were applied separately or in combination 1 h before exposure of HT-22 neurons to glutamate. Cell viability was determined 18 h later by the MTT assay. Note, that there was no additive effect when UCF-101 and Z-VAD-FMK were applied in combination. The graph shows mean values and SD of 8 experiments per group. *** $p < 0.001$ compared to glutamate-treated cells.

Since the data above suggested a role for Omi/HtrA2 upstream the activation of Bid, the ability of Omi/HtrA2 to cleave Bid was checked. However, recombinant serine protease Omi/HtrA2 was neither able to cleave Bid nor to accelerate Bid cleavage mediated by caspases in HT-22 cell protein extracts containing full length Bid (Figure 37A/B) suggesting that caspases can activate Bid in a direct manner while Omi/HtrA2 may operate through different mechanisms and acts on Bid in an indirect manner.

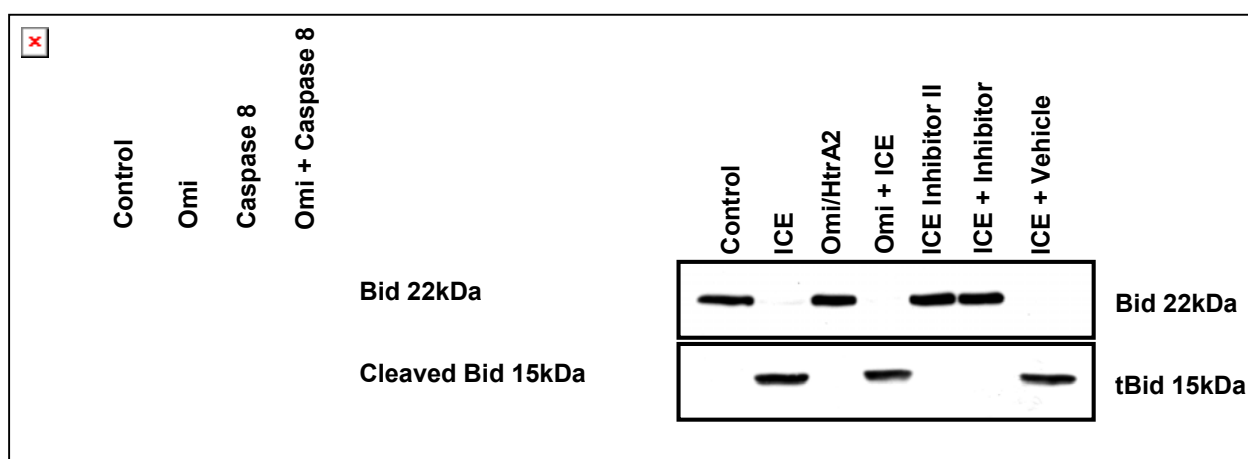


Figure 37: Bid is not a direct target of Omi/HtrA2.

A. Total protein extracts of HT-22 neurons were exposed to recombinant Omi/HtrA2 or caspase-8 for 10 min. Immunoblot analysis of the incubated extracts with a Bid antibody reveals Bid cleavage by caspase-8 but not by Omi/HtrA2. **B.** Total protein extracts of HT-22 neurons were exposed to recombinant caspase-1 [100 U], Omi/HtrA2 or a combination of both proteins for 10 min. Immunoblot analysis show Bid cleavage by 100 U of caspase-1. Bid cleavage was not detected at caspase-1 incubation in presence of its specific inhibitor (ICE inhibitor II, 25 μ M), and neither Omi/HtrA2 alone nor combinations of both proteases resulted in enhanced Bid cleavage.

3.2 Bid and AIF are not required in staurosporine-induced apoptosis

It remained to be clarified, however, whether this Bid-dependent pathway was a specific feature of glutamate-induced cell death or a general mechanism of apoptosis in neurons. Therefore, effects of the Bid inhibitor and AIF-siRNA were investigated after induction of apoptosis by staurosporine, an inducer of caspase-dependent apoptosis.

3.2.1 No protection from STS-induced cell death by Bid-inhibition

The Bid inhibitor BI-6C9 did not prevent STS-induced cell death as confirmed by the MTT assay (Figure 38A) and did not reduce the percentage of Annexin-V-positive cells after STS-damage in HT-22 neurons as confirmed by Annexin-V / PI-staining (Figure 38B/C).

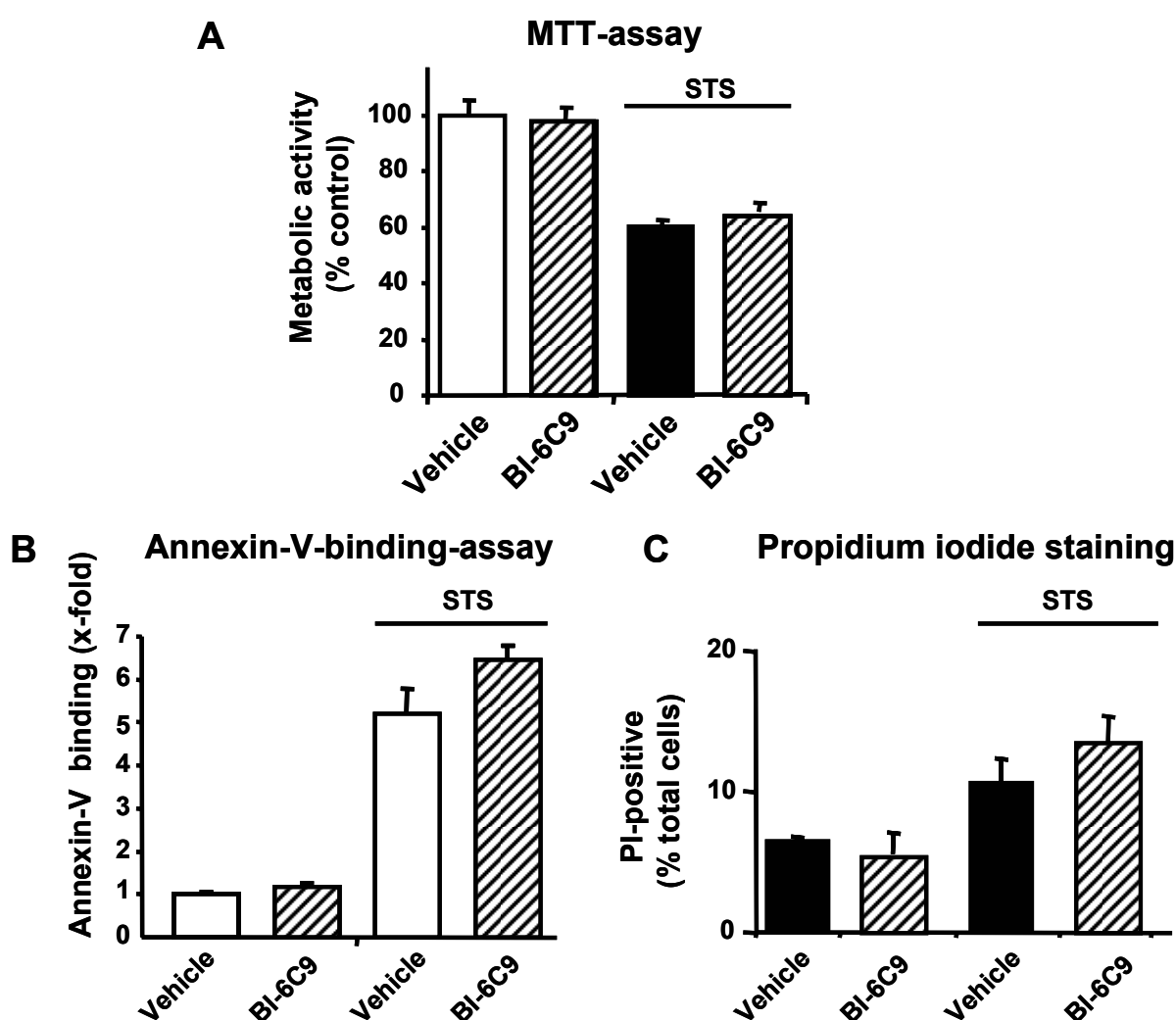


Figure 38: Bid is not required for staurosporine-induced apoptosis in HT-22 neurons.

A. Cell viability of HT-22 was determined by MTT assay 18 h after treatment with STS (300 nM). Pretreatment of HT-22 neurons with 10 μ M BI-6C9 1 h prior to onset of STS treatment did not attenuate cell death. **B.** FACS analysis of HT-22 neurons binding FITC-labeled Annexin-V 18 h after exposure to staurosporine (300 nM). The Bid inhibitor BI-6C9 (10 μ M, 1 h prior to damage) did not reduce apoptosis induced by STS. **C.** FACS analysis of necrotic HT-22 neurons after labeling with propidium iodide (PI). Note that the increase in PI positive cells after STS exposure (300 nM) is far less pronounced compared to the increase in Annexin-V-labeling. BI-6C9 (10 μ M) treatment before STS-exposure did not significantly affect the percentage of PI positive cells to control levels.

3.2.2 STS-induced cell death does not involve AIF translocation

Analysis of AIF translocation after the STS challenge in AIF-GFP fusion protein transfected HT-22 neurons revealed that AIF was not released from mitochondria and did not translocate to the nucleus in damaged neurons (Figure 39).

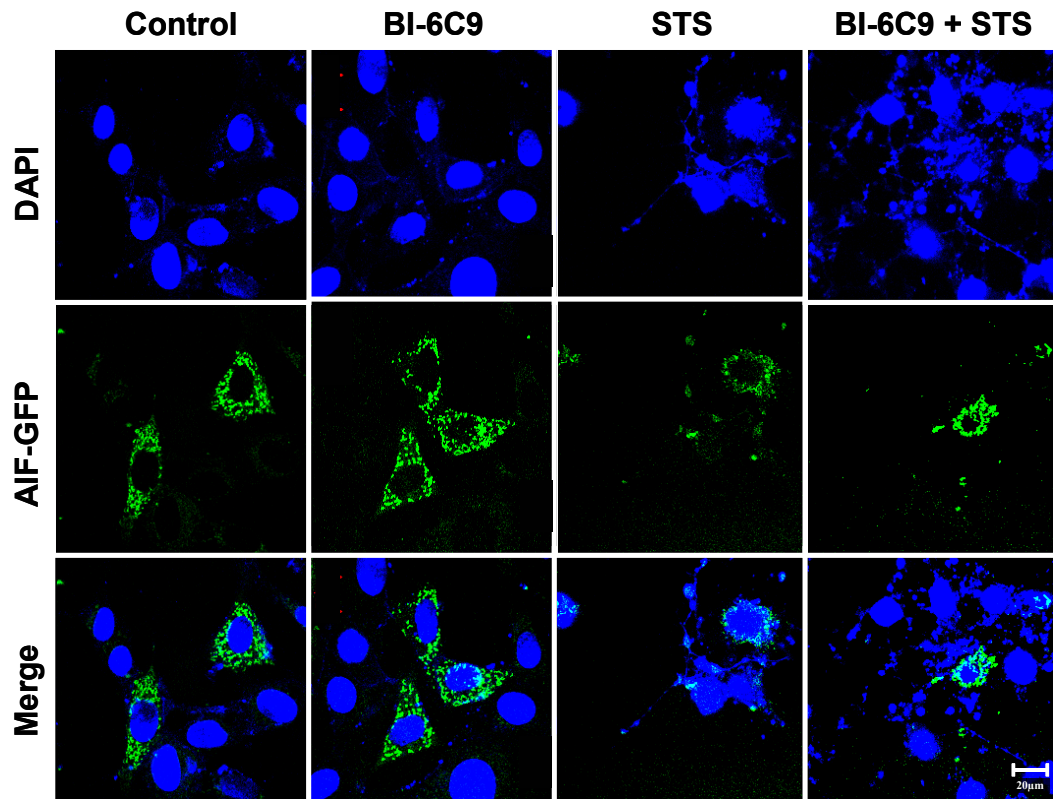


Figure 39: AIF does not translocate to the nucleus in STS-treated neurons.

HT-22 neurons expressing AIF-GFP fusion protein (green) were treated with STS for 18 h, before staining with DAPI (blue) and analysis by confocal fluorescent microscopy. The Bid inhibitor BI-6C9 does not prevent DNA condensation and nuclear fragmentation of HT-22 neurons, and AIF remains located in the mitochondria of and does not translocate to the nucleus of damaged cells.

3.2.3 AIF-knockdown does not rescue HT-22 neurons from apoptosis by STS-treatment

After demonstrating a non-involvement of AIF in STS-induced apoptosis, AIF gene silencing by AIF-siRNA transfection did not affect STS-induced apoptosis, neither. In contrast, there was a pronounced protection against glutamate toxicity.

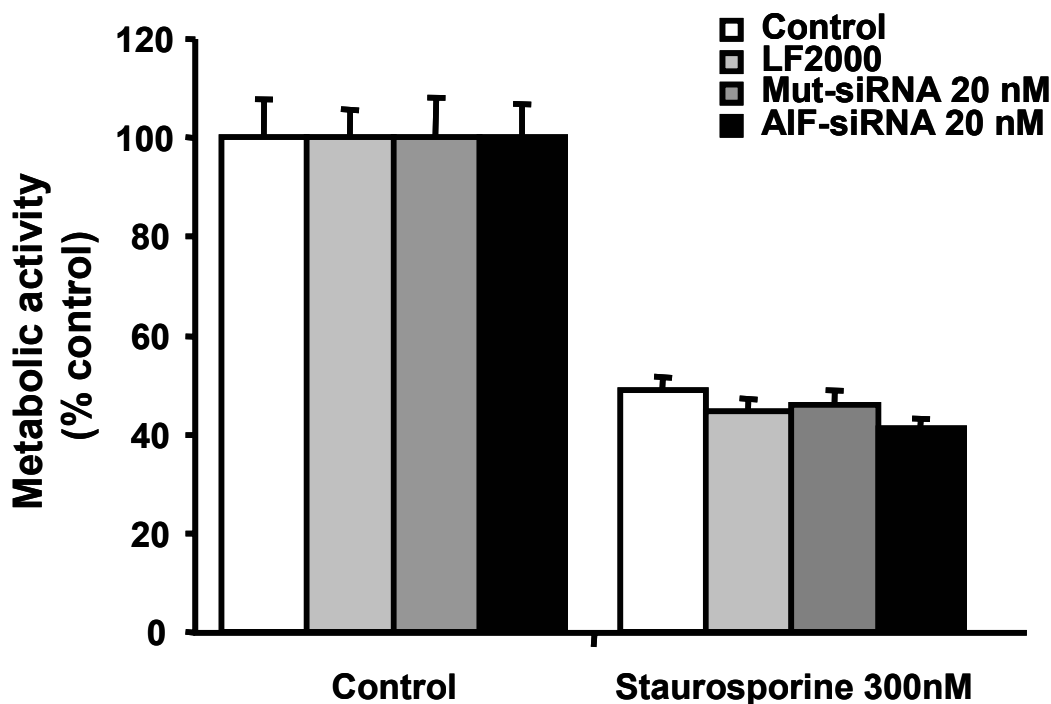


Figure 40: AIF is not required for staurosporine-induced apoptosis in HT-22 neurons.

Cells were transfected with mutant siRNA or AIF-siRNA (20 nM, 48 h) before STS (300 nM, 18 h) exposure. Cell viability in STS-exposed cultures was significantly decreased by STS and was not influenced by AIF-siRNA.

3.3 Role of Bid and AIF in glutamate-induced apoptosis of primary rat neurons

Since HT-22 neurons do not express glutamate receptors, they can not be used as a model for excitotoxic glutamate damage as it occurs in primary rat neurons for example in stroke and brain trauma. But glutamate-induced apoptosis in HT-22 neurons as well as excitotoxicity induced by glutamate in primary neurons, both end up in an increase of reactive oxygen species and subsequent mitochondrial damage.

Therefore, glutamate damage of HT-22 neurons was used as a reproducible, easy to handle model of apoptosis in neuronal cells. To confirm the data found in HT-22 neurons, different tests in primary rat neurons were established. Thereby a key role for AIF and Bid was found as it was pronounced in glutamate-induced apoptosis of HT-22 neurons.

3.3.1 AIF-knockdown rescues primary neurons from apoptosis

In primary hippocampal neurons, AIF-siRNA (dicer product) induced complete loss of AIF mRNA within 48 h and significant reduction of AIF protein 48 h after onset siRNA treatment (Figure 41A). Housekeeping proteins such as GAPDH or α -Tubulin were not affected by AIF-siRNA, and mutant siRNA control sequences affected neither AIF mRNA nor protein levels nor the housekeeping proteins GAPDH or α -Tubulin (Figure 41A). SiRNA-mediated knock-down of AIF resulted in a significant reduction of apoptotic nuclei after glutamate-induced neuronal cell death (Figure 41B). After glutamate treatment, >90% of cells displayed condensed nuclei in control cultures, whereas only $58 \pm 8\%$ of AIF-siRNA-treated cells showed signs of nuclear apoptosis ($p < 0.01$) (Figure 41C).

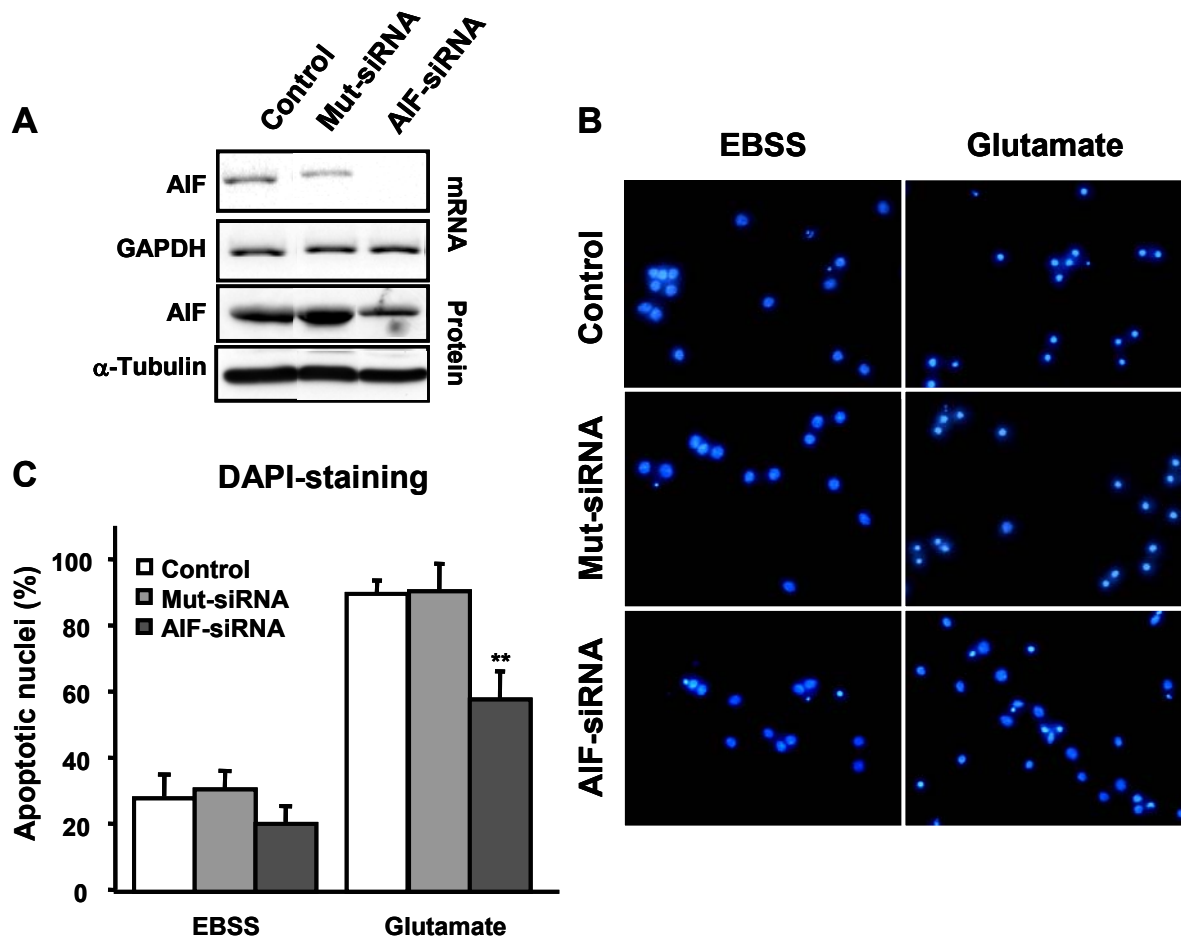


Figure 41: Reduced glutamate-induced apoptosis in primary neurons pretreated with AIF-siRNA.

A. AIF mRNA and protein were significantly downregulated, as demonstrated by RT-PCR (top 2 rows) and Western blot analysis (bottom 2 rows), respectively, in primary hippocampal neurons pretreated with AIF-siRNA for 48 h. RT-PCR for GAPDH (bottom) and Western blotting for α -tubulin were performed as controls. **B.** Fluorescence microscope images of DAPI-stained embryonic hippocampal neurons were obtained after 48 h of exposure to 20 μ M glutamate in EBSS medium. Only cultures pretreated with 20 nM AIF-siRNA contained >50% healthy nuclei, whereas all other glutamate-treated groups showed >85% pyknotic and/or fragmented nuclei, indicating apoptotic damage (Glutamate, right column). The respective control cultures with EBSS medium contained only very few apoptotic nuclei (Control, left column). **C.** Primary hippocampal neurons were left untreated (Controls) or were pretreated with 20 nM nonfunctional mutant siRNA (mut-siRNA), or 20 nM AIF-siRNA for 48 h. On day 9, cells were exposed to 20 μ M glutamate in EBSS medium for 48 h. Thereafter, neurons were fixed with paraformaldehyde, and apoptotic nuclei were quantified after staining with DAPI. Pretreatment with AIF-siRNA significantly reduced apoptotic cell death compared with the other cultures exposed to glutamate ($n=4$; ** $p<0.01$ versus all other glutamate-treated groups).

3.3.2 Bid inhibitor prevents translocation of AIF

Inhibition of Bid by 2 μM BI-11A7, which was always applied in primary neurons, because of the insolubility of BI-6C9 in EBSS, reduced nuclear AIF translocation and neuronal cell death after glutamate treatment (20 μM , 6 h) compared to control levels (Figure 42A/B). This result suggests that similar to glutamate-induced apoptosis in HT-22 neurons, in excitotoxic apoptosis of primary cortical neurons nuclear AIF translocation occurs downstream of Bid activation and that Bid may be responsible for the release of AIF from mitochondria.

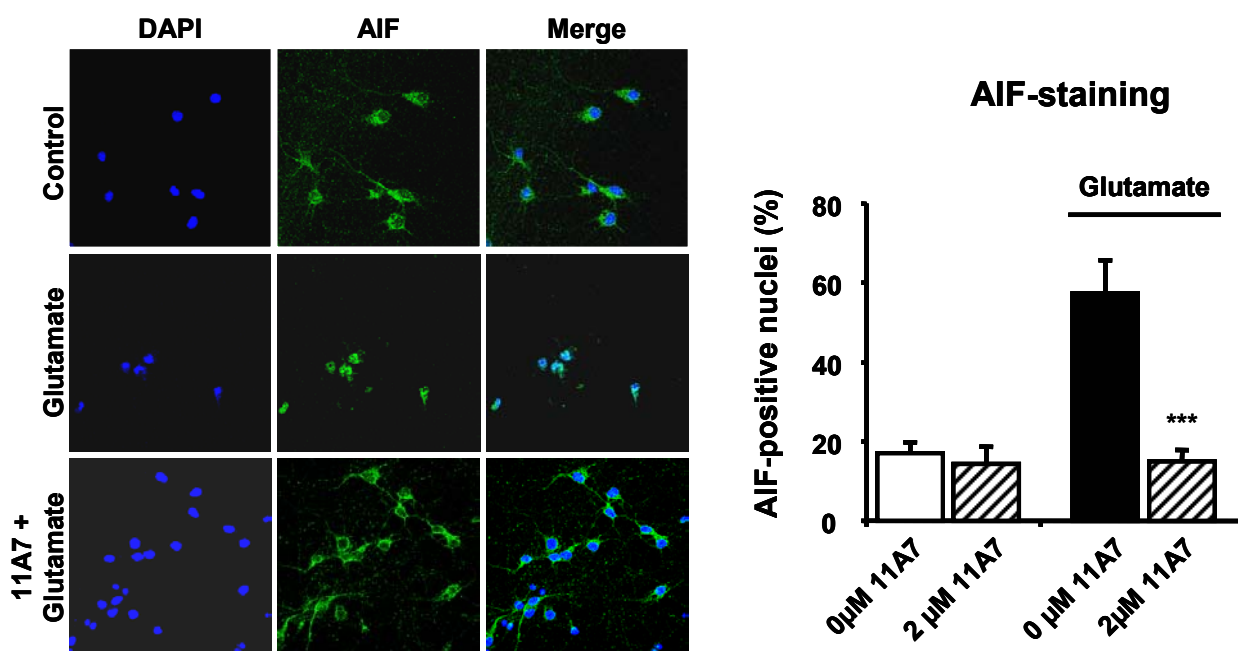


Figure 42: BI-11A7 prevents AIF translocation after excitotoxicity by glutamate in primary cortical neurons.

A. Immunostaining of rat embryonic cortical neurons shows translocation of AIF (green fluorescence) to the nucleus 6 h after exposure to glutamate. Pretreatment with BI-11A7 (2 μM) preserves nuclear morphology (blue fluorescence, Hoechst 33342) and prevents AIF translocation. **B.** Quantification of AIF positive nuclei in rat embryonic neurons exposed to glutamate (20 μM) for 6 h. Mean values and SD of four dishes per group are presented. *** $p < 0.001$ compared to glutamate-treated cells.

3.3.3 Bid-inhibition prevents apoptosis of primary rat neurons

In addition it could be shown that prevention of AIF translocation in primary neurons resulted in the prevention of cell death, i.e. apoptosis. Pretreatment with Bid inhibitor BI-11A7 1 h prior to glutamate (20 μM , 24 h) exposure showed a significant reduction

of apoptotic nuclei (Figure 43A). After glutamate treatment, >80% of cells displayed condensed nuclei in control cultures, whereas only 25% of BI-11A7-pretreated cells showed signs of nuclear apoptosis (Figure 43B). It is interesting to note that the Bid inhibitor provided neuroprotective effects in a dose dependent manner. Quantification of pyknotic nuclei could be confirmed by the MTT-assay.

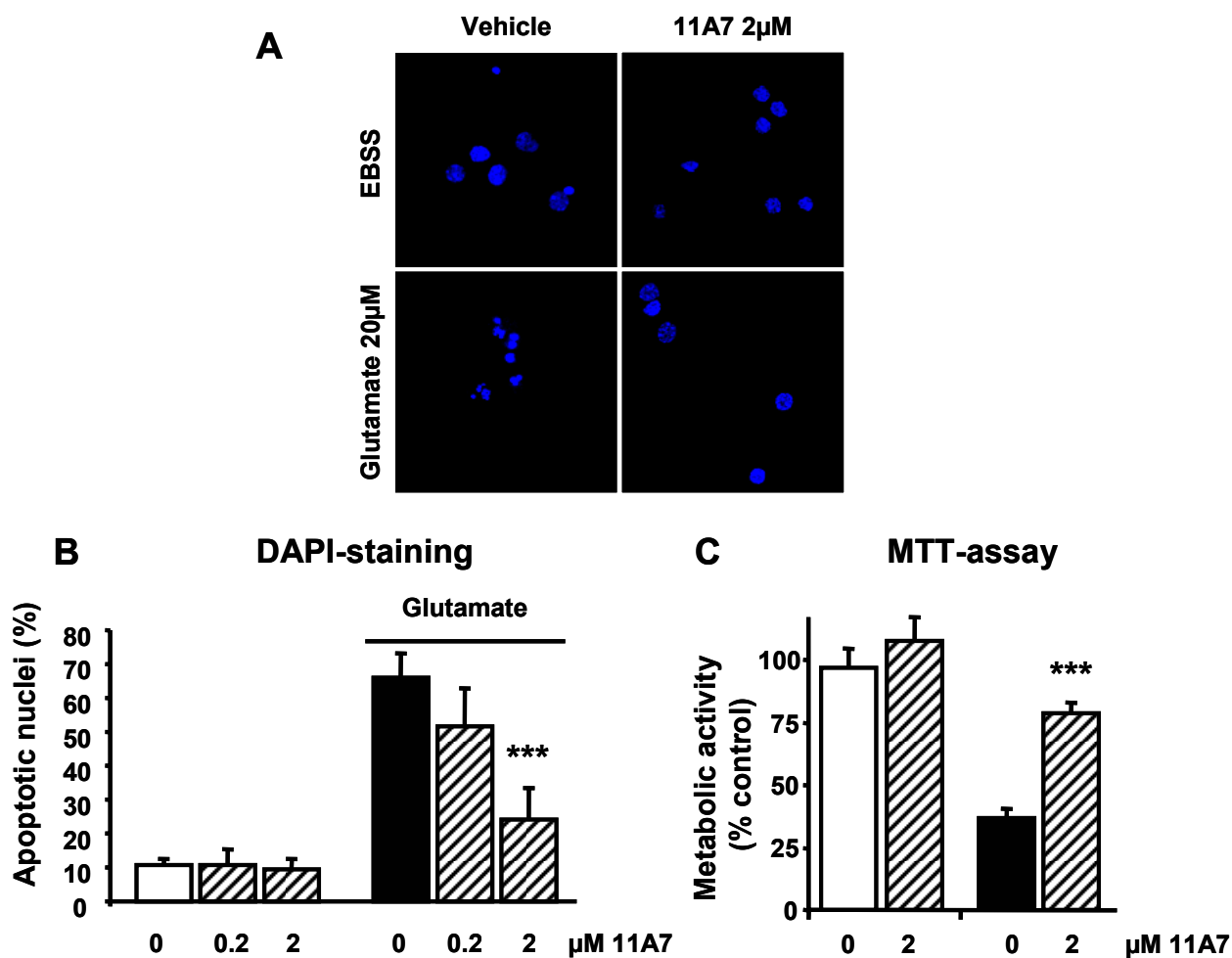


Figure 43: Bid inhibitor BI-11A7 prevents excitotoxicity-induced apoptosis of primary rat hippocampal and cortical neurons.

Hippocampal (A) or cortical (B, C) neurons were pretreated with BI-11A7 at the indicated concentrations 1 h before exposure to glutamate (20 µM) in EBSS. After 24 h, apoptotic nuclei were quantified after staining with Hoechst 33342. C. In a separate experiment, the protective effect of BI-11A7 against glutamate-induced cell death was quantified by the MTT-assay. The graphs show mean percentages of apoptotic nuclei (A) or cell viability (C) and SD of five separate dishes per group. *** $p < 0.001$ compared with glutamate-treated cells (ANOVA, Scheffé's).

4 Discussion

The present thesis demonstrates a key role for Bid in mitochondrial membrane permeabilization and the subsequent release of AIF after glutamate-induced cell death in HT-22 neurons. Both, Bid gene silencing and pharmacological inhibition of Bid significantly protected HT-22 neurons against glutamate toxicity and inhibition of Bid prevented breakdown of mitochondrial membrane potential and AIF translocation to the nucleus. Strikingly, AIF gene silencing prevented tBid induced neurotoxicity, which strongly suggests a particular role for AIF and thus caspase-independent execution of cell death downstream of Bid. Many factors which have been previously discussed to mediate the activation of Bid, including calpains, cathepsins and caspase-2 were not found to be involved in glutamate-induced apoptosis of HT-22 neurons. In contrast, caspase-1 and Omi/HtrA2 were suggested to act upstream mitochondrial damage and to be involved in the activation of Bid. Additionally, it has been demonstrated that excitotoxic cell death in primary neurons depends on Bid and AIF as well. Therefore, it is proposed that the model of glutamate-damage in HT-22 is relevant for mechanisms involved in excitotoxic cell death of primary neurons.

4.1 Glutamate damage in HT-22 neurons: A model for oxidative stress induced apoptosis

Glutamate causes cell death in HT22 neurons by oxidative stress, not by excitotoxicity through glutamate receptor-mediated calcium influx. In HT-22 neurons, which lack functional glutamate receptors, glutamate blocks the glutamate-cystine antiporter system [20]. Therefore, cysteine, which is required for glutathione synthesis, is missing and glutathione levels decrease in the cell. As a consequence, levels of reactive oxygen species (ROS) increase within a few hours after glutamate treatment of HT-22 neurons by the initial breakdown of the free radical detoxification system. This initial ROS formation leads to mitochondrial damage which is the reason for a secondary explosive burst of ROS levels [21]. In addition, an elevation of cytosolic calcium levels occurs [95], similar to the increase of calcium levels induced

by excitotoxicity in primary neurons, which suggests glutamate toxicity in HT-22 neurons as an adequate model for glutamate-induced cell death of neurons. Bid-siRNA significantly inhibited the burst of free radical generation in HT-22 neurons exposed to glutamate suggesting that the initial oxidative stress by glutathione depletion requires Bid-mediated mitochondrial amplification. Therefore, the present findings expose Bid as a major mediator of ROS-induced cell death through mitochondrial pathways. It is important to note that the small molecule Bid inhibitors do not prevent cell death after exposure to H₂O₂. This excludes free radical scavenger properties of these Bid inhibitors. In contrast to the protective effect by inhibition of Bid, inhibition of Bax, a Bcl-2 family member which interacts with Bid to permeabilize the mitochondrial membrane [96], could not protect HT-22 neurons from glutamate damage. Similar results were obtained in excitotoxicity-induced apoptosis in primary neurons. In these primary cells, Bax-knockdown had not protective effect, whereas knockdown of Bid and AIF protected neurons against glutamate [Cardoso et al., FENS meeting, Vienna, 2006]. These findings and the current results of this thesis indicate a major involvement of Bid in mitochondrial damage and the subsequent execution of apoptosis, which may occur independently of the interaction of Bid with Bax.

4.2 Bid-dependent AIF-release in glutamate-induced apoptosis of HT-22 neurons

A second important aspect of the present study addresses the role of AIF mediating caspase-independent cell death downstream of Bid activation. Using the AIF-GFP construct mitochondrial release of AIF and translocation to the nucleus could be demonstrated, which occurred around 8-10 h after the onset of glutamate exposure. Time laps video recordings showed that the time point of massive AIF translocation to the nucleus after onset of the glutamate challenge may vary from cell to cell, but once started, the AIF translocation takes place within 15 min and is followed by rapid nuclear condensation and fragmentation of the cells. AIF-siRNA significantly attenuated glutamate-induced neurotoxicity in HT-22 neurons (Figure 20, 22) and in primary neurons (Figure 41); most intriguingly, AIF siRNA prevented tBid-induced cell

death in HT-22 neurons, clearly demonstrating that Bid-induced cell death was executed by AIF. Of note, confocal microscopy of AIF-GFP expressing HT-22 neurons as well as western blot analysis of cytosolic and nuclear protein extracts revealed that the Bid inhibitors prevented the translocation of AIF from mitochondria to the cytosol. These results suggest that AIF dominates the potential pathways to neuronal cell death triggered by Bid after the glutamate challenge. This finding is well in line with recent data where we and others demonstrated a key role for AIF in delayed neuronal cell death after excitotoxic, or hypoxia/ischemia insults in vitro and in vivo. It has been shown that Hq mice, which express only about 20% AIF in comparison to their wildtype littermates, exhibit protection against different stimuli such as excitotoxicity by glutamate or kainate or even ischemia by middle cerebral artery occlusion (MCAO). Similar results were obtained in the corresponding in vitro models of glutamate and kainate toxicity or oxygen-glucose deprivation [97, 98].

Further, these results propose that the release of pro-apoptotic factors is a coordinated process where the release of a particular apoptotic factor and its role in the execution of apoptosis also depends on the stress challenge and the pathway to mitochondrial damage. Very little is known on the proposed regulated release of particular mitochondrial factors in apoptotic cells and in damaged neurons in particular. Recent data demonstrated that AIF release requires cleavage of the protein which is localized at the inner membrane of the mitochondrial intermembrane space [99, 100], and possible candidates for such proteolytic processing of AIF for mitochondrial release are, for example, calpains [75]. However, other proteases which may be activated independent of calcium levels have been postulated but not yet identified to mediate such AIF processing [100]. In addition, inhibition of poly (ADP-ribose) polymerase 1 (PARP1), a molecule responsible for neuronal cell death for example after cerebral ischemia [101], resulted in an attenuated damage of HT-22 neurons after glutamate exposure. These results confirmed previous studies which demonstrated a protective effect of PARP1 inhibition in oxygen glucose deprivation of primary neurons and focal cerebral ischemia in mice [98]. In these models it has been suggested that mitochondrial NAD^+ depletion, which is caused by overactivation of PARP1, may represent the link between PARP activation and the

release of AIF from mitochondria [91]. In contrast, inhibition of PARP1 was not able to prevent cell death in HT-22 neurons overexpressing tBid. Together these data suggest that activation of PARP1 during glutamate-damage of HT-22 neurons leads to a decrease of mitochondrial NAD^+ that induces Bid-mediated translocation of AIF to the nucleus, in which it initiates nuclear condensation [102]. Silencing of the poly (ADP-ribose) glycohydrolase gene (PARG) has been recently shown to be protective in H_2O_2 -treated MCF-7 and HeLa cells [86]. In these models, the catabolism of poly (ADP) ribose (PAR) was delayed, and cells were protected against genotoxic stress, suggesting that not PAR accumulation, but fast PAR degradation is a trigger of genotoxic stress-induced apoptosis. In our model, HT-22 neurons were not protected against glutamate by PARG knockdown with PARG-siRNA, suggesting that PAR degradation does not play a leading part in glutamate toxicity in this model system.

Other mitochondrial pro-apoptotic factors than AIF may as well be located in particular compartments of the mitochondrial intermembrane space and may require activation of different release mechanisms [103, 104]. For example, recent studies provided evidence for the entrapment of cytochrome c in the mitochondrial cristae, and the release of cytochrome c during apoptosis required disruption of Optic Atrophy 1 (OPA1) oligomers [105, 106]. The proposed differential distribution and individual mechanisms of release from the mitochondrial intermembrane space may explain why AIF release occurs as an early event and is independent of the release of other pro-apoptotic factors after ischemic or excitotoxic brain lesions. In line with this model, our data propose a preferential release of AIF from mitochondria in glutamate-induced cell death in neurons that is not compensated after AIF gene silencing by cytochrome c release and caspase-dependent mechanisms.

4.2.1 Caspase-dependent versus caspase-independent apoptosis

It has been well established that mitochondrial membrane permeabilization results in the release of pro-apoptotic factors such as cytochrome c, Smac/Diablo, Omi/HtrA2 and AIF, which may execute cell death via caspase-dependent or caspase-independent mechanisms. For example, formation of the apoptosome by cytochrome c, Apaf-1 and procaspase-9 and downstream catalytic activation of executor

caspases (caspase-3, -6, or -7) is a widely established mechanism of caspase-dependent cell death execution downstream of mitochondrial damage in many cells, including neurons. In the present study, activation of caspase-3 downstream of Bid was detected suggesting that this pathway was also activated in HT-22 neurons. Caspase-3 inhibition alone, however, did not prevent glutamate-induced cell death (Figure 17) and other indicators of executor caspase activities, as for example lamin cleavage as a prerequisite for caspase-6, were also not detected (Figure 18). Similarly activation of caspase-8, which is widely described as an initiator in caspase-dependent apoptosis upstream of Bid, was not detected (Figure 29), and the specific caspase-8 inhibitor did not protect the neurons against glutamate toxicity. Previous findings in cerebral ischemia of mice demonstrated that AIF release and caspase-3 activation occurred in parallel [98] as found here in the glutamate-damage model of HT-22 neurons. However, the present and the previous studies suggested a merely partial involvement of caspase-3 in these models of neuronal apoptosis. Strikingly, inhibition of caspase-3 had no protective effect in glutamate-treated HT-22 neurons which is in line with findings in cerebral ischemia of mice where only a part of the detected apoptotic DNA fragmentation was associated with caspase-3 activity [98]. In contrast, previous findings demonstrated that caspase-3 knock-out mice showed neuroprotection in models of cerebral ischemia [70]. However, this protective effect was less pronounced than anticipated regarding the strong evidence for caspase activation in ischemic brain tissue. In the present in vitro models, AIF gene silencing did not push cells toward caspase-3-mediated cell death. In sum these data strongly suggest a major role for AIF-mediated caspase-independent execution of apoptotic cell death downstream of mitochondrial membrane permeabilization. This fits well with observations in vivo, where AIF translocation to the nucleus of ischemic neurons occurred prior to detectable caspase activation and correlated well with signs of cell death; further, in models of cerebral ischemia protective effects in animals with low AIF protein levels were far more pronounced than protective effects in caspase-knockout animals or after caspase inhibition [65, 98, 107].

Another mitochondrial factor that has been linked to caspase-dependent as well as caspase-independent apoptosis is the serine protease Omi/HtrA2 [93, 94]. Omi/HtrA2

is localized in the mitochondria and in the cytosol and after apoptotic stress increased mitochondrial release of activated Omi/HtrA2 may lead to proteolysis of IAPs, in particular cleavage of XIAP or survivin, and subsequent acceleration of caspase activity [93, 94, 108-110]. In addition Omi/HtrA2 can mediate cell death through caspase-independent mechanisms through its serine protease activity [39, 94]. In contrast, in Omi/HtrA2 knock-out mice, it has been shown that Omi/HtrA2 plays a neuroprotective role for striatal neurons. Mice lacking the Omi/HtrA2-gene, developed a parkinsonian phenotype, that led to death around 30 days after birth [111]. However, a recent study demonstrated protective effects of the Omi/HtrA2 inhibitor UCF-101 in a model of focal cerebral ischemia, suggesting a pro-apoptotic role for Omi/HtrA2 in acute ischemic neuronal death [37]. Furthermore, Omi/HtrA2 plays a role in apoptotic cell death after myocardial ischemia [112]. These data suggest that, similar to AIF, Omi/HtrA2 plays an important role in the maintenance of neurons under physiological conditions but takes over detrimental functions after acute apoptotic stress. In the present model, Omi/HtrA2 appears to act upstream of mitochondrial AIF release rather than in downstream caspase-dependent execution mechanisms since inhibition of Omi/HtrA2 clearly prevented AIF translocation and glutamate-induced neuronal cell death. Most importantly, the Omi/HtrA2 inhibitor failed to prevent tBid-induced apoptosis, which puts Omi/HtrA2-mediated apoptosis pathways upstream of or independent of Bid. If and how Omi/HtrA2 contributes to Bid-mediated AIF release has to be addressed in further studies; data from the present study demonstrate that Omi/HtrA2 neither cleaves Bid in a direct manner nor accelerates Bid cleavage by caspase-1 or caspase-8. It is also interesting to note, that AIF-siRNA and Omi/HtrA2 inhibitor UCF-101 did not show an additional protective effect. This suggests that AIF and Omi/HtrA2 are connected to each other in their pro-apoptotic function.

4.2.2 Staurosporine-induced apoptosis is independent of Bid

The present model of glutamate toxicity in HT-22 neurons features Bid-mediated mitochondrial membrane permeabilization and nuclear translocation of AIF, whereas activation of Bid and translocation of AIF to the nucleus have not been detected as

essential features for STS-induced apoptosis which is consistent with previous observations in non-neuronal cells [113, 114]. STS is a low molecular weight inhibitor of protein kinases, especially of typical, calcium dependent protein kinase C (PKC). Damaging neurons with STS leads to apoptosis on a pathway different from the mechanisms after excitotoxic insults and calcium elevation. For example the typical apoptotic DNA laddering occurs after STS-treatment while calcium levels stay constant. Indeed, high extracellular potassium levels attenuated STS-induced cell death by increasing calcium influx through voltage-dependent calcium channels [115, 116]. Downstream of the PKC-inhibition, treatment of neurons with STS leads to an activation of caspase-8 and caspase-3. It is interesting to note that despite an activation of caspase-8 and potential subsequent Bid cleavage with mitochondrial membrane permeabilization, there was no breakdown of the mitochondrial membrane potential shown [117]. In contrast, glutamate-induced excitotoxic apoptosis was mediated caspase-8-independent but with a breakdown of the mitochondrial membrane potential. This is in line with the present findings in the STS-damage model of HT-22 neurons: Bid inhibitors could not prevent STS-induced apoptosis in HT-22 neurons. Consequently, without a Bid-mediated breakdown of the mitochondrial membrane potential, there was no mitochondrial release and nuclear translocation of AIF, and AIF siRNA did not protect HT-22 neurons from STS-induced apoptosis. In sum these findings show, that apoptosis is a flexible mechanism, changing the involved cascades depending from its specific stimuli. Therefore many cell death models are needed to further clarify the interrelations between the single pro-apoptotic factors upon activation by different initiators of apoptosis. For research on mechanisms of neurodegeneration cell damage models involving increased intracellular calcium levels and oxidative stress, such as glutamate toxicity, OGD or amyloid- β toxicity, are likely more suitable than STS-induced apoptosis which bears no reference to a distinct neurological disorder and which was used as a counter-example to glutamate-induced cell death in the present study.

4.3 Activation of Bid

Since Bid is apparently a key regulator in glutamate-induced neuronal apoptosis further experiments focused on the activation of Bid after the glutamate challenge. As outlined above, a direct involvement of Omi/HtrA2 in Bid cleavage could be excluded. Similar negative results were obtained when addressing other prominent candidates that have been linked to Bid cleavage and activation: Caspase-8 and caspase-2 have been shown to cleave Bid mediating apoptosis induced by Fas/TNF or TRAIL receptor stimuli, respectively [118, 119]. Increases in intracellular calcium levels activate Calpain I, which is also suggested to cleave Bid thereby triggering tBid mediated mitochondrial damage [120]. In addition, calpain has been identified to mediate cleavage and release of AIF from isolated mitochondria, after entering the mitochondrial intermembrane space through the tBid-generated pore in the mitochondrial outer membrane [75]. The lysosomal involvement in neuronal apoptosis triggered by oxidative stress is being increasingly recognized and may involve mitochondrial membrane permeabilization either directly through activation of phospholipases or indirectly through cleavage of Bid. For example, the lysosomal cysteine proteases such as Cathepsin B, D, H and L have been reported to mediate Bid cleavage, subsequent activation of Bax by tBid, and mitochondrial release of cytochrome c, AIF, and Smac/Diablo [90]. The findings of this work, however, strongly suggest that none of these factors that may act upstream of Bid cleavage and mitochondrial AIF release are involved in glutamate-induced apoptosis of HT-22 neurons: Inhibition of caspase-8 or caspase-2, calpains or cathepsins failed to prevent glutamate-induced cell death in HT-22 neurons.

In addition, blocking of p38 MAP kinase, a stress responding cellular serine/threonine kinase, did not protect HT-22 neurons exposed to glutamate. For example, in Parkinson's models of cell death, p38 has been shown to be activated, with subsequent cleavage of Bid, but these findings apparently had no relevance for glutamate-induced cell death of neurons.

In contrast, the caspase-1 inhibitor (ICE inhibitor II) provided moderate protection against glutamate neurotoxicity, confirming previous reports suggesting the

involvement of caspase-1 in this model system [21]. Here Bid was confirmed as a substrate for caspase-1 in the in vitro assay. In sharp contrast to the pronounced protective effects of the Bid inhibitor over a wide range of glutamate concentrations, however, inhibition of caspase-1 only provided moderate protection against the glutamate challenge and this protective effect was hardly detectable at high concentrations of glutamate, i.e. strong apoptotic stress. Therefore, other mechanisms are likely involved in Bid activation and the apoptotic signaling in addition to the activation of caspase-1. It is interesting to note, that the combination of caspase-1 inhibitor and the Omi/HtrA2 inhibitor provided additive protective effects. This finding suggests that caspase-1 and Omi/HtrA2 may act in parallel pathways of apoptotic signaling towards Bid activation and AIF release after glutamate challenge. In addition, Omi/HtrA2 may support the upstream activation of caspase-1 by enhanced cleavage of IAPs which may result in an acceleration of Caspase activity. In addition, recent data suggested that activation of Bid and translocation to the mitochondria does not necessarily require Bid cleavage [81, 82]. In particular, a recent study by Prehn and co-workers demonstrated translocation of full length Bid to the mitochondria in glutamate-treated cells prior to disruption of the mitochondrial membrane potential [81]. Further, phosphorylation of Bid by ATM at Serin 61 or Serin 78 has been suggested as a mechanism of activity regulation, e.g. in response to DNA damage [71, 72, 90]. On the other hand, phosphorylation of Bid by casein kinases I + II at Threonine 58 and / or Serine 61, which are adjacent to the caspase-8 cleavage residue Aspartate 59, prevents Bid truncation by caspase-8 and has therefore been suggested as a mechanism to control mitochondrial amplification of apoptotic signaling [121, 122]. Thus, cleavage of Bid by caspase-1 may be just one possible mechanism among others to regulate Bid activity and mitochondrial translocation of truncated or full length Bid in glutamate neurotoxicity. These mechanisms may involve activation of Omi/HtrA2 or alterations of Bid phosphorylation and require further investigation. The following scheme shows possible Bid-activation mechanisms for glutamate-induced apoptotic pathways.

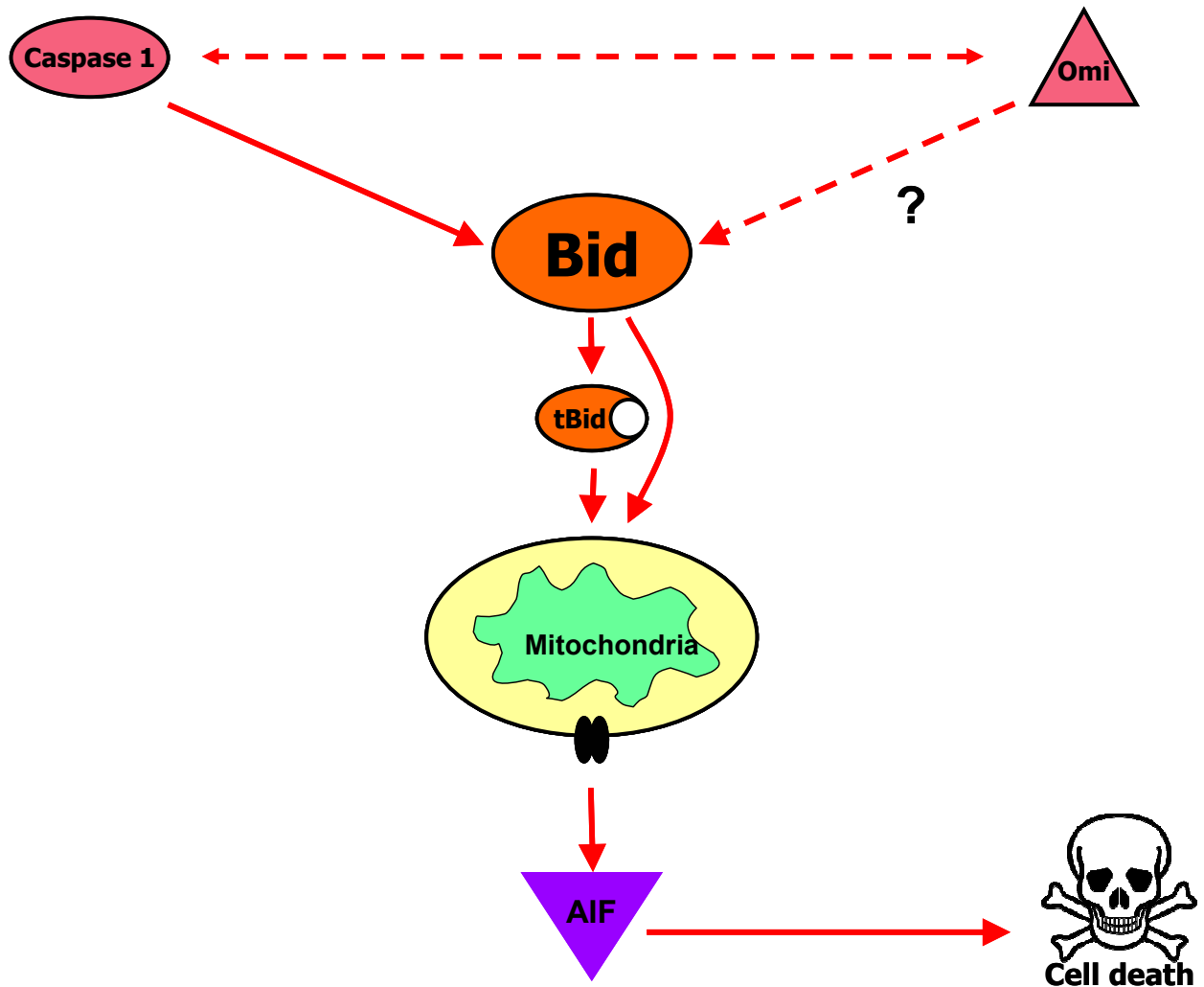


Figure 44: Bid-activating mechanism in glutamate-treated neurons

Caspase-1, but not Omi/HtrA2 is able to cleave Bid. After glutamate damage of neurons, Bid is activated by caspase-1 and in parallel by Omi/HtrA2 which may support the activity of caspase-1. Bid or tBid mediate the mitochondrial release of AIF and subsequent cell death.

4.4 Glutamate toxicity in HT-22 neurons is a relevant model for neurodegenerative diseases:

As shown above, glutamate-treatment of HT-22 neurons leads to oxidative stress, elevation of intracellular calcium levels and mitochondrial damage. Since oxidative stress, increased calcium levels and subsequent trigger of mitochondrial cell death pathways are key mechanisms in various models of neuronal cell death, glutamate-

treatment of HT-22 neurons is a relevant in vitro model for neurodegenerative diseases: For example, parallel experiments in primary cultured neurons demonstrated pronounced neuroprotective effects of different Bid inhibitors in models of glutamate-induced apoptosis or oxygen-glucose deprivation. In both models of neuronal cell death, activation of glutamate receptors mediates rapid increase of intracellular calcium levels and an excitotoxic death program that involves the formation of ROS, permeabilization of the mitochondrial membrane and mitochondrial release of AIF [98, 123]. It is therefore concluded that Bid plays a key role in neuronal cell death induced by excitotoxic stimuli and oxidative stress which both have been associated with a wide variety of neurodegenerative conditions following acute brain injury by cerebral ischemia or brain trauma as well as chronic neurodegenerative diseases, such as Alzheimer's disease [124]. It is interesting to note that very similar to the presented protection against glutamate toxicity pharmacological inhibition of Bid also prevented AIF translocation to the nucleus and cell death in HT-22 neurons exposed to amyloid-beta peptide (data not shown). The relevance of the current data on the key role for Bid in neuronal cell death in vitro is further underlined by recent data obtained in mouse models of cerebral ischemia [65] and brain trauma [67]. In both models of acute brain injury, Bid cleavage has been detected after the respective insults, and Bid knockout resulted in significant cerebroprotective effects compared to wildtype animals. Therefore the presently used Bid inhibitors, BI-6C9 and BI-11A7, may emerge as promising lead structures for neuroprotective drugs in the treatment of neurodegenerative diseases. These two compounds expose different solubility in the different media depending on the serum content and were therefore used in serum-containing medium for HT-22 neurons (BI-6C9) or in serum-free medium for primary neurons (BI-11A7), respectively. The effectivity of both these compounds was similar in the respective model system. Based on these findings in HT-22 and primary neurons it could be shown that glutamate damage of HT-22 neurons is an appropriate model to investigate neuronal apoptosis. Since apoptosis for example in Alzheimer's disease [125], stroke [126] and also in models of excitotoxicity in primary neurons (see above) is related to oxidative stress, intracellular increase of calcium levels and mitochondrial

dysfunction, a scheme universally valid for different models of neurodegenerative disorders, could be developed. This involves Bid as a pivotal factor upstream of the breakdown of mitochondrial membrane potential and AIF as the leading executor of neuronal apoptosis induced by intrinsic mechanisms (Figure 45).

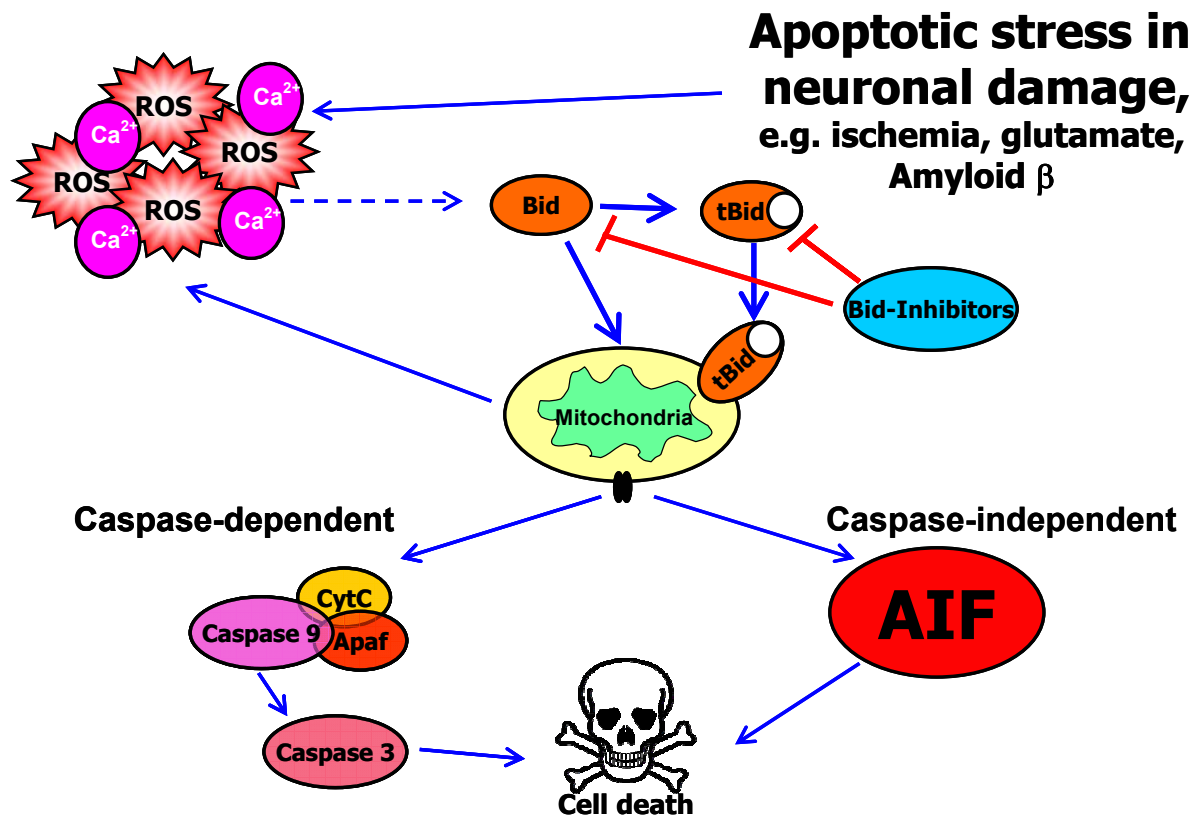


Figure 45: Proposed mechanism of apoptosis by neurodegeneration based on findings in the glutamate-damage model of HT-22 neurons.

Neurodegeneration induced by ischemia in stroke, glutamate in trauma or Amyloid-beta in Alzheimer's disease is followed by an increase of reactive oxygen species and Calcium levels in the neurons. This results in cleavage of Bid to tBid, which together with Bax or alone can form pores in the mitochondrial outer membrane, breakdown of the mitochondrial membrane potential, and further enhanced production of ROS. This vicious circle can lead to the activation of caspases and, most importantly, to the release and activation of caspase-independent proteins such as AIF which causes DNA damage, nuclear condensation and cell death. Bid inhibitors were able to interrupt the pathway upstream of mitochondrial damage.

5 Summary

The Bcl-2 family members play an important role in the control of programmed cell death by either promoting or preventing the release of pro-apoptotic mitochondrial proteins. In the present thesis the roles of the pro-apoptotic Bcl-2 family member Bid and mitochondrial protein AIF were investigated in glutamate-induced neuronal apoptosis. After exposure to glutamate, neuronal cell death was determined by MTT assay and annexin-V-FITC staining with subsequent FACS analysis in immortalized hippocampal mouse neurons (HT-22), or by quantification of apoptotic nuclei by Hoechst staining in primary rat neurons. In addition, caspase-3 activity was determined as well as caspase-independent death signaling, such as mitochondrial release of AIF. Bid-siRNA or pharmacological inhibition of Bid rescued HT-22 neurons from glutamate-induced apoptosis with similar efficiency. In addition, a small molecule Bid inhibitor significantly attenuated the loss of mitochondrial membrane potential, reduced activation of caspase-3, and prevented AIF translocation to the nucleus in HT-22 neurons exposed to glutamate. The specificity of the Bid-inhibitor was demonstrated in tBid overexpression experiments. It is interesting to note that AIF-siRNA also attenuated glutamate toxicity in HT22 cells whereas the general caspase inhibitor Z-VAD-fmk alone did not exert neuroprotection, suggesting that mainly caspase-independent mechanisms executed glutamate-induced cell death in this experimental paradigm. In addition, inhibition of Omi/HtrA2, which can promote apoptotic death signaling in a caspase-dependent and caspase-independent manner, also rescued HT-22 neurons from glutamate-induced apoptosis by prevention of AIF translocation. Similar findings were observed in primary embryonic rat neurons where Bid inhibitors prevented AIF-translocation and cell death after exposure to glutamate. Overall, the data of this thesis reveal that Bid plays a key role for the release of pro-apoptotic molecules such as AIF from mitochondria thereby promoting caspase-independent cell death. Small molecule inhibitors of Bid may therefore emerge as promising therapeutics in neurodegenerative diseases where programmed cell death is prominent. In addition it has been shown that glutamate damage of HT-22 neurons is an appropriate model for apoptotic cell death induced by glutamate, relevant to mechanisms that occur in many neurodegenerative diseases.

6 Appendix

6.1 Abbreviations

A	Ampere
AIF	apoptosis inducing factor
AMPA	alpha-amino-3-hydroxy-5-methyl-4-isoxazolepropionic acid
Apaf-1	apoptosis protease-activating factor-1
APS	ammonium persulfate
ATM	ataxia telangiectasia mutated
ATP	adenosine triphosphate
Bcl-2	B-cell lymphoma-2
bp	base pairs
CAD	caspase-activated deoxyribonuclease
CARD	caspase recruitment domain
CCCP	carbonyl cyanide m-chlorophenylhydrazone
cDNA	copy DNA
CHAPS	3-[(3-Cholamidopropyl)dimethylammonio]-1-propanesulfonate
CO ₂	carbon dioxide
DAPI	4', 6-diamidino-2-phenylindole dihydrochloride
dATP	deoxy Adenosine triphosphate
dCTP	deoxy cytosine triphosphate
DD	death domain
DED	death effector domain
dGTP	deoxy guanosine triphosphate
DMEM	Dulbecco's modified Eagle medium
DMSO	dimethyl sulfoxide

DNA	deoxyribonucleic acid
dNTP	deoxy nucleotide triphosphate
dsRNA	double-stranded RNA
DTT	D,L-dithiotreitol
dTTP	deoxy thymidine triphosphate
EBSS	Earle's balanced salt solution
EDTA	ethylenediaminetetraacetic acid disodium salt
EGFP	enhanced green fluorescent protein
EGTA	ethylene glycol-bis(2-aminoethylether)-N,N,N',N'-tetraacetic acid
ER	endoplasmatic reticulum
FAD	flavin adenine dinucleotide
FasL	Fas ligand
FCS	fetal calf serum
FENS	Federation of European Neurosciences
FITC	fluorescein isothiocyanate
g	relative centrifugal force
GAPDH	glyceraldehyde-3-phosphate dehydrogenase
GFP	green fluorescent protein (=EGFP)
h	hour(s)
HBSS	Hanks' balanced salt solution
HEPES	4-(2-Hydroxyethyl)piperazine-1-ethanesulfonic acid
Hq	harlequin
HRP	horse reddish peroxidase
IAP	inhibitor of apoptosis
ICAD	inhibitor of caspase-activated deoxyribonuclease
ICE	interleukin converting enzyme (caspase-1)
IgG	immunoglobulin G

IP ₃	inositol triphosphate
JC-1	5,5',6,6'-tetrachloro-1,1',3,3'-tetraethylbenzimidazolylcarbocyanine iodide
kb	kilo base
KCl	potassium chloride
LiCl	lithium chloride
mAIF_pd2EGFP-N1	plasmid encoding for a AIF, coupled to EGFP under control of the CMV promoter/enhancer
MAPK	mitogen activated protein kinase
MEM	Eagle's minimum essential medium
MgCl ₂	magnesium chloride
Min	minute(s)
MLS	mitochondrial localization sequence
MTT	3-(4,5-Dimethylthiazol-2-yl)-2,5-diphenyltetrazolium bromide
NA	numeric aperture
NaHCO ₃	sodium hydrogen carbonate
NaOH	sodium hydroxide
NB	neurobasal medium
NB+	neurobasal medium plus B27 supplement
NLS	nuclear localization sequence
NMDA	N-methyl-D-aspartate
OGD	oxygen glucose deprivation
Omi/HtrA2	high temperature requirement protein A2
p.a.	pro analysi
Parg	poly(ADP-ribose) glycohydrolase
PARP	poly(ADP-ribose) polymerase
PBS	phosphate-buffered saline
pcDNA 3.1+	empty plasmid with a CMV promoter/enhancer

PCR	polymerase chain reaction
pd2pEGFP-N1	plasmid encoding for EGFP under control of the CMV promoter/enhancer
pDsRed2-Bid	plasmid encoding for a fusion protein of red fluorescent protein and Bid under control of the CMV promoter/enhancer
pEGFP-Luc	plasmid encoding for EGFP and Luciferase under control of the CMV promoter/enhancer
pEGFP-N1	plasmid encoding for EGFP under control of the CMV promoter/enhancer
PFA	paraformaldehyde
pgWIZ-GFP	plasmid encoding for EGFP under control of the CMV promoter/enhancer
pH	potentia hydrogenii
PI	propidium iodide
poly-hema	polyhydroxyethylmethacrylate
PVDV	polyvinylidenfluorid
RIP 2	receptor interacting protein 2
RNA	ribonucleic acid
ROCK	Rho-associated kinase
ROS	reactive oxygen species
RT	room temperature
RT-PCR	reverse transcription polymerase chain reaction
SD	standard deviation
SDS	sodium dodecyl sulfate
siRNA	small interfering ribonucleic acid
Smac/Diablo	second mitochondrial derived activator of caspase
SOD	superoxide dismutase
STS	staurosporine
TBE	buffer containing Tris, boric acid and EDTA
tBid	truncated Bid
TBST	Tris-buffered saline with Tween 20

TE	PBS containing 0.05% trypsin and 0.02% EDTA
TEMED	N,N,N',N'-tetramethylethylenediamine
TNF	tumor necrosis factor
Tris	Tris(hydroxymethyl)aminomethane
U	unit(s)
UV	ultraviolet
V	Volt
XIAP	X-chromosomal linked inhibitors of apoptosis

6.2 Publications

6.2.1 Original papers

Culmsee C, Zhu C, Landshamer S, Becattini B, Wagner E, Pellecchia M, Blomgren K, Plesnila N (2005). Apoptosis-inducing factor triggered by poly(ADP-ribose) polymerase and Bid mediates neuronal cell death after oxygen-glucose deprivation and focal cerebral ischemia. ***Journal of Neuroscience***, 25:10262-10272.

Culmsee C, Gerling N, Landshamer S, Rickerts B, Duchstein HJ, Umezawa K, Klumpp S, Kriegelstein J (2005). Nitric oxide donors induce neurotrophin-like survival signaling and protect neurons against apoptosis. ***Molecular Pharmacology***, 68:1006-1017.

Barbara Becattini, Carsten Culmsee, Marilisa Leone, Dayong Zhai, Xiyun Zhang, Kevin J. Crowell, Stefan Landshamer, John C. Reed, Nikolaus Plesnila and Maurizio Pellecchia (2006). SAR by ILOEs-based design and synthesis of anti-apoptotic compounds targeting Bid. ***Proceedings of the National Academy of Sciences***, 103:12602-12606.

Isele NB, Lee HS, Landshamer S, Straube A, Plesnila N, Padovan C, Culmsee C (2007). The antiapoptotic effect of bone marrow stromal cells on primary neurons is

mediated through Erk1/2/MAPK and PI3-K/Akt. *Neurochemistry International*, 50:243-250.

Nikolaus Plesnila, Louisa von Baumgarten, Marina Retiounskaia, Doortje Engel, Ardeshir Ardeshiri, Ricarda Zimmermann, Stefan Landshamer, Ernst Wagner, Carsten Culmsee (2007). Delayed neuronal death after brain trauma involves p53-dependent inhibition of NF- κ B transcriptional activity. *Cell Death & Differentiation*, under revision.

Stefan Landshamer, Miriam Hoehn, Nicole Barth, Gerlinde Schwake, Irene Kazhdan, Barbara Becattini, Stefan Zahler, Angelika Vollmar, Maurizio Pellecchia, Nikolaus Plesnila, Ernst Wagner, Carsten Culmsee (2007). Glutamate induces neuronal death through activation of Bid and mitochondrial release of AIF. *Journal of Cell Biology*, submitted.

Ardavan Ardeshiri, Ardeshir Ardeshiri, Jennifer E. Slemmer, Changlian Zhu, Stefan Landshamer, Ernst Wagner, Klas Blomgren, Carsten Culmsee, John T. Weber, Nikolaus Plesnila. Causal role of AIF for secondary neuronal death following traumatic injury. In preparation.

6.2.2 Reviews

Culmsee C, Landshamer S (2006). Molecular insights into mechanisms of the cell death program: role in the progression of neurodegenerative disorders. *Journal of Current Alzheimer's Research*, 3:269-283 (Cover illustration).

6.2.3 Oral presentations and posters

Landshamer S., Hoehn M., Becattini B., Pellecchia M., Plesnila N., Culmsee C. (2006). Pharmacological inhibition of Bid blocks caspase-dependent and caspase-

independent cell death pathways in neurons. ***Naunyn-Schmiedeberg's Archives of Pharmacology***, 374:281.

Culmsee C., Zhu C., Landshamer S., Becattini B., Wagner E., Pellechia M., Blomgren K., Plesnila N. (2006). Causal role of apoptosis-inducing factor in ischemic neuronal cell death. ***Naunyn-Schmiedeberg's Archives of Pharmacology***, 374:297.

Isele N.B., Lee H.S., Landshamer S., Straube A., Plesnila N., Padovan C.S., Culmsee C. (2006). Bone marrow stromal cells mediate neuroprotection through stimulation of PI3/AKT- and MAPK signaling in neurons. ***Naunyn-Schmiedeberg's Archives of Pharmacology***, 374:299.

Landshamer S., Culmsee C, Hoehn M, Pellecchia M, Wagner E, Plesnila N 2006. Targeting Bid to prevent caspase-dependent and caspase-independent cell death in neurons. ***Joint Meeting of the Czech, German and Hungarian Pharmaceutical Societies***, Marburg, 04-07. October 2006.

S. Landshamer, M. Hoehn, B. Becattini, M. Pellecchia, E. Wagner, N. Plesnila, C. Culmsee (2006). Role of Bid for the release of AIF and Omi/HtrA2 from mitochondria and subsequent execution of caspase-independent cell death. ***Annual Meeting of the Society for Neuroscience***, Atlanta, Poster No. 184.19/LL84.

7 References

- [1] Kerr JF, Wyllie AH, Currie AR. Apoptosis: a basic biological phenomenon with wide-ranging implications in tissue kinetics. *Br J Cancer* 1972; 26: 239-57.
- [2] Dive C, Gregory CD, Phipps DJ, Evans DL, Milner AE, Wyllie AH. Analysis and discrimination of necrosis and apoptosis (programmed cell death) by multiparameter flow cytometry. *Biochim Biophys Acta* 1992; 1133: 275-85.
- [3] Vaux DL and Korsmeyer SJ. Cell death in development. *Cell* 1999; 96: 245-54.
- [4] Oppenheim RW. Cell death during development of the nervous system. *Annu Rev Neurosci* 1991; 14: 453-501.
- [5] Mattson MP. Apoptosis in neurodegenerative disorders. *Nat Rev Mol Cell Biol* 2000; 1: 120-9.
- [6] McKay SE, Purcell AL, Carew TJ. Regulation of synaptic function by neurotrophic factors in vertebrates and invertebrates: implications for development and learning. *Learn Mem* 1999; 6: 193-215.
- [7] Ankarcrona M, Dypbukt JM, Bonfoco E, Zhivotovsky B, Orrenius S, Lipton SA, Nicotera P. Glutamate-induced neuronal death: a succession of necrosis or apoptosis depending on mitochondrial function. *Neuron* 1995; 15: 961-73.
- [8] Mattson MP. Modification of ion homeostasis by lipid peroxidation: roles in neuronal degeneration and adaptive plasticity. *Trends Neurosci* 1998; 21: 53-7.
- [9] Mattson MP, Keller JN, Begley JG. Evidence for synaptic apoptosis. *Exp Neurol* 1998; 153: 35-48.
- [10] Duan W, Zhang Z, Gash DM, Mattson MP. Participation of prostate apoptosis response-4 in degeneration of dopaminergic neurons in models of Parkinson's disease. *Ann Neurol* 1999; 46: 587-97.
- [11] Zhang L, Rzigalinski BA, Ellis EF, Satin LS. Reduction of voltage-dependent Mg²⁺ blockade of NMDA current in mechanically injured neurons. *Science* 1996; 274: 1921-3.
- [12] Choi DW. Calcium and excitotoxic neuronal injury. *Ann N Y Acad Sci* 1994; 747: 162-71.
- [13] Portera-Cailliau C, Price DL, Martin LJ. Non-NMDA and NMDA receptor-mediated excitotoxic neuronal deaths in adult brain are morphologically

- distinct: further evidence for an apoptosis-necrosis continuum. *J Comp Neurol* 1997; 378: 88-104.
- [14] Loo DT, Copani A, Pike CJ, Whittemore ER, Walencewicz AJ, Cotman CW. Apoptosis is induced by beta-amyloid in cultured central nervous system neurons. *Proc Natl Acad Sci U S A* 1993; 90: 7951-5.
- [15] Roth KA. Caspases, apoptosis, and Alzheimer disease: causation, correlation, and confusion. *J Neuropathol Exp Neurol* 2001; 60: 829-38.
- [16] Hartmann A, Hunot S, Michel PP, Muriel MP, Vyas S, Faucheux BA, Mouatt-Prigent A, Turmel H, Srinivasan A, Ruberg M, Evan GI, Agid Y, Hirsch EC. Caspase-3: A vulnerability factor and final effector in apoptotic death of dopaminergic neurons in Parkinson's disease. *Proc Natl Acad Sci U S A* 2000; 97: 2875-80.
- [17] Andersen JK. Does neuronal loss in Parkinson's disease involve programmed cell death? *Bioessays* 2001; 23: 640-6.
- [18] Jenner P and Olanow CW. The pathogenesis of cell death in Parkinson's disease. *Neurology* 2006; 66: S24-S36.
- [19] Yuan J, Lipinski M, Degterev A. Diversity in the mechanisms of neuronal cell death. *Neuron* 2003; 40: 401-13.
- [20] van Leyen K, Siddiq A, Ratan RR, Lo EH. Proteasome inhibition protects HT22 neuronal cells from oxidative glutamate toxicity. *J Neurochem* 2005; 92: 824-30.
- [21] Tan S, Sagara Y, Liu Y, Maher P, Schubert D. The regulation of reactive oxygen species production during programmed cell death. *J Cell Biol* 1998; 141: 1423-32.
- [22] Stefanis L. Caspase-dependent and -independent neuronal death: two distinct pathways to neuronal injury. *Neuroscientist* 2005; 11: 50-62.
- [23] Alnemri ES, Livingston DJ, Nicholson DW, Salvesen G, Thornberry NA, Wong WW, Yuan J. Human ICE/CED-3 protease nomenclature. *Cell* 1996; 87: 171.
- [24] Oliver L and Vallette FM. The role of caspases in cell death and differentiation. *Drug Resist Updat* 2005; 8: 163-70.
- [25] Creagh EM and Martin SJ. Caspases: cellular demolition experts. *Biochem Soc Trans* 2001; 29: 696-702.
- [26] Slee EA, Adrain C, Martin SJ. Executioner caspase-3, -6, and -7 perform distinct, non-redundant roles during the demolition phase of apoptosis. *J Biol Chem* 2001; 276: 7320-6.

-
- [27] Coleman ML, Sahai EA, Yeo M, Bosch M, Dewar A, Olson MF. Membrane blebbing during apoptosis results from caspase-mediated activation of ROCK I. *Nat Cell Biol* 2001; 3: 339-45.
- [28] Takahashi A, Alnemri ES, Lazebnik YA, Fernandes-Alnemri T, Litwack G, Moir RD, Goldman RD, Poirier GG, Kaufmann SH, Earnshaw WC. Cleavage of lamin A by Mch2 alpha but not CPP32: multiple interleukin 1 beta-converting enzyme-related proteases with distinct substrate recognition properties are active in apoptosis. *Proc Natl Acad Sci U S A* 1996; 93: 8395-400.
- [29] Lazebnik YA, Kaufmann SH, Desnoyers S, Poirier GG, Earnshaw WC. Cleavage of poly(ADP-ribose) polymerase by a proteinase with properties like ICE. *Nature* 1994; 371: 346-7.
- [30] Enari M, Sakahira H, Yokoyama H, Okawa K, Iwamatsu A, Nagata S. A caspase-activated DNase that degrades DNA during apoptosis, and its inhibitor ICAD. *Nature* 1998; 391: 43-50.
- [31] Oberhammer F, Wilson JW, Dive C, Morris ID, Hickman JA, Wakeling AE, Walker PR, Sikorska M. Apoptotic death in epithelial cells: cleavage of DNA to 300 and/or 50 kb fragments prior to or in the absence of internucleosomal fragmentation. *EMBO J* 1993; 12: 3679-84.
- [32] Peter ME and Krammer PH. Mechanisms of CD95 (APO-1/Fas)-mediated apoptosis. *Curr Opin Immunol* 1998; 10: 545-51.
- [33] Nicholls DG and Budd SL. Mitochondria and neuronal survival. *Physiol Rev* 2000; 80: 315-60.
- [34] Zou H, Li Y, Liu X, Wang X. An APAF-1.cytochrome c multimeric complex is a functional apoptosome that activates procaspase-9. *J Biol Chem* 1999; 274: 11549-56.
- [35] Rodriguez J and Lazebnik Y. Caspase-9 and APAF-1 form an active holoenzyme. *Genes Dev* 1999; 13: 3179-84.
- [36] Tikoo A, O'Reilly L, Day CL, Verhagen AM, Pakusch M, Vaux DL. Tissue distribution of Diablo/Smac revealed by monoclonal antibodies. *Cell Death Differ* 2002; 9: 710-6.
- [37] Althaus J, Siegelin MD, Dehghani F, Cilenti L, Zervos AS, Rami A. The serine protease Omi/HtrA2 is involved in XIAP cleavage and in neuronal cell death following focal cerebral ischemia/reperfusion. *Neurochem Int* 2007; 50: 172-80.
- [38] Cilenti L, Lee Y, Hess S, Srinivasula S, Park KM, Junqueira D, Davis H, Bonventre JV, Alnemri ES, Zervos AS. Characterization of a novel and specific

- inhibitor for the pro-apoptotic protease Omi/HtrA2. *J Biol Chem* 2003; 278: 11489-94.
- [39] Egger L, Schneider J, Rheme C, Tapernoux M, Hacki J, Borner C. Serine proteases mediate apoptosis-like cell death and phagocytosis under caspase-inhibiting conditions. *Cell Death Differ* 2003; 10: 1188-203.
- [40] Ye H, Cande C, Stephanou NC, Jiang S, Gurbuxani S, Larochette N, Daugas E, Garrido C, Kroemer G, Wu H. DNA binding is required for the apoptogenic action of apoptosis inducing factor. *Nat Struct Biol* 2002; 9: 680-4.
- [41] Lipton SA and Bossy-Wetzel E. Dueling activities of AIF in cell death versus survival: DNA binding and redox activity. *Cell* 2002; 111: 147-50.
- [42] Daugas E, Susin SA, Zamzami N, Ferri KF, Irinopoulou T, Larochette N, Prevost MC, Leber B, Andrews D, Penninger J, Kroemer G. Mitochondrio-nuclear translocation of AIF in apoptosis and necrosis. *Faseb J* 2000; 14: 729-39.
- [43] Modjtahedi N, Giordanetto F, Madeo F, Kroemer G. Apoptosis-inducing factor: vital and lethal. *Trends Cell Biol* 2006; 16: 264-72.
- [44] Klein JA, Longo-Guess CM, Rossmann MP, Seburn KL, Hurd RE, Frankel WN, Bronson RT, Ackerman SL. The harlequin mouse mutation downregulates apoptosis-inducing factor. *Nature* 2002; 419: 367-74.
- [45] Zhu C, Qiu L, Wang X, Hallin U, Cande C, Kroemer G, Hagberg H, Blomgren K. Involvement of apoptosis-inducing factor in neuronal death after hypoxia-ischemia in the neonatal rat brain. *J Neurochem* 2003; 86: 306-17.
- [46] Eckert A, Keil U, Marques CA, Bonert A, Frey C, Schussel K, Muller WE. Mitochondrial dysfunction, apoptotic cell death, and Alzheimer's disease. *Biochem Pharmacol* 2003; 66: 1627-34.
- [47] Regula KM, Ens K, Kirshenbaum LA. Mitochondria-assisted cell suicide: a license to kill. *J Mol Cell Cardiol* 2003; 35: 559-67.
- [48] Mattson MP and Kroemer G. Mitochondria in cell death: novel targets for neuroprotection and cardioprotection. *Trends Mol Med* 2003; 9: 196-205.
- [49] Sherratt HS. Mitochondria: structure and function. *Rev Neurol (Paris)* 1991; 147: 417-30.
- [50] Bernardi P, Scorrano L, Colonna R, Petronilli V, Di Lisa F. Mitochondria and cell death. Mechanistic aspects and methodological issues. *Eur J Biochem* 1999; 264: 687-701.

-
- [51] Szegezdi E, Logue SE, Gorman AM, Samali A. Mediators of endoplasmic reticulum stress-induced apoptosis. *EMBO Rep* 2006; 7: 880-5.
- [52] Szalai G, Krishnamurthy R, Hajnoczky G. Apoptosis driven by IP(3)-linked mitochondrial calcium signals. *EMBO J* 1999; 18: 6349-61.
- [53] Katayama T, Imaizumi K, Manabe T, Hitomi J, Kudo T, Tohyama M. Induction of neuronal death by ER stress in Alzheimer's disease. *J Chem Neuroanat* 2004; 28: 67-78.
- [54] Nakagawa T, Zhu H, Morishima N, Li E, Xu J, Yankner BA, Yuan J. Caspase-12 mediates endoplasmic-reticulum-specific apoptosis and cytotoxicity by amyloid-beta. *Nature* 2000; 403: 98-103.
- [55] Hitomi J, Katayama T, Eguchi Y, Kudo T, Taniguchi M, Koyama Y, Manabe T, Yamagishi S, Bando Y, Imaizumi K, Tsujimoto Y, Tohyama M. Involvement of caspase-4 in endoplasmic reticulum stress-induced apoptosis and Abeta-induced cell death. *J Cell Biol* 2004; 165: 347-56.
- [56] Kroemer G and Reed JC. Mitochondrial control of cell death. *Nat Med* 2000; 6: 513-9.
- [57] Zamzami N and Kroemer G. Apoptosis: mitochondrial membrane permeabilization--the (w)hole story? *Curr Biol* 2003; 13: R71-R73.
- [58] Polster BM and Fiskum G. Mitochondrial mechanisms of neural cell apoptosis. *J Neurochem* 2004; 90: 1281-9.
- [59] Kim R. Unknotting the roles of Bcl-2 and Bcl-xL in cell death. *Biochem Biophys Res Commun* 2005; 333: 336-43.
- [60] Ward MW, Kogel D, Prehn JH. Neuronal apoptosis: BH3-only proteins the real killers? *J Bioenerg Biomembr* 2004; 36: 295-8.
- [61] Uo T, Kinoshita Y, Morrison RS. Neurons exclusively express N-Bak, a BH3 domain-only Bak isoform that promotes neuronal apoptosis. *J Biol Chem* 2005; 280: 9065-73.
- [62] Desagher S, Osen-Sand A, Nichols A, Eskes R, Montessuit S, Lauper S, Maundrell K, Antonsson B, Martinou JC. Bid-induced conformational change of Bax is responsible for mitochondrial cytochrome c release during apoptosis. *J Cell Biol* 1999; 144: 891-901.
- [63] Eskes R, Desagher S, Antonsson B, Martinou JC. Bid induces the oligomerization and insertion of Bax into the outer mitochondrial membrane. *Mol Cell Biol* 2000; 20: 929-35.

-
- [64] Martin-Villalba A, Herr I, Jeremias I, Hahne M, Brandt R, Vogel J, Schenkel J, Herdegen T, Debatin KM. CD95 ligand (Fas-L/APO-1L) and tumor necrosis factor-related apoptosis-inducing ligand mediate ischemia-induced apoptosis in neurons. *J Neurosci* 1999; 19: 3809-17.
- [65] Plesnila N, Zinkel S, Le DA, Amin-Hanjani S, Wu Y, Qiu J, Chiarugi A, Thomas SS, Kohane DS, Korsmeyer SJ, Moskowitz MA. BID mediates neuronal cell death after oxygen/ glucose deprivation and focal cerebral ischemia. *Proc Natl Acad Sci U S A* 2001; 98: 15318-23.
- [66] Yin XM, Luo Y, Cao G, Bai L, Pei W, Kuharsky DK, Chen J. Bid-mediated mitochondrial pathway is critical to ischemic neuronal apoptosis and focal cerebral ischemia. *J Biol Chem* 2002; 277: 42074-81.
- [67] Bermpohl D, You Z, Korsmeyer SJ, Moskowitz MA, Whalen MJ. Traumatic brain injury in mice deficient in Bid: effects on histopathology and functional outcome. *J Cereb Blood Flow Metab* 2006; 26: 625-33.
- [68] Schendel SL, Azimov R, Pawlowski K, Godzik A, Kagan BL, Reed JC. Ion channel activity of the BH3 only Bcl-2 family member, BID. *J Biol Chem* 1999; 274: 21932-6.
- [69] Culmsee C, Zhu Y, Kriegelstein J, Mattson MP. Evidence for the involvement of Par-4 in ischemic neuron cell death. *J Cereb Blood Flow Metab* 2001; 21: 334-43.
- [70] Le DA, Wu Y, Huang Z, Matsushita K, Plesnila N, Augustinack JC, Hyman BT, Yuan J, Kuida K, Flavell RA, Moskowitz MA. Caspase activation and neuroprotection in caspase-3- deficient mice after in vivo cerebral ischemia and in vitro oxygen glucose deprivation. *Proc Natl Acad Sci U S A* 2002; 99: 15188-93.
- [71] Zinkel SS, Hurov KE, Ong C, Abtahi FM, Gross A, Korsmeyer SJ. A role for proapoptotic BID in the DNA-damage response. *Cell* 2005; 122: 579-91.
- [72] Kamer I, Sarig R, Zaltsman Y, Niv H, Oberkovitz G, Regev L, Haimovich G, Lerenthal Y, Marcellus RC, Gross A. Proapoptotic BID is an ATM effector in the DNA-damage response. *Cell* 2005; 122: 593-603.
- [73] Chan SL and Mattson MP. Caspase and calpain substrates: roles in synaptic plasticity and cell death. *J Neurosci Res* 1999; 58: 167-90.
- [74] Goll DE, Thompson VF, Li H, Wei W, Cong J. The calpain system. *Physiol Rev* 2003; 83: 731-801.
- [75] Polster BM, Basanez G, Etxebarria A, Hardwick JM, Nicholls DG. Calpain I induces cleavage and release of apoptosis-inducing factor from isolated mitochondria. *J Biol Chem* 2005; 280: 6447-54.

-
- [76] Rami A. Ischemic neuronal death in the rat hippocampus: the calpain-calpastatin-caspase hypothesis. *Neurobiol Dis* 2003; 13: 75-88.
- [77] McCollum AT, Jafarifar F, Lynn BC, Agu RU, Stinchcomb AL, Wang S, Chen Q, Guttman RP. Inhibition of calpain-mediated cell death by a novel peptide inhibitor. *Exp Neurol* 2006; 202: 506-13.
- [78] Ray SK and Banik NL. Calpain and its involvement in the pathophysiology of CNS injuries and diseases: therapeutic potential of calpain inhibitors for prevention of neurodegeneration. *Curr Drug Targets CNS Neurol Disord* 2003; 2: 173-89.
- [79] Seth R, Yang C, Kaushal V, Shah SV, Kaushal GP. p53-dependent caspase-2 activation in mitochondrial release of apoptosis-inducing factor and its role in renal tubular epithelial cell injury. *J Biol Chem* 2005; 280: 31230-9.
- [80] Zhang WH, Wang X, Narayanan M, Zhang Y, Huo C, Reed JC, Friedlander RM. Fundamental role of the Rip2/caspase-1 pathway in hypoxia and ischemia-induced neuronal cell death. *Proc Natl Acad Sci U S A* 2003; 100: 16012-7.
- [81] Ward MW, Rehm M, Duesmann H, Kacmar S, Concannon CG, Prehn JH. Real time single cell analysis of Bid cleavage and Bid translocation during caspase-dependent and neuronal caspase-independent apoptosis. *J Biol Chem* 2006; 281: 5837-44.
- [82] Valentijn AJ and Gilmore AP. Translocation of full-length Bid to mitochondria during anoikis. *J Biol Chem* 2004; 279: 32848-57.
- [83] Becattini B, Sareth S, Zhai D, Crowell KJ, Leone M, Reed JC, Pellecchia M. Targeting apoptosis via chemical design: inhibition of bid-induced cell death by small organic molecules. *Chem Biol* 2004; 11: 1107-17.
- [84] Gil-Parrado S, Assfalg-Machleidt I, Fiorino F, Deluca D, Pfeiler D, Schaschke N, Moroder L, Machleidt W. Calpastatin exon 1B-derived peptide, a selective inhibitor of calpain: enhancing cell permeability by conjugation with penetratin. *Biol Chem* 2003; 384: 395-402.
- [85] Kazhdan I, Long L, Montellano R, Cavazos DA, Marciniak RA. Targeted gene therapy for breast cancer with truncated Bid. *Cancer Gene Ther* 2006; 13: 141-9.
- [86] Blenn C, Althaus FR, Malanga M. Poly(ADP-ribose) glycohydrolase silencing protects against H₂O₂-induced cell death. *Biochem J* 2006; 396: 419-29.
- [87] Morimoto BH and Koshland DE, Jr. Excitatory amino acid uptake and N-methyl-D-aspartate-mediated secretion in a neural cell line. *Proc Natl Acad Sci U S A* 1990; 87: 3518-21.

-
- [88] van Engeland M, Nieland LJ, Ramaekers FC, Schutte B, Reutelingsperger CP. Annexin V-affinity assay: a review on an apoptosis detection system based on phosphatidylserine exposure. *Cytometry* 1998; 31: 1-9.
- [89] Culmsee C and Plesnila N. Targeting Bid to prevent programmed cell death in neurons. *Biochem Soc Trans* 2006; 34: 1334-40.
- [90] Yin XM. Bid, a BH3-only multi-functional molecule, is at the cross road of life and death. *Gene* 2006; 369: 7-19.
- [91] Yu SW, Wang H, Poitras MF, Coombs C, Bowers WJ, Federoff HJ, Poirier GG, Dawson TM, Dawson VL. Mediation of poly(ADP-ribose) polymerase-1-dependent cell death by apoptosis-inducing factor. *Science* 2002; 297: 259-63.
- [92] Stoica BA, Movsesyan VA, Knoblach SM, Faden AI. Ceramide induces neuronal apoptosis through mitogen-activated protein kinases and causes release of multiple mitochondrial proteins. *Mol Cell Neurosci* 2005; 29: 355-71.
- [93] Suzuki Y, Imai Y, Nakayama H, Takahashi K, Takio K, Takahashi R. A serine protease, HtrA2, is released from the mitochondria and interacts with XIAP, inducing cell death. *Mol Cell* 2001; 8: 613-21.
- [94] Martins LM, Iaccarino I, Tenev T, Gschmeissner S, Totty NF, Lemoine NR, Savopoulos J, Gray CW, Creasy CL, Dingwall C, Downward J. The serine protease Omi/HtrA2 regulates apoptosis by binding XIAP through a reaper-like motif. *J Biol Chem* 2002; 277: 439-44.
- [95] Tan S, Wood M, Maher P. Oxidative stress induces a form of programmed cell death with characteristics of both apoptosis and necrosis in neuronal cells. *J Neurochem* 1998; 71: 95-105.
- [96] Chao DT and Korsmeyer SJ. BCL-2 family: regulators of cell death. *Annu Rev Immunol* 1998; 16: 395-419.
- [97] Cheung EC, Melanson-Drapeau L, Cregan SP, Vanderluit JL, Ferguson KL, McIntosh WC, Park DS, Bennett SA, Slack RS. Apoptosis-inducing factor is a key factor in neuronal cell death propagated by BAX-dependent and BAX-independent mechanisms. *J Neurosci* 2005; 25: 1324-34.
- [98] Culmsee C, Zhu C, Landshamer S, Becattini B, Wagner E, Pellicchia M, Blomgren K, Plesnila N. Apoptosis-inducing factor triggered by poly(ADP-ribose) polymerase and Bid mediates neuronal cell death after oxygen-glucose deprivation and focal cerebral ischemia. *J Neurosci* 2005; 25: 10262-72.

-
- [99] Otera H, Ohsakaya S, Nagaura Z, Ishihara N, Mihara K. Export of mitochondrial AIF in response to proapoptotic stimuli depends on processing at the intermembrane space. *EMBO J* 2005; 24: 1375-86.
- [100] Yuste VJ, Moubarak RS, Delettre C, Bras M, Sancho P, Robert N, d'Alayer J, Susin SA. Cysteine protease inhibition prevents mitochondrial apoptosis-inducing factor (AIF) release. *Cell Death Differ* 2005; 12: 1445-8.
- [101] Endres M, Ahmadi M, Kruman I, Biniszkievicz D, Meisel A, Gertz K. Folate deficiency increases postischemic brain injury. *Stroke* 2005; 36: 321-5.
- [102] Susin SA, Lorenzo HK, Zamzami N, Marzo I, Snow BE, Brothers GM, Mangion J, Jacotot E, Costantini P, Loeffler M, Larochette N, Goodlett DR, Aebersold R, Siderovski DP, Penninger JM, Kroemer G. Molecular characterization of mitochondrial apoptosis-inducing factor. *Nature* 1999; 397: 441-6.
- [103] Munoz-Pinedo C, Guio-Carrion A, Goldstein JC, Fitzgerald P, Newmeyer DD, Green DR. Different mitochondrial intermembrane space proteins are released during apoptosis in a manner that is coordinately initiated but can vary in duration. *Proc Natl Acad Sci U S A* 2006; 103: 11573-8.
- [104] Gottlieb E. OPA1 and PARL keep a lid on apoptosis. *Cell* 2006; 126: 27-9.
- [105] Frezza C, Cipolat S, Martins dB, Micaroni M, Beznoussenko GV, Rudka T, Bartoli D, Polishuck RS, Danial NN, De Strooper B, Scorrano L. OPA1 controls apoptotic cristae remodeling independently from mitochondrial fusion. *Cell* 2006; 126: 177-89.
- [106] Cipolat S, Rudka T, Hartmann D, Costa V, Serneels L, Craessaerts K, Metzger K, Frezza C, Annaert W, D'Adamio L, Derks C, Dejaegere T, Pellegrini L, D'Hooge R, Scorrano L, De Strooper B. Mitochondrial rhomboid PARL regulates cytochrome c release during apoptosis via OPA1-dependent cristae remodeling. *Cell* 2006; 126: 163-75.
- [107] Zhu C, Wang X, Huang Z, Qiu L, Xu F, Vahsen N, Nilsson M, Eriksson PS, Hagberg H, Culmsee C, Plesnila N, Kroemer G, Blomgren K. Apoptosis-inducing factor is a major contributor to neuronal loss induced by neonatal cerebral hypoxia-ischemia. *Cell Death Differ* 2006.
- [108] Hegde R, Srinivasula SM, Zhang Z, Wassell R, Mukattash R, Cilenti L, DuBois G, Lazebnik Y, Zervos AS, Fernandes-Alnemri T, Alnemri ES. Identification of Omi/HtrA2 as a mitochondrial apoptotic serine protease that disrupts inhibitor of apoptosis protein-caspase interaction. *J Biol Chem* 2002; 277: 432-8.
- [109] Verhagen AM, Silke J, Ekert PG, Pakusch M, Kaufmann H, Connolly LM, Day CL, Tikoo A, Burke R, Wrobel C, Moritz RL, Simpson RJ, Vaux DL. HtrA2

- promotes cell death through its serine protease activity and its ability to antagonize inhibitor of apoptosis proteins. *J Biol Chem* 2002; 277: 445-54.
- [110] van Loo G, van Gurp M, Depuydt B, Srinivasula SM, Rodriguez I, Alnemri ES, Gevaert K, Vandekerckhove J, Declercq W, Vandenabeele P. The serine protease Omi/HtrA2 is released from mitochondria during apoptosis. Omi interacts with caspase-inhibitor XIAP and induces enhanced caspase activity. *Cell Death Differ* 2002; 9: 20-6.
- [111] Martins LM, Morrison A, Klupsch K, Fedele V, Moiso N, Teismann P, Abuin A, Grau E, Geppert M, Livi GP, Creasy CL, Martin A, Hargreaves I, Heales SJ, Okada H, Brandner S, Schulz JB, Mak T, Downward J. Neuroprotective role of the Reaper-related serine protease HtrA2/Omi revealed by targeted deletion in mice. *Mol Cell Biol* 2004; 24: 9848-62.
- [112] Liu HR, Gao E, Hu A, Tao L, Qu Y, Most P, Koch WJ, Christopher TA, Lopez BL, Alnemri ES, Zervos AS, Ma XL. Role of Omi/HtrA2 in apoptotic cell death after myocardial ischemia and reperfusion. *Circulation* 2005; 111: 90-6.
- [113] Cande C, Vahsen N, Kouranti I, Schmitt E, Daugas E, Spahr C, Luban J, Kroemer RT, Giordanetto F, Garrido C, Penninger JM, Kroemer G. AIF and cyclophilin A cooperate in apoptosis-associated chromatinolysis. *Oncogene* 2004; 23: 1514-21.
- [114] Susin SA, Daugas E, Ravagnan L, Samejima K, Zamzami N, Loeffler M, Costantini P, Ferri KF, Irinopoulou T, Prevost MC, Brothers G, Mak TW, Penninger J, Earnshaw WC, Kroemer G. Two distinct pathways leading to nuclear apoptosis. *J Exp Med* 2000; 192: 571-80.
- [115] Koh JY, Wie MB, Gwag BJ, Sensi SL, Canzoniero LM, Demaro J, Csernansky C, Choi DW. Staurosporine-induced neuronal apoptosis. *Exp Neurol* 1995; 135: 153-9.
- [116] Prehn JH, Jordan J, Ghadge GD, Preis E, Galindo MF, Roos RP, Kriegstein J, Miller RJ. Ca²⁺ and reactive oxygen species in staurosporine-induced neuronal apoptosis. *J Neurochem* 1997; 68: 1679-85.
- [117] Budd SL, Tanneti L, Lishnak T, Lipton SA. Mitochondrial and extramitochondrial apoptotic signaling pathways in cerebrocortical neurons. *Proc Natl Acad Sci U S A* 2000; 97: 6161-6.
- [118] Luo X, Budihardjo I, Zou H, Slaughter C, Wang X. Bid, a Bcl2 interacting protein, mediates cytochrome c release from mitochondria in response to activation of cell surface death receptors. *Cell* 1998; 94: 481-90.

-
- [119] Wagner KW, Engels IH, Deveraux QL. Caspase-2 can function upstream of bid cleavage in the TRAIL apoptosis pathway. *J Biol Chem* 2004; 279: 35047-52.
- [120] Chen M, He H, Zhan S, Krajewski S, Reed JC, Gottlieb RA. Bid is cleaved by calpain to an active fragment in vitro and during myocardial ischemia/reperfusion. *J Biol Chem* 2001; 276: 30724-8.
- [121] Degli EM, Ferry G, Masdehors P, Boutin JA, Hickman JA, Dive C. Post-translational modification of Bid has differential effects on its susceptibility to cleavage by caspase 8 or caspase 3. *J Biol Chem* 2003; 278: 15749-57.
- [122] Desagher S, Osen-Sand A, Montessuit S, Magnenat E, Vilbois F, Hochmann A, Journot L, Antonsson B, Martinou JC. Phosphorylation of bid by casein kinases I and II regulates its cleavage by caspase 8. *Mol Cell* 2001; 8: 601-11.
- [123] Becattini B, Culmsee C, Leone M, Zhai D, Zhang X, Crowell KJ, Rega MF, Landshamer S, Reed JC, Plesnila N, Pellecchia M. Structure-activity relationships by interligand NOE-based design and synthesis of antiapoptotic compounds targeting Bid. *Proc Natl Acad Sci U S A* 2006; 103: 12602-6.
- [124] Tanovic A and Alfaro V. [Glutamate-related excitotoxicity neuroprotection with memantine, an uncompetitive antagonist of NMDA-glutamate receptor, in Alzheimer's disease and vascular dementia]. *Rev Neurol* 2006; 42: 607-16.
- [125] Mark RJ, Blanc EM, Mattson MP. Amyloid beta-peptide and oxidative cellular injury in Alzheimer's disease. *Mol Neurobiol* 1996; 12: 211-24.
- [126] Mattson MP, Culmsee C, Yu ZF. Apoptotic and antiapoptotic mechanisms in stroke. *Cell Tissue Res* 2000; 301: 173-87.

8 Acknowledgements

My first word of thanks goes to all my colleagues of the 'AK Wagner'. Without their support, my research would not have been as much fun and as successful as it turned out to be, and writing this thesis would have been impossible.

First of all, I would like to thank Prof. Dr. Ernst Wagner for providing me with a place in his group, for enabling me to attend both national and international meetings, and for advancing this thesis through helpful discussions.

It should be mentioned that without my direct supervisor PD Dr. Carsten Culmsee, I would never have started writing this thesis. He supported me and my projects in an excellent manner, always motivating me, always being around for help and always guiding me into the right direction. With his most outstanding assistance during work and his ability to make every congress or private event funny and pleasant, he earns a special and sincere thankyou.

Thankyou also to Professor Dr. Nikolaus 'Nick' Plesnila who always had competent advises, supported my projects in different manners and made the time at the 2006 Annual Meeting of the Society for Neuroscience in Atlanta unforgettable.

I would also like to thank Dr. Manfred Ogris for so much fun during lab-work, holding mouse tails, talking bullshit and teaching me walking up the walls in 'Matrix' style. I am very grateful to Dr. Martina Ruffer for supervising me in the biochemistry students' courses and for organizing the according lab work.

A really big thankyou to Miriam Höhn for her great technical assistance, which was marked by a maximum of efficiency and precision, as well as speedy results whenever it came to conducting cell culture experiments. Her experience helped me so much during lab work.

Thanks to Melinda Kiss and Wolfgang Rödl, who helped me with gene vectors and protein analytics and with some computer problems, respectively.

Thank you to Professor Dr. Heike Beck: I had a great time in Atlanta at the Annual Meeting of the Society for Neuroscience with you.

Very special thanks to my colleagues Julia Klöckner, Julia Fahrmeir, Lilja Thoenes, Lars Gädtke, Michael Günter and Clemens Thoma for endless fun both during and after work. Without you, I would never have learned dancing Salsa, founding 'wire companies' and preparing sixty molar sodium chloride solutions. In addition, I discovered that girls can belch, salad is food, Reggaton is a kind of music and French assistants do not like students' underwear on their desk. Thank you for all these important lessons and for all private events with you.

I would also like to say thank you to all my 'Wahlpflichtfach'-students, especially to Natalie Pfeiffer, Eva Röder, Gertraud Helf and Markus Hofer, who did an excellent job during their time in my lab and never forgot how to have fun at work.

A really big thankyou goes to Angela Maier, Michael Grintz, and the whole 'Bienen family' in general. Without you, I would eventually have forgotten the fun and pleasure that comes with a pharmacist's work.

I also thank my best friends Manuel Flecker, Markus Durst and Marlon Kwasnik. It was the anticipation of spending some of my rare spare time during my period of research with you that made me always look forward to evenings and weekends.

A very special and heartfelt thankyou to Constanza Hagn for her continuous help, her enduring patience with me and her sincere appreciation.

Finally, I thank my parents and my sisters Christina and Maria. Without their support, I would never have been able to complete this thesis.

9 Curriculum Vitae

Personal data

Date of birth: 25.07.1978

Place of birth: Munich, Germany

Marital status: unmarried

Education

02/2004 to present	PhD thesis at the Department of Pharmaceutical Biology-Biotechnology, Ludwig-Maximilian-University, Munich, Germany; supervisors: PD Dr. Carsten Culmsee, Prof. Dr. Ernst Wagner
12/2003	Licensure as pharmacist
05/2003-10/2003	Internship at Bienen-Apotheke OHG, Munich, Germany
11/2002-04/2003	Internship at Technical Research / Chemical analytics, Roche Diagnostics, Penzberg, Germany
09/1997-10/2002	Studies of pharmacy, Ludwig-Maximilian-University, Munich, Germany (stopping out for alternative civilian service from 09/1998 to 09/1999 at the surgical intensive care unit of the Dr. von Haunersches Kinderspital, Munich
09/1989-06/1997	Secondary school, Theresien Gymnasium, Munich, Germany